UNIVERSITY OF CALIFORNIA, SAN DIEGO

ALS-linked TDP-43 mutations produce aberrant RNA splicing and adult-onset motor disease without aggregation or loss of nuclear TDP-43

A dissertation submitted in partial satisfaction of the requirements for the degree

Doctor of Philosophy

in

Biomedical Sciences

by

Eveline Sun Arnold

Committee in charge:

Professor Don W. Cleveland, Chair
Professor Lawrence S.B. Goldstein
Professor Bruce A. Hamilton
Professor Albert La Spada
Professor Bing Ren

2012

The Dissertation of Eveline Sun Arnold is approved, and it is acceptable in quality and form for publication on microfilm and electronically:

_____

_____

_____

_____

_____

Chair

University of California, San Diego

2012

Dedication

I dedicate this thesis to the family and friends who have made this journey possible.

Table of Contents

List of Figures

List of Tables

List of Abbreviations

ALS	Amyotrophic lateral sclerosis
BAC	Bacterial artificial chromosome
ChAT	Choline acetyl-transferase
CNS	Central nervous system
CTF	C-terminal fragment
dTDP-43	Drosophila TDP-43, or TBPH
eGFP	Enhanced green fluorescent protein
EDTA	Ethylenediaminetetraacetic acid
EMG	electromyography or electromyogram
FALS	Familial amyotrophic lateral sclerosis
FTD	Frontotemporal dementia
FTLD	Frontotemporal lobar degeneration
FTLD-U	Frontotemporal lobar degeneration with ubiquitinated inclusions
FUS/TLS	Fused in sarcoma/translocated in liposarcoma
hTDP-43	human TDP-43
PCR	Polymerase chain reaction
PFA	Paraformaldehyde
MEP	Motor-evoked potential
MMEP	Myogenic motor evoked potential
MND	Motor neuron disease
mRNA	Messenger ribonucleic acid
mTDP-43	mouse TDP-43

NMJ	Neuromuscular junction
NES	Nuclear export signal
NLS	Nuclear localization signal
RRM	RNA recognition motif
RT-PCR	Reverse transcription polymerase chain reaction
RT-qPCR	Reverse transcription quantitative polymerase chain reaction
SALS	Sporadic amyotrophic lateral sclerosis
SCMEP	Spinal cord motor-evoked potential
SOD1	Cu/Zn superoxide dismutase 1
TBE	Tris/Borate/EDTA
TEMED	Tetramethylethylenediamine
TDP-43	Trans-activating response region (TAR) DNA binding protein with a molecular mass of 43 KDa
UTR	Untranslated region
VAchT	Vesicular acetylcholine transporter
VChAt	Vesicular choline acetyltransferase

Acknowledgements

This work has been the result of help and support from many extraordinarily generous, talented and helpful individuals, and I have many to thank. I apologize in advance if I have inadvertently omitted anyone.

Firstly, to my thesis advisor, Don W. Cleveland, thank you for the privilege and opportunity to work in the extraordinary intellectual environment of your laboratory. Thank you for continuously challenging me to be a better scientist, setting high intellectual expectations and, lastly, teaching me to swim with (scientific) sharks. There are many lessons I have learned from you and others in the laboratory that I will carry with me throughout my career.

To my committee members, Drs. Bruce A. Hamilton, Lawrence S.B. Goldstein, Albert R. La Spada, and Bing Ren, thank you for your helpful scientific insight and constructive criticism. I give special thanks to Dr. Hamilton for his support and enthusiastic mentorship of all Genetics Training Program trainees, past and present. Thank you to Gina Butcher, Leanne Nordeman and Kathy Klingenberg for working tirelessly in the Biomedical Sciences students' interests, and for making all BMS administrative requirements as painless as possible.

To my undergraduate mentors and advisors, Drs. Virginia M.-Y. Lee and John Q. Trojanowski: I owe both my decision to pursue a graduate career and, coincidentally, the initiating discovery that formed the foundation of my thesis project to the both of you. To say that you, along with Dr. Cleveland, are among my many scientific role models would be a vast understatement. To Dr. Matthew

Winton, thank you for the encouragement, support, and training that allowed me to pursue my scientific goals.

To the many friends and family who made this work possible, I cannot thank you enough for the endless support and words of encouragement you have provided me through the years. To my mother and father, Mei-Hwei and Sey-Shing Sun, and my little sister, Vicki, a few short sentences are insufficient to express my gratitude, but needless to say, I would not be who I am without you. To my husband, Grant, thank you for your unwavering support and patience, despite the distance and time. I could not have done it without all of you behind me.

To the members of the Cleveland lab, it goes without saying that I owe much of my intellectual development as a scientist to all of you. I am exceedingly thankful for the privilege of working with so many tremendously talented and driven individuals. Thanks especially to Dr. Holly Kordasiewicz for the patience and enthusiasm you showed in mentoring me, from the beginning of my graduate career to the end. To Dr. Shuo-Chien Ling: thank you for the endless discussions and mentorship. I hope that all your incredible hard work and dedication will pay off soon. To my past baymates: Drs. Hristelina Ilieva and Andrew Holland: thank you for holding my hand as an inexperienced beginning graduate student. To my current baymates, Drs. Desiree Salazar and Shuying Sun: thank you for the emotional and intellectual support in the final years of this journey. To Melissa Downes: thank you for being a bedrock of help, technically, scientifically, management-wise, or otherwise! To the past Cleveland graduate students, Drs.

Alain Silk, Anita Kulukian and Yumi Kim: I am likely the last in the line of Cleveland Lab graduate students, and I had a lot to live up to. You were one of the reasons I joined this laboratory and I still look up to all of you. Thank you for being scientific big siblings. Finally, I wish to give special thanks to the dedicated Cleveland lab undergraduate research assistants who have helped me at one time or another: Han Jin Park, Sandra Lee, Anne Vetto and Kevin Clutario.

Chapter 2, in part, is being prepared for publication. The dissertation author was the primary researcher and author of this paper. Oleksandr Platoshyn, Melissa Downes, and Dr. Martin Marsala (Marsala Lab, La Jolla, CA) performed electrophysiology experiments and analysis of the resulting data. Ling Ouyang (Salk Institute, La Jolla, CA) performed microarray experiments and Stephanie Huelga and Dr. Gene Yeo (Yeo Lab, La Jolla, CA) performed analysis of the resulting data. Drs. Clotilde Lagier-Tourenne and Magdalini Polymenidou performed RT-qPCR experiments. Dr. Holly Kordasiewicz provided assistance with and performed rotarod experiments. Nuclear-cytoplasmic and biochemical fractionations were performed by Dr. Dara Ditsworth. Drs. Sandrine Da Cruz, and Philippe Parone performed histological staining and quantification for neuromuscular junctions and upper motor neurons. Dr. Chris Shaw (King's College, London, U.K.) very kindly provided clones containing wild-type and mutant human TDP-43 cDNA.

Vita

2002-2006 Bachelor of Arts, University of Pennsylvania, Philadelphia

2006-2012 Doctor of Philosophy, University of California, San Diego

Fellowships

2007-2009 Genetics Training Grant
University of California, San Diego
National Institute for General Medical Sciences, T32 GM008666

Publications

Arnold E.S., Ling, S.C., Lagier-Tourenne, C., Polymenidou, M., Huelga, S.C., Ditsworth, D., Kordasiewicz, H., Platoshyn, O., Downes, M., Parone, P., Da Cruz, S., Marsala, M., Yeo, G., Shaw, C.E., and Cleveland, D.W. ALS-linked TDP-43 mutations produce aberrant RNA splicing and adult-onset motor disease without aggregation or loss of nuclear TDP-43. *Manuscript in Preparation.*

Winton, M.J., Lee. E.B., **Sun, E.,** Wong, M.M., Leight, S., Zhang, B., Trojanowski, J.Q. and Lee, V.M. (2011). Intraneuronal APP, Not Free Abeta Peptides In 3xTg-AD Mice: Implications For Tau Versus Abeta-Mediated Alzheimer Neurodegeneration. **J. Neurosci.** 31:7691-9.

Polymenidou, M., Lagier-Tourenne, C., Hutt, K.R., Huelga, S.C., Moran, J., Liang, T.Y., Ling S.C., Zhong, Z., **Sun, E.,** Wancewicz. E., Mazur, C., Kordasiewicz, H., Sedaghat, Y., Bennett, F.C., Yeo, G.W. and Cleveland, D.W. (2011). Disrupted processing of long pre-mRNAs and widespread RNA missplicing are components of neuronal vulnerability from loss of nuclear TDP-43. **Nat. Neurosci**. 14, 459-468.

Uryu K., Richter-Landsberg C., Welch W., **Sun E.,** Goldbaum O., Norris E.H., Pham C.T., Yazawa I., Hilburger K., Micsenyi M., Giasson B.I., Bonini N.M., Lee V.M., Trojanowski J.Q. (2006). Convergence of heat shock protein 90 with ubiquitin in filamentous alpha-synuclein inclusions of alpha-synucleinopathies. **Am. J. Pathol.** 168, 947-961.

Abstract of the Dissertation

ALS-linked TDP-43 mutations produce aberrant RNA splicing and adult-onset motor disease without aggregation or loss of nuclear TDP-43

by

Eveline Sun Arnold

Doctor of Philosophy in Biomedical Sciences

University of California, San Diego, 2012

Professor Don W. Cleveland, Chair

Amyotrophic lateral sclerosis (ALS) is an adult-onset neurodegenerative disease symptomatically characterized by progressive, fatal paralysis resulting from the degeneration of the upper and lower motor neurons of the nervous system. Although 10% of ALS is inherited in a dominant, autosomal fashion, the remaining 90% of ALS cases do not have a known genetic cause. Since the discovery of the first gene linked to familial ALS (FALS), much progress has been made towards understanding the pathological mechanisms underlying this disease. Like many neurodegenerative diseases, ALS as well as a second neurodegenerative disease, frontotemporal lobar degeneration (FTLD), are characterized by the appearance of ubiquitinated inclusions within the cytoplasm of neurons and glia. As the most common cause of frontotemporal dementia, a class of neurodegenerative diseases in adults under 65, FTLD shares clinical and pathological signs with ALS. The discovery that the protein TAR DNA binding protein (TDP-43) comprises the major protein component in these

ubiquitinated inclusions in ALS and FTLD in 2006 represented a major shift in the understanding of ALS and FTLD pathogenesis.

Since 2008, over 40 mutations linked to sporadic and familial ALS have been reported in TDP-43, as well as in a second structurally and functionally related nucleic acid binding protein, FUS/TLS. At present, the mechanism underlying TDP-43 and FUS/TLS-mediated neurodegeneration is not well understood. Much of the molecular understanding of ALS and neurodegeneration pathogenesis comes from the use of genetic models expressing disease-linked mutations in the causative genes. The study presented here demonstrates that mutations in TDP-43 are sufficient to induce adult onset, mutant-dependent neurodegeneration in the absence of robust cytoplasmic accumulation, through the generation and use of rodent models expressing mutant human TDP-43. Furthermore, targets directly bound by TDP-43 are aberrantly spliced in a mutant-dependent, dose-dependent manner, with mutations in TDP-43 conferring both gain and loss of function. Thus, mutant-dependent alterations in splicing may contribute to motor neuron degeneration prior to the accumulation of aberrant cytoplasmic species of TDP-43.

Chapter 1: Introduction

1.1 Background

1.1.1 Lou Gehrig's Disease, or Amyotrophic Lateral Sclerosis

. More commonly known as Lou Gehrig's Disease in the United States and Canada and as motor neuron disease (MND) in the United Kingdom, amyotrophic lateral sclerosis (ALS) is an adult-onset neurodegenerative disease clinically characterized by progressive paralysis eventually leading to death. ALS affects 2-4 per 100,000 individuals per year (Boillee et al., 2006a; Buratti and Baralle, 2008). On average, death results within 2-5 years of diagnosis, typically due to loss of respiratory function following the loss of innervation to the muscles required for respiration. At present, there is no prophylactic or curative treatment available for ALS beyond the anti-glutamatergic drug riluzole, which may only extend life a few months (Bensimon et al., 1994). Since its first description in 1869 by the French neurologist Jean-Martin Charcot (Charcot, 1869), great strides have been made towards understanding the genetic, cellular and molecular mechanisms underlying this terrible disease.

Like many neurodegenerative diseases, ALS is primarily a sporadic disease (90%) without a known underlying genetic cause (sporadic ALS, or SALS). The remaining 10% of cases (familial ALS, or FALS) are inherited in an autosomal dominant manner. Both familial and sporadic ALS present with overlapping clinical and pathological hallmarks, including muscle weakness, spasticity and eventually paralysis due to the selective loss of both the upper and

lower motor neurons (Boillee et al., 2006a). The common clinical and pathological hallmarks underlying the familial and sporadic forms of ALS have focused research efforts towards uncovering and understanding the common pathways underlying both forms of the disease.

The discovery of mutations in Cu/Zn superoxide dismutase 1, or SOD1, linked to familial ALS in 1993 (Rosen et al., 1993) represented a major breakthrough in the molecular understanding of the disease. Since 2000, eight more genes have been reported to carry mutations linked to classical presentations of adult onset ALS (Table 1.1) . Despite the recent discovery of these mutations, overall, the majority of research on the molecular mechanisms underlying the pathogenesis of ALS has been accomplished using cellular and animal models expressing mutations in SOD1.

1.1.2 Use of SOD1 transgenic animal models in ALS and non-cell autonomy

The discovery of mutations in SOD1 heralded a new era in the understanding of ALS disease mechanisms. SOD1 is an ubiquitously expressed, cytoplasmic enzyme that performs a critical function of catalytically converting reactive superoxide (oxygen with an extra electron) to hydrogen peroxide or oxygen (Ilieva et al., 2009). SOD1 is a 153 amino acid protein encoded by five exons, and mutations associated with disease occur throughout the coding region of the protein, with an increased propensity for mutations in exon four and five. Currently, over 150 mutations in SOD1 are known to cause inherited ALS

and account for approximately 2-3% of FALS (Da Cruz and Cleveland, 2011). FALS associated with mutations in SOD1 are typically inherited in an autosomal dominant fashion, although rare variants N86S and D90A are inherited as recessive alleles (Turner and Talbot, 2008).

The generation of transgenic mice constitutively expressing mutant human SOD1 rapidly followed the discovery of FALS-linked mutations. These mice generally utilized the endogenous human SOD1 promoter and associated regulatory elements and recapitulated many key features of human disease, including lower motor neuron loss and progressive paralysis. Although many mechanisms have been proposed, unfortunately, there is no current consensus on the primary pathogenic process underlying ALS. Nevertheless, studies using rodent models genetically ablated for SOD1 or expressing mutant forms of human SOD1 have uncovered several critical observations about the disease process.

Firstly, SOD1-mediated toxicity is not due a loss of function of the protein, but rather, due to a gain of one or more toxic properties. Based on the observation that patient erythrocytes heterozygous for SOD1 mutations showed reduced dismutase activity (Deng et al., 1993), one early hypothesis proposed that a loss of SOD1 activity was a component of disease. SOD1 null mice were therefore generated to test this hypothesis, but were viable without overt motor deficits (Ho et al., 1998; Reaume et al., 1996). Further studies showed that SOD1-null mice were hypersensitive to certain insults, including paraquat-induced toxicity (Ho et al., 1998), ischemia (Kawase et al., 1999; Kondo et al.,

1997) and axotomy (Reaume et al., 1996). However, ablation of SOD1 alone was not sufficient to induce motor neuron disease. Indeed, initial studies showed that the mutant SOD1-induced phenotype occurred in the presence of endogenous mouse SOD1, supporting the proposal of a dominant, gain of toxic property associated with mutant SOD1 (Gurney et al., 1994). Secondly, the generation of transgenic mice expressing dismutase-inactive mutant SOD1 that also develop fatal motor neuron disease demonstrated that SOD1 dismutase activity was not a critical component of disease (Bruijn et al., 1997; Ripps et al., 1995).

Finally, experiments using restricted expression of mutant SOD1 in neurons indicated that neuronal-expression of mutant SOD1 was not sufficient to provoke a robust neurodegenerative phenotype (Lino et al., 2002; Pramatarova et al., 2001). Subsequent experiments exploiting chimeric mice expressing variable amounts of mutant SOD1 in neuronal and glial populations (Clement et al., 2003; Lino et al., 2002; Yamanaka et al., 2008a) demonstrated a critical role for non-neuronal cell-types in the initiation and progression of disease. Subsequent experiments using cre-mediated excision of mutant SOD1 in motor neurons, astrocytes and microglia (Boillee et al., 2006b; Yamanaka et al., 2008b), as well as ablation and replacement experiments using wild-type myeloid cells (Beers et al., 2006), showed that wild-type motor neurons or glia could respectively delay onset and progression of the ALS phenotype. Together, these experiments established the non-cell-autonomous nature of ALS disease onset and progression.

1.1.3 Identification of TDP-43 as the major protein component of ubiquitinated inclusions in ALS and FTLD and mutations in TDP

Pathologically, a key feature of many neurodegenerative diseases is the accumulation of cytoplasmic or nuclear protein inclusions within the neurons and glia central nervous system. The identification of these misfolded proteins has been crucial to understanding pathogenic mechanisms underlying many neurodegenerative diseases. Until recently, the identity of these ubiquitinated protein aggregates found in sporadic ALS as well as a second neurodegenerative disorder called frontotemporal lobar degeneration (FTLD or FTLD-U) was unknown.

FTLD is the most common form of frontotemporal dementia (FTD), which is the most prevalent cause of dementia in patients under the age of 65 after Alzheimer's disease (Neumann et al., 2006). FTDs present as progressive deficits in cognition, language, and/or social inhibition. Notably, although the primary presentation is characterized by cognitive involvement, some FTLD patients present with concomitant parkinsonism or MND. Conversely, ALS patients may present with signs of dementia, although the rate of clinical overlap is not well characterized, due to variations in diagnostic criteria (Hodges et al., 2004; Liscic et al., 2008; Lomen-Hoerth et al., 2002). The overlap of pathological and clinical symptoms between ALS and FTLD led to the proposal that the two disorders coexist on a wide continuum of neurodegenerative disorders.

A new chapter in the study of ALS therefore arrived in 2006 with the groundbreaking identification of the major ubiquitinated component of protein aggregates in patients with FTLD and sporadic ALS (Arai et al., 2006; Neumann et al., 2006). Using monoclonal antibodies that specifically recognized the ubiquitinated inclusions found in FTLD brains, Neumann et al. systematically screened FTLD patient samples with a series of biochemical analyses to identify the nucleic acid binding protein TAR DNA binding protein with a molecular mass of 43 kDa (TDP-43) as the major component of these inclusions. This landmark discovery motivated the direct sequencing of the gene encoding TDP-43, *TARDBP*, in FTLD and ALS patients and the identification of the first mutations in TDP-43 linked to ALS (Gitcho et al., 2008; Kabashi et al., 2008; Sreedharan et al., 2008). In 2009, mutations in a structurally and functionally related protein, fused in sarcoma/translocated in liposarcoma (FUS/TLS) were subsequently identified in familial ALS patients (Vance et al., 2009). Since 2008, over forty mutations in TDP-43 and FUS/TLS, respectively, have been reported in sporadic and familial ALS cases. Together, these mutations, as well as the observation of pathological mislocalization of both TDP-43 and FUS/TLS, have led to a paradigm shift that places defects in RNA processing as a probable mechanism underlying the development of both familial and sporadic motor neuron disease. In 2011, the most common cause of inherited ALS and FTLD was revealed with the report of hexanucleotide repeat expansions in the gene *C9ORF72* (DeJesus-Hernandez et al., 2011; Renton et al., 2011). The report of RNA foci within the nuclei of patient samples as well as the loss of an alternatively spliced *C9ORF72*

transcript has further emphasized the potential contribution of defects in RNA processing to the development of motor neuron disease.

1.1.4 TDP-43's Normal Function in Transcription and RNA Metabolism

TDP-43 was initially identified in a screen for transcriptional repressors that bind TAR DNA of the human immunodeficiency virus type 1 (HIV-1) (Ou et al., 1995). TDP-43 is a 414 amino acid encoded by six exons in the human gene, *TARDBP*, located on chromosome 1 (1p36.22). Structurally, TDP-43 is related to a family of heterogenous ribonucleoproteins (hnRNPs). TDP-43 contains a nuclear export signal, nuclear localization signal (Winton et al., 2008), two RNA recognition motifs (RRM1 and RRM2), and a C-terminal glycine-rich region thought to be involved in association with other proteins including components of the RNA splicing machinery (Buratti et al., 2005; D'Ambrogio et al., 2009; Kuo et al., 2009; Wang et al., 2004). Strikingly, with the exception of a two mutations found in the NLS (A90V – reported in an FTLD/ALS patient) and RRM1 (D169G), mutations in TDP-43 overwhelmingly cluster within the C-terminal glycine-rich region (Da Cruz and Cleveland, 2011). All currently reported mutations in TDP-43 are dominant missense changes, with the exception of a truncation mutant Y374X at the C-terminus of the protein (Daoud et al., 2008). Although its full normal function is not completely understood, in vivo and in vitro studies have established that TDP-43 plays a critical role in transcriptional regulation and RNA metabolism (Buratti and Baralle, 2008; Da Cruz and Cleveland, 2011; Lagier-Tourenne et al., 2010).

As a nucleic acid binding protein, TDP-43 binds both RNA and DNA, with a strong affinity for single stranded DNA (Acharya et al., 2006; Buratti and Baralle, 2001; Buratti et al., 2001). TDP-43 was initially described as a transcriptional repressor of both TAR DNA (Ou et al., 1995) as well as the mammalian SP-10 promoter (Abhyankar et al., 2007), although the mechanisms underlying its role as a transcriptional regulator are not well defined. Further studies have defined its role at multiple steps of RNA processing and metabolism, specifically its regulation of mRNA splicing (Buratti and Baralle, 2008; Da Cruz and Cleveland, 2011). Consistent with its role in RNA metabolism, under normal conditions, TDP-43 is found within the nucleus. However, under pathological conditions, TDP-43 is depleted from the nucleus and accumulates cytoplasmically in both neurons and glia (Igaz et al., 2008; Van Deerlin et al., 2008). Based on these pathological findings, one proposal for the mechanism of TDP-43-mediated neurodegeneration is the loss of its normal function. However, it is unclear whether a toxic gain of property, loss of normal function, or a combination of both is the primary pathogenic trigger underlying neurodegeneration.

1.1.5 Identification of TDP-43's RNA Targets

A potential avenue towards understanding the contribution of TDP-43 to neurodegeneration is through the identification of the normal RNA targets of TDP-43 that may be disrupted in disease. In addition to its role as a transcriptional regulator, TDP-43 was also identified as a splicing enhancer of the

cystic fibrosis transmembrane conductance regulator (Buratti and Baralle, 2001). In the context of the central nervous system, the use of high throughput sequencing following immunoprecipitation of TDP-43-bound RNA has been instrumental in identifying targets that may be dysregulated in neurodegenerative disease (Polymenidou et al., 2011; Tollervey et al., 2011).

Using cross-linking of TDP-43 to its RNA targets (called CLIP-seq or iCLIP), two studies have established that TDP-43 binds to approximately a third of the mouse brain transcriptome (Polymenidou et al., 2011), representing approximately 6000 transcripts, and likely an equivalent percentage of the human transcriptome as well (Tollervey et al., 2011). In addition to identifying targets bound by TDP-43, the use of cross-linking allowed for the identification of TDP-43 binding sites on their targets. Immunoprecipitation of TDP-43 without crosslinking (RIP-seq) identified approximately 4000 transcripts bound by TDP-43 in rat cortical neurons, but this approach cannot identify the binding sites due to technical limitations (Sephton et al., 2011). A fourth study using UV-CLIP of human neuroblastoma cells also identified approximately120 TDP-43-bound transcripts (Xiao et al., 2011). Together, these studies have emphasized a broad role for TDP-43 in the maintenance of the CNS transcriptome.

Through the *in vitro* (Ayala et al., 2011; Sephton et al., 2011; Xiao et al., 2011) and *in vivo* approaches (Polymenidou et al., 2011; Tollervey et al., 2011) described, the TDP-43 *in vivo* binding site was confirmed to consist of a GU-rich motif, as initially described *in vitro* (Buratti et al., 2004). However, a GU-rich motifi is neither necessary nor sufficient for TDP-43 binding (Polymenidou et al., 2011).

Furthermore, the majority of TDP-43 binding sites occur deep within introns away from splice junctions (Polymenidou et al., 2011; Sephton et al., 2011; Tollervey et al., 2011; Xiao et al., 2011). Upon depletion of TDP-43 using a siRNA approach in cell culture (Tollervey et al., 2011) or infusion of antisense oligonucleotides into the adult mouse nervous system (Polymenidou et al., 2011), two groups further demonstrated a broad role for TDP-43 in the maintenance of mRNA levels and alternative splicing. The latter approach also identified changes in the levels of over 600 RNAs and altered splicing of 965 mRNAs in the adult mouse brain following depletion of TDP-43.

Importantly, both studies identified mRNA targets bound by TDP-43 that encode proteins that are involved in neuronal function or development, or are implicated in neurological disease. Furthermore, targets whose levels were most significantly altered following loss of TDP-43 were also targets with the longest introns (average size >100kb), as well as targets that encode proteins involved in synaptic transmission (Polymenidou et al., 2011). Preferential expression of genes containing long introns relative to other tissues characterizes both the mouse and human nervous system. As such, depletion of nuclear TDP-43 in ALS and FTLD and subsequent loss of these long transcripts could plausibly represent a pathway for selective neuronal vulnerability in disease pathogenesis. Indeed, iCLIP and RNAseq analysis of FTLD patient brains have provided evidence of alterations in neuronal transcript levels associated with levels of TDP-43 binding (Tollervey et al., 2011). A study using laser capture microdissection of motor neurons from sporadic ALS patients followed by

genome exon splicing microarrays has also identified alterations in the splicing in 411 genes and changes in the levels of 148 transcripts, although the study did not find changes in TDP-43 or FUS/TLS levels (Rabin et al., 2010).

In addition to alterations in transcript levels, several studies have now identified changes in splicing in mRNA transcripts whose protein products are directly implicated in neurodegenerative disease, including FUS/TLS, parkin, huntingtin and the ataxins (Polymenidou et al., 2011; Tollervey et al., 2011; Xiao et al., 2011). These studies also confirmed previously proposed TDP-43 binding targets HDAC6 (Fiesel et al.; Kim et al., 2008) and the NF-L neurofilament subunit (Strong et al., 2007), both of which have been reported as being reduced in ALS patients. However, despite the large number of neuronal and disease-related genes reported to be targets of TDP-43 regulation, two studies have reported that there is no TDP-43 binding or reduction in SOD1 transcript levels in either mice or humans (Belzil et al., 2011; Polymenidou et al., 2011). Nevertheless, these studies have illustrated a wide range of transcripts that are affected in the CNS that are dependent upon the levels of TDP-43, with TDP-43 likely acting at multiple levels of RNA processing.

1.1.6 Autoregulation of TDP-43

In addition to binding many of the transcripts previously described, TDP-43 has been shown to bind its own transcript in the 3’ UTR region and alter its own splicing and transcript levels (Polymenidou et al., 2011; Tollervey et al., 2011). In the absence of a functional 3’UTR regulatory sequence, expression of

exogenous TDP-43 has been found to downregulate endogenous TDP-43 in both cell culture models (Ayala et al., 2011; Polymenidou et al., 2011; Tollervey et al., 2011) and transgenic mouse models (Igaz et al., 2011; Polymenidou et al., 2011; Xu et al., 2010). One study has shown evidence for binding to and enhancement of splicing of an intron within the TDP-43 3'UTR, thus promoting the downregulation of TDP-43 through nonsense-mediated decay (Polymenidou et al., 2011). A second group has proposed a model in which direct TDP-43 binding to its 3'UTR directly leads to instability and degradation of the TDP-43 transcript through what is referred to as the exosome machinery (Ayala et al., 2011). Although there is not yet a consensus on the precise mechanisms underlying TDP-43 autoregulation, the two studies have highlighted a key feature of TDP-43 biology: TDP-43 is a protein whose nuclear levels are highly regulated. Disturbance of nuclear accumulation may result in a feed-forward mechanism driving unregulated TDP-43 synthesis that may play a role in ALS pathogenesis.

1.1.7 Non-rodent Animal Models of TDP-43 Proteinopathy

Many efforts have been focused towards generating *in vivo* models of TDP-43 proteinopathy. TDP-43 is highly conserved protein across many species, including *Drosophila melanogaster*, *Caenorhabditis elegans* and *Danio rerio* (zebrafish). Several groups have taken advantage of the tractability of genetic modeling in these organisms to study the effects of overexpression of either wild-type or mutant human TDP-43 and disruption of TDP-43 homologs.

Disruption of the Drosophila homolog to TDP-43, known as TBPH or dTDP-43, either through a partial or complete genetic null or reduction using RNAi resulted in partial lethality in on study (Lu et al., 2009) and reduced life span in another (Feiguin et al., 2009). Reduction of dTDP-43, resulted in defects in dendritic branching (Lu et al., 2009) or axon loss in the mushroom body (Li et al., 2010), as well as defects in locomotion and neuromuscular junctions (Feiguin et al., 2009). Notably, ectopic expression of human TDP-43 (hTDP-43) was shown to promote dendritic branching, as did dTDP-43, whereas expression of human TDP-43 mutants Q331K and M337V resulted in a reduction in dendritic branching, much like what was observed upon dTDP-43 reduction (Lu et al., 2009). In the second study, cell-type restricted ectopic expression of human TDP-43 in motor neurons following reduction of dTDP-43 rescued the reported motor deficits (Feiguin et al., 2009). A similar approach to deplete TDP-43 with antisense morpholinos was also used in zebrafish, although no apparent reduction in viability was observed. Defects in axon length and disorganized branching were observed, which were accompanied by swimming deficits (Kabashi et al., 2009). As was observed in the rescue studies in Drosophila, replacement of zebrafish TDP-43 with wild-type human, but not mutant TDP-43, could rescue the deficits reported. Together, these studies have established the importance of TDP-43's function in the nervous system through multiple organisms.

In addition to TDP-43 depletion studies, several groups have now produced transgenic C. elegans (Ash et al., 2010; Liachko et al., 2010),

Drosophila (Hanson et al., 2010; Li et al., 2010; Miguel et al., 2011; Ritson et al., 2010), and zebrafish models (Kabashi et al., 2009; Laird et al., 2010) expressing human wild-type or mutant TDP-43. All of these studies have arrived at the consensus that overexpression of both wild-type and mutant human TDP-43 promotes motor deficits and/or cellular toxicity, albeit not in a cell-type specific manner and likely more correlated to transgene dosage (Laird et al., 2010). However, it appears that across multiple studies, the mutant forms of TDP-43 are more detrimental than wild-type human TDP-43 (Kabashi et al., 2009; Laird et al., 2010).

1.1.8 Rodent Models of TDP-43 Proteinopathy

In addition to genetic modeling in lower organisms, many groups have also focused their efforts towards generating transgenic rodent models of TDP-43 proteinopathy. To better understand the normal role of TDP-43 in the CNS, several groups have generated mice that are either constitutively or conditionally disrupted for *Tardbp*. TDP-43 is essential during the development of the mouse embryo, and disruption of both alleles of mouse *Tardbp* results in early lethality at approximately E3.5 to 8.5 due to abnormal expansion of the inner cell mass (Chiang et al., 2010; Kraemer et al., 2010; Sephton et al., 2009; Wu et al., 2010). Heterozygous *Tardbp* gene disruption mice are reported to be phenotypically normal, although one study has reported mild decreases in grip strength and hang time (Kraemer et al., 2010). Interestingly, all studies reporting constitutive disruption of TDP-43 demonstrate accumulation of TDP-43 protein at normal

levels in heterozygous mice, demonstrating a tight control of TDP-43 levels (Chiang et al., 2010; Kraemer et al., 2010; Sephton et al., 2009; Wu et al., 2010). Postnatal deletion of TDP-43 using a tamoxifen-inducible Cre-recombinase gene transcribed from the Rosa-26 promoter and two cre-exciseable conditional alleles resulted in rapid death within 9 days following TDP-43 excision. Use of a weaker driver line of tamoxifen-inducible CAG-cre resulted in slightly prolonged survival (minimum 18 days after induction), but resulted in a significant decrease in body weight due to loss of stored body fat. This dramatic loss of body fat was accompanied by TDP-43-dependent downregulation of the obesity-associated gene *Tbc1d1* in skeletal muscle. In sum, these studies have demonstrated a tight regulation of TDP-43 levels and a critical role for TDP-43 in early embryogenesis.

Since the initial report of mutations in TDP-43 in 2008, multiple efforts have been undertaken to generate transgenic rodent models expressing wild-type and mutant TDP-43. Most of these efforts have pursued a strategy employing heterologous promoters (mouse Thy1, prion promoter, calcium/calmodulin-dependent kinase II or CaMKII) to drive expression of human cDNA encoding wild-type or carrying ALS-linked mutations. One published study has used the native human TDP-43 gene sequence with the surrounding regulatory regions (Swarup et al., 2011a). Similar to what is observed in C. elegans, zebrafish and drosophila transgenic models, elevated expression of both wild-type (Igaz et al., 2011; Shan et al., 2010; Wils et al., 2010; Xu et al., 2010) and disease-linked mutant TDP-43 (Stallings et al., 2010; Wegorzewska et al., 2009; Xu et al., 2011) induce a wide variety of motor deficits and

neurodegenerative phenotypes in mice. Toxicity from elevated wild-type TDP-43 levels was not limited to human TDP-43 alone, as increased mouse wild-type TDP-43 expression under control of the CamKII (Tsai et al., 2010) was sufficient to induce a reduction in hippocampal neurons and brain weight, with a shortened lifespan in transgenic mice (mean 495 days vs. 632 days). As wild-type (mouse or human) TDP-43 and mutant TDP-43 are sufficient to induce neurological deficits, demonstration of mutant-dependent toxicity has proven a challenge. Discrepancies in cell-type expression as well as the levels of TDP-43 among studies have emphasized the need for careful interpretation of the resulting data.

Consistent with the highly regulated nature of TDP-43 during embryogenesis, early and rapid lethality of transgenic mice expressing high levels of wild-type or mutant TDP-43 (Shan et al., 2010; Stallings et al., 2010; Wegorzewska et al., 2009; Wils et al., 2010; Xu et al., 2010) have highlighted additional challenges in generating appropriate rodent models of age-dependent disease. Several groups have attempted to generate transgenic rodent models using inducible promoters to bypass this difficulty. One strategy to generate a rat model expressing TDP-43 has exploited a Tet-repressible system (rtTA) that utilizes a tetracycline-controlled transactivator (tTA) transcribed from a CAG-promoter and a doxycycline-repressible promoter (TRE-miniCMV) that is rendered inactive in the presence of doxycycline. Removal of doxycycline drives CNS and non-CNS expression of human TDP-43 carrying the FALS-linked mutation M337V. Unfortunately, no equivalent inducible wild-type transgene was established (Zhou et al., 2010). Following activation of the transgene after

removal of doxycycline, rapid paralysis and death occurred between postnatal days 35 and 50 with one line exhibiting sexual dimorphism in age of onset. However, despite the widespread CNS expression (non-CNS tissues were not evaluated for rat or human TDP-43 expression), TRE-TDP-43^{M337V} developed a phenotype clinically and pathologically similar to ALS, with weakness and eventual paralysis, albeit very early in life.

A parallel study was performed with motor neuron-restricted expression of mutant TDP-43^{M337V}. Similar to what was observed with widespread expression of TDP-43^{M337V}, the rats also developed rapid paralysis (reaching endstage 75 days after doxycycline removal on average) upon induction of the mutant transgene. Of note, however, was the reversibility of the phenotype. Rats with surviving motor neurons recovered from motor deficits upon repression of the transgene. Additionally, although end-stage rats showed increased cytoplasmic accumulation of ubiquitin, this was not accompanied by formation of cytoplasmic TDP-43 inclusions. Furthermore, this cytoplasmic ubiquitin accumulation was reversible, as they largely disappeared upon repression of the transgene.

Another group has attempted to test whether the accumulation of cytoplasmic TDP-43 is directly responsible for the development of TDP-43-dependent neurodegeneration, also using a CamKIIa-tTA inducible transgene drive expression of wild-type or a non-disease-linked NLS-deleted mutant (Igaz et al., 2011). Both cytoplasmically-restricted TDP-43 and nuclear TDP-43 were sufficient to induce neuronal loss in this model. Notably, in the presence of nuclear wild-type TDP-43, the authors observed a distinct downregulation of

mouse-TDP-43, consistent with the autoregulation of TDP-43. Furthermore, the authors found that the amount of neurodegeneration correlated best with depletion of nuclear endogenous TDP-43, rather than accumulation of cytoplasmic TDP-43. This downregulation of endogenous TDP-43 has been consistently reported in several transgenic TDP-43 rodent models (Cannon et al., 2012; Polymenidou et al., 2011; Shan et al., 2010; Wegorzewska et al., 2009; Xu et al., 2010), consistent with the autoregulation of TDP-43 that has been reported in cell culture models (Ayala et al., 2011; Polymenidou et al., 2011). In sum, non-rodent and rodent models have illustrated an integral role for TDP-43 in the developing nervous system. Under normal conditions, the levels of TDP-43 are tightly regulated, and it is highly likely that perturbation of this regulation contributes to neurodegeneration. However, the mechanisms through which mutations in TDP-43 contribute to disruption of TDP-43 function remains unresolved.

1.1.9 Cytoplasmic and Nuclear TDP-43 in Disease

Although it is clear that TDP-43 performs a wide variety of functions in the processing and metabolism of RNA, it is of interest that the overwhelming majority of mutations in TDP-43 fall within the glycine-rich C-terminus and not within either of the two RRMs. Several proposals have now been put forward towards the mechanism of toxicity deriving from these mutations. Firstly, purified TDP-43 has been shown to be intrinsically aggregation prone (Johnson et al., 2009b), and mutations in TDP-43 increase both the stability (Ling et al., 2010)

propensity of the protein to aggregate (Johnson et al., 2009b). Furthermore, the C-terminus of TDP-43 has been shown to possess prion-like properties similar to other Q/N-rich domains found in RNA-binding proteins (Alberti et al., 2009; Couthouis et al., 2011; Wang et al., 2012). This prion-like property is not unique to TDP-43, as it has been identified not only in FUS/TLS, which also contains mutations linked to FALS, but for a variety of other human RNA binding proteins (Alberti et al., 2009; Couthouis et al., 2011). The propensity of these related RNA-binding proteins to aggregate has been proposed as one mechanism underlying the initiation and spread of neurodegeneration, not only in ALS but other neurodegenerative disorders as well (King et al., 2012; Polymenidou and Cleveland, 2012).

Secondly, one key finding from biochemical characterization of patient samples was the observation of phosphorylation and production of 20-25 and 35 kDa cleavage products (Arai et al., 2006; Neumann et al., 2006). Exogenous expression of this predicted C-terminal fragment (CTF) has been shown to aggregate and induce toxicity in cell culture (Igaz et al., 2009). Coupled with the prion-like properties associated this region, toxicity derived from production of these aggregation-prone fragments has also been a proposed as a mechanism for neurodegeneration. However, production of these fragments from de novo intranuclear cleavage in cell culture produced fragments that were rapidly degraded. These fragments also only aggregated upon the introduction of already misfolded CTFs or following RNase treatment, suggesting (1) a requirement for a “second hit” for the induction of aggregation (2) that association

with RNA maintains the solubility of these fragments. Coupled with the report that inclusions in SALS patient spinal cords are comprised of what is likely full-length TDP-43 (Igaz et al., 2008), the exact contribution of truncated TDP-43 fragments to neurodegeneration and motor neuron vulnerability remains to be determined.

Although the intrinsic toxicity of aggregated or TDP-43 CTFs has been demonstrated in yeast (Johnson et al., 2009a) or in cell culture (Igaz et al., 2009), emerging evidence from Drosophila (Voigt et al., 2010), C. elegans (Ash et al., 2010), and yeast models (Elden et al., 2010) suggests that full-length TDP-43 is the neurotoxic species, and that retention of the RRMs is also required. Furthermore, although several studies in transgenic rodent models have shown the accumulation of CTFs, these CTFs appear biochemically divergent from what is found in human patients; namely that they are found at higher levels than in human brains, remain largely soluble, and accumulate intranuclearly (Stallings et al., 2010; Tsai et al., 2010; Wegorzewska et al., 2009; Wils et al., 2010; Xu et al., 2010). Furthermore, not all rodent models report the presence of these CTFs despite displaying similar neurodegenerative phenotypes, implying that the formation of CTFs is not required for neurodegeneration (Igaz et al., 2011; Shan et al., 2010). A study examining the relative contributions of cytoplasmic or nuclear TDP-43 found that although both were able to confer toxicity, the toxicity was correlated to the loss of endogenous TDP-43 rather than accumulated cytoplasmic TDP-43 (Igaz et al., 2011). Additionally, the relative scarcity of inclusions in these mice suggests that although cytoplasmic TDP-43 contributes to toxicity, it is not absolutely required for the development of neurodegeneration.

Additional studies defining the relative contributions of dysregulated TDP-43 function and cytoplasmic accumulation of toxic TDP-43 species are certainly required.

1.2 Dissertation Overview

1.2.1 Research History

In 2006, the landmark discovery of the nucleic acid binding protein TDP-43 as the major component of ubiquitinated inclusions found in sporadic ALS and FTLD-U began a paradigm shift in our understanding of ALS pathogenesis. The subsequent discovery of mutations in TDP-43 provided a hint of a converging mechanism underlying the development of both FALS and SALS. As rodent models expressing mutant human SOD1 had proven invaluable to our understanding of potential pathogenic mechanisms underlying familial ALS, the generation of rodent models expressing wild-type and mutant TDP-43 was similarly necessary.

The work presented in this dissertation was therefore aimed at answering the following questions regarding the biology TDP-43 and the functional consequences of mutations therein.

Aim1: Define the functional consequences of expressing wild-type versus mutant TDP-43 in the mammalian CNS

To define the functional consequences of expressing wild-type versus mutant TDP-43 in the mammalian CNS, I selected the strategy of using a heterologous promoter to drive expression of a human cDNA containing either wild-type or either of two ALS-linked mutants, Q331K and M337V. I initially selected the mouse Prion (*Prnp*) promoter, due to its use in previous models of neurodegeneration (Borchelt et al., 1996) and its ability to drive wide and robust expression of transgenes in a variety of cell types in the nervous system (Borchelt et al., 1996; Wang et al., 2005). The primary advantages to this strategy over either a genetic knock-in or the use of the full human gene with accompanying promoter and regulatory regions were (1) the ability to generate a variety of founder lines and (2) the ability to override the endogenous autoregulation of mouse TDP-43 that is abrogated with the use of the human promoter (unpublished results, discussion with S.-C. Ling and D.W. Cleveland). The generation of multiple founders allowed for the selection of multiple lines expressing differing levels of transgene dosage, which facilitated the study of both dosage as well as mutant-dependent effects. With this approach, I have generated a new genetic model that develops mutant-dependent, adult-onset motor deficits that clinically mimics aspects of human ALS.

Aim 2: Define whether toxicity resulting from expression of mutant TDP-43 in the CNS results from gain or loss of normal TDP-43 function, or a combination of both

Although the pathological link between mutations in TDP-43 and ALS has been established, it remains unresolved whether mutations in TDP-43 result in a gain-of-toxic function, or loss of normal function. In collaboration with the Yeo group, I sought to define the molecular consequences of mutations in TDP-43 using a splicing-sensitive microarrays. We selected this strategy as an extension of a previous collaboration between the Cleveland and Yeo groups that defined the normal RNA targets of TDP-43 and the alterations that occur following TDP-43 depletion (Polymenidou et al., 2011). I elected to perform this experiment during an early stage of disease in order to distinguish early alterations in splicing that may contribute to disease pathogenesis from splicing changes that occur as a consequence of the disease process.

Chapter 2 contains the results of Aims 1 and 2, and forms the basis for a manuscript that is currently in preparation for publication.

In Chapter 3, I will discuss future directions and additional strategies in modeling TDP-43-dependent neurodegeneration in rodent models that others may pursue.

Chapter 2: ALS-linked TDP-43 mutations produce aberrant RNA splicing and adult-onset motor disease without aggregation or loss of nuclear TDP-43

2.1 Abstract:

TAR DNA Binding Protein (TDP-43) is the major protein component of ubiquitinated inclusions found in amyotrophic lateral sclerosis (ALS) and frontotemporal lobar degeneration with ubiquitinated inclusions (FTLD-U). Two ALS-causing mutants (TDP-43^{Q331K} and TDP-43^{M337V}), but not wild type human TDP-43, are shown here to provoke age-dependent, mutant-dependent, progressive motor axon degeneration and motor neuron death when expressed in mice at levels and in a cell type selective pattern similar to endogenous TDP-43. Mutant TDP-43-dependent degeneration of lower motor neurons occurs without 1) loss of TDP-43 from the corresponding nuclei, 2) accumulation of TDP-43 aggregates, and 3) accumulation of insoluble TDP-43. Computational analysis using splicing sensitive microarrays demonstrates an augmentation of endogenous TDP-43- dependent alternative splicing changes conferred by both human wild-type and mutant TDP-43^{Q331K}, but with high levels of mutant TDP-43 preferentially enhancing exon exclusion of some target pre-mRNAs affecting genes involved in neurological transmission and function. Comparison to splicing alterations following TDP-43 depletion demonstrates that TDP-43^{Q331K} enhances normal TDP-43 splicing function for some targets but loss of function for others. Thus, adult onset motor neuron disease does not require aggregation or loss of

nuclear TDP-43, with ALS-linked mutants producing loss and gain of splicing function of selected RNA targets at an early disease stage.

2.2 Introduction

Amyotrophic lateral sclerosis (ALS) and frontotemporal lobar degeneration with ubiquitinated inclusions (FTLD-U) are progressive, adult-onset neurodegenerative diseases with overlapping clinical and pathological features (Da Cruz and Cleveland, 2011; Liscic et al., 2008; Lomen-Hoerth et al., 2002). ALS is characterized by the selective loss of upper and lower motor neurons leading to progressive fatal paralysis and muscle atrophy. A large majority (~90%) of ALS and FTLD-U cases are without a known genetic cause. Importantly, in these sporadic cases, the appearance of ubiquitinated inclusions within the affected neurons of the nervous system characterizes both ALS and FTLD-U patients, suggesting an overlapping mechanism underlying both diseases. Biochemical characterization of brains and spinal cords from ALS and FTLD-U patients identified TAR DNA Binding Protein (TDP-43) as the major protein component of these ubiquitinated inclusions (Arai et al., 2006; Neumann et al., 2006). The discovery of ALS-linked mutations in the glycine-rich C-terminal domain of TDP-43 (Gitcho et al., 2008; Kabashi et al., 2008; Sreedharan et al., 2008) demonstrated a pathological role of TDP-43 in both diseases. The subsequent identification of mutations in a structurally and functionally related nucleic acid binding protein, FUS/TLS (fused in sarcoma/translocated in

liposarcoma) (Kwiatkowski et al., 2009; Vance et al., 2009), further implicated defects in RNA processing in ALS pathogenesis.

TDP-43 is a multi-functional nucleic acid binding protein. Within the nervous system, TDP-43 binds to >6,000 pre-mRNAs and affects the levels of ~600 mRNAs and the splicing patterns of another 950 (Polymenidou et al., 2011). Structurally, the 414 amino acid protein consists of two RNA recognition motifs (RRM1 and RRM2) (Buratti et al., 2001; Ou et al., 1995), nuclear import and export signal (Winton et al., 2008), and a glycine-rich region implicated in protein-protein interactions (Ayala et al., 2005; Wang et al., 2004) that include components of the RNA splicing machinery (Buratti et al., 2005; D'Ambrogio et al., 2009).

Disruption in mice of the highly conserved *Tardbp* gene is embryonically lethal (Chiang et al., 2010; Kraemer et al.; Sephton et al., 2009; Wu et al., 2010). Similarly, post-natal inactivation of *Tardbp* (by Cre recombinase-mediated gene excision encoded by an ubiquitously-expressed CAG-Cre transgene) results in rapid postnatal death accompanied by defects in fat metabolism (Chiang et al., 2010). TDP-43 autoregulates its own RNA level (Ayala et al., 2011; Polymenidou et al., 2011) at least in part by stimulating excision of an intron in its 3' untranslated region thereby making the spliced RNA a substrate for non-sense mediated RNA degradation (Polymenidou et al., 2011). Furthermore, transgenic rodent models have been used to demonstrate that overriding the autoregulatory mechanism by overexpression of unregulated wild-type (Igaz et al., 2011; Shan et al., 2010; Tsai et al., 2010; Wils et al., 2010; Xu et al., 2010) or disease-linked

mutant (Cannon et al., 2012; Huang et al., 2012; Stallings et al., 2010; Swarup et al., 2011a; Wegorzewska et al., 2009; Wils et al., 2010; Xu et al., 2010; Xu et al., 2011; Zhou et al., 2010) TDP-43 transgenes can produce neurodegeneration in mice.

ALS and FTLD-U patient brain and spinal cord samples are characterized by the accumulation of cytoplasmic TDP-43 aggregates accompanied by a distinct clearing of nuclear TDP-43 within affected neurons and glia (Igaz et al., 2008; Van Deerlin et al., 2008), implicating possible loss of nuclear TDP-43 function in disease pathogenesis. In human disease, TDP-43 has been reported to be abnormally phosphorylated, ubiquitinated and cleaved to produce C-terminal fragments (Arai et al., 2006; Arai et al., 2010; Neumann et al., 2009; Neumann et al., 2006). Ectopic expression of these C-terminal fragments in cell culture models (Igaz et al., 2009; Zhang et al., 2009; Zhang et al., 2007) has shown that they are aggregation-prone and confer an intrinsic toxicity. However, the extent of the contribution of these C-terminal fragments to disease pathogenesis is undetermined. Indeed, double immunofluorescent labeling of ALS patient spinal cords using N-terminal specific and C-terminal specific antibodies suggests that inclusions in spinal cord motor neurons are comprised primarily of full-length TDP-43 (Igaz et al., 2008). Importantly, retention of RNA-binding by full-length TDP-43 has been demonstrated to be required for toxicity in yeast, fly, and C. elegans models (Ash et al., 2010; Elden et al., 2010; Johnson et al., 2008; Voigt et al., 2010).

Nevertheless, it remains unresolved whether toxicity to motor neurons from mutations in TDP-43 is mediated through a gain of toxic property, loss of function, or a combination of both. By generation of transgenic mice encoding levels of wild-type or mutant human TDP-43 comparable to endogenous TDP-43, we demonstrate mutant-dependent, age-dependent motor neuron disease from ALS-linked TDP-43 mutants in the absence of overexpression, cytoplasmic accumulation of a 35 kD TDP-43 fragment, or insoluble TDP-43 aggregates. Accompanying autoregulation-mediated reduction of endogenous wild type TDP-43 are splicing alterations previously identified to be TDP-43 dependent (Polymenidou et al., 2011). Additional splicing alterations are identified by systematic genome-wide analyses of alternative splicing that are indicative of enhancement or loss of function by the TDP-43 mutants for individual RNA substrates, from which we conclude that ALS-linked mutations confer both loss and gain of function properties to TDP-43 and that these act intranuclearly to induce splicing alterations that can underlie age-dependent motor neuron disease.

2.3 Results

2.3.1 Generation and establishment of “floxed” TDP-43 transgenic mice expressing wild-type and mutant TDP-43 broadly in the central nervous system

Transgenic mice were produced that express either wild type or ALS-linked mutant TDP-43 broadly throughout the central nervous system using the murine prion-promoter (Borchelt et al., 1996) previously reported to drive transgene expression most abundantly in the central nervous system, both in neurons and astrocytes (Wang et al., 2005). cDNAs encoding wild-type or either of two ALS-linked mutants of TDP-43 (Sreedharan et al., 2008) [Q331K (glutamine to lysine substitution at amino acid position 331) and M337V (methionine to valine substitution at amino acid position 337)] were fused to an N-terminal myc-tag under control of the murine prion promoter (Figure 2.1A). From >20 founders for each gene, three lines were selected and established for TDP-43$^{\text{Wild-Type}}$, TDP-43$^{\text{Q331K}}$, and TDP-43$^{\text{M337V}}$, respectively.

Analysis of whole tissue lysates by immunoblotting with a polyclonal anti-TDP-43 antibody recognizing recombinant mouse and human TDP-43 protein with equal affinity confirmed that transgene expression was confined primarily to the brain and spinal cord, with very low to no expression in some other tissues (Figure 2.1B). Immunoblotting and qRT-PCR of whole brain extracts or total RNAs, respectively, identified level of transgene expression for each of the nine lines (Figure 2.8). Analysis of cortex and spinal cord identified lines expressing comparable levels of human TDP-43 mRNA, ranging from 1x to 1.5x the level of endogenous TDP-43 in non-transgenic mice, which was recapitulated in the accumulated protein levels from whole brain and spinal cord lysates (Figure 2.1C, D, and Figure 2.8A). Immunofluorescent staining with myc antibody to detect human TDP-43 showed that it accumulated in neurons and glia of the spinal cord

(Figure 2.1E) in a pattern that mimicked the endogenous expression pattern of TDP-43. For in-depth analysis, four lines mice were selected in which wild-type TDP-43, TDP-43^{M337V} or TDP-43^{Q331K} were accumulated to levels comparable to endogenous TDP-43 in non-transgenic mice, as well as one line with a lower level (referred TDP-43$^{Q331K\text{-}low}$).

2.3.2 Mice expressing mutant human TDP-43 develop adult-onset motor deficits and hindlimb weakness

In order to determine whether expression of mutant human TDP-43 at levels comparable to endogenous TDP-43 in normal mice is sufficient to produce mutant-specific clinical phenotypes, we examined mice expressing wild-type TDP-43, both moderate and low levels of TDP-43^{Q331K} (referred to as TDP-43^{Q331K} and TDP-43$^{Q331K\text{-}low}$), and TDP-43^{M337V}. At birth, mice expressing wild-type human TDP-43 or either TDP-43 mutant were indistinguishable from their non-transgenic littermates. However, in contrast to their non-transgenic littermates or TDP-43$^{Wild\text{-}Type}$ mice, TDP-43^{Q331K} transgenic mice developed a tremor at as early as three months of age (Figure 2.9A). This tremor worsened with aging and was accompanied by the development of hindlimb clasping indicative of spastic motor impairment (Igaz et al., 2011; Yazawa et al., 2005) (Figure 2.9B).

Motor performance of TDP-43$^{Wild\text{-}Type}$, TDP-43$^{Q331K\text{-}Low}$, TDP-43^{Q331K}, and TDP-43^{M337V} mice was followed during aging. Motor performance (on an accelerating rotarod) was normal at the earliest times points analyzed in each of

the mutant TDP-43 expressing lines (Figure 2.2A, B). In contrast with non-transgenic and TDP-43$^{Wild\text{-}Type}$ mice, all three mutant TDP-43 lines developed significant age-dependent motor deficits by 10 months of age, with the deficit most severe and developing at the earliest age (3 months) in the higher expressing TDP-43^{Q331K} line (Figure 2.2B). A significant decrease in hindlimb grip strength by 10 months of age accompanied age-dependent motor impairment in TDP-43^{Q331K} animals (Figure 2.2C). Analysis of animals at later time points (e.g., after 17 months of age) showed no further exacerbation of motor impairment (2.10A), indicating a window of adult onset, active degeneration up to 10 months of age, after which there is little further worsening of motor phenotype despite continued transgene accumulation in the remaining motor neurons and surrounding glia (see below, Figure 2.5).

To determine whether the motor deficits and hindlimb weakness observed in TDP-43^{Q331K} transgenic mice were accompanied by neuromuscular abnormalities similar to those clinically observed in human patients, we performed electrophysiological analyses on TDP-43$^{Wild\text{-}Type}$ and TDP-43^{Q331K} transgenic mice (Figure 2.3A). Resting electro-myographic (EMG) recordings from the gastrocnemius muscle (i.e., in the absence of any stimulus in isoflurane-anesthetized animals). As expected, in SOD1^{G37R} symptomatic mice that will go on to develop fatal paralytic disease, high frequency fibrillations (spontaneous firings of the motor units) were recorded (Figure 2.3B - v), consistent with the known widespread denervation. Recordings in TDP-43^{Q331K} mice (Figure 2.3B – iii) revealed the presence of muscle fibrillations similar to those observed in

presymptomatic SOD1^{G37R} mice (Figure 2.3B – iv), indicating neuromuscular denervation and motor unit degeneration and regeneration. These spontaneous firings were mutant TDP-43-dependent, as recordings in non-transgenic and expression matched TDP-43$^{Wild\text{-}Type}$ mice (Figure 2.3B, i and ii) lacked such spontaneous EMG activity.

As both upper and lower motor neuron deficits can develop in ALS patients, we tested if the spontaneous EMG activity associated with neuromuscular denervation observed in TDP-43^{Q331K} mice was accompanied by upper motor neuron deficits. To this end, myogenic motor evoked potentials (MMEPs), which report a measure of connectivity of the entire neuromuscular unit, including the motor cortex, inter-neurons, a-motorneurons and the neuromuscular junction, were recorded from the gastrocnemius muscle after electrical stimulation of the motor cortex (Figure 2.3C). Use of this measure in SOD1^{G37R} mice revealed that, as expected, MMEPs were decreased (from ~2.4 mV in non-transgenic animals) to 1.5 mV at pre-symptomatic stages and were almost completely lost in symptomatic SOD1^{G37R} mice (0.03 mV). TDP-43^{Q331K} transgenic mice also developed significant decreases (to 0.18 mV; n=3) in MMEP amplitude (Figure 2.3C) compared to non-transgenic (2.4 mV; n=4) and TDP-43$^{Wild\text{-}Type}$ transgenic mice (1.8 mV; n=3), indicating a disruption of the neuromuscular unit.

To determine whether the decrease in MMEPs reported above involved disruption of the connectivity between the upper and lower motor neurons, spinal cord motor evoked potentials (MEPs) were then recorded from the dorsal surface

of an exposed thoracic (T12) segment after electrical stimulation of the motor cortex. MEPs consist of multiple waves, with the two earliest peaks (N1, N2) corresponding to the activation of the extrapyramidal system. No significant differences were found in the amplitude of the N1 wave when comparing non-transgenic (0.20 mV; n=4), TDP-43$^{Wild\text{-}Type}$ (0.21 mV; n=5) and TDP-43^{Q331K} transgenic mice (0.20 mV; n=4) (Figure 2.3D). Quantification of immunofluorescently-labeled Ctip2-positive upper motor neurons in cortex layer V in TDP-43^{Q331K} transgenic animals showed no loss of upper motor neurons, consistent with the retention of upper motor neuron function indicated by the persistence of cortical MEPs (Figure 2.11A). Therefore, spontaneous muscle firing recorded using EMGs, accompanied by decreased MMEP amplitudes, must reflect motor dysfunction associated primarily with lower motor neuron degeneration in TDP-43^{Q331K} mice.

2.3.3 TDP-43^{Q331K} transgenic mice develop age-dependent motor neuron disease, including motor neuron loss and motor axon degeneration

Having observed the development of motor deficits and electrophysiological abnormalities, we examined the central nervous system for signs of neurodegeneration. Immunofluorescent staining for the astrocytic marker GFAP and the microglial marker Iba-1 revealed immunoreactive astrocytes and infiltrating microglia (Figure 2.11B) in the ventral horn of the spinal cord in 10-12 month old TDP-43^{Q331K} transgenic mice. Consistent with the initial identification of the Q331K mutation in an ALS patient with classic lower motor neuron

involvement (Sreedharan et al., 2008), quantification of choline acetyl-transferase (ChAT)-positive lower motor neurons in lumbar spinal cords from TDP-43^{Q331K} mice revealed a significant, age-dependent decrease ($p=0.04$, $n=3$) in motor neuron number. Loss of motor neurons initiated prior to 2 months of age and continued until about 12 months of age, yielding a reduction of ~35% when compared to age-matched non-transgenic or TDP-43$^{Wild\text{-}Type}$ transgenic animals (Figure 2.4A). Additionally, the milder motor deficits seen by 10-12 months of age in both TDP-43$^{Q331K\text{-}Low}$ and TDP-43^{M337V} mice were accompanied by a trend in age-dependent reduction in ChAT-positive motor neurons compared with non-transgenic or TDP-43$^{Wild\text{-}Type}$ transgenic animals in the ventral lumbar horns at 10-12 months of age (Figure 2.4A).

Quantification of axons remaining in the fifth lumbar (L5) roots of TDP-43^{Q331K} transgenic mice revealed a significant reduction (623 versus 923 in non-transgenic, ***$p<0.001$) of total motor axons by 10-12 months of age (Figure 2.4B), with the most significant reduction in large caliber a-motor axons (>3.5 mm) that innervate muscle (Ilieva et al., 2008) (Figure 2.4C). Morphological examination of the remaining motor axons revealed the presence of degenerating axons, characterized by the appearance of vacuolization and myelin defects (Figure 2.4D). Similar to what was demonstrated behaviorally, there was no further loss of L5 motor axons at 20 months of age (Figure 2.10B-D), indicating a period of active degeneration up to 10 months of age.

We therefore focused our remaining analyses within this disease period. Morphological examination of hematoxylin and eosin (H&E) stained sections of

gastrocnemius muscle from 10 month old TDP-43^{Q331K} animals revealed regions of damaged muscle fibers and regions of regeneration characterized by the appearance of centralized nuclei (Figure 2.4E). TDP-43$^{Wild\text{-}Type}$, TDP-43$^{Q331K\text{-}low}$ and TDP-43^{M337V} animals lacked similar morphological abnormalities in the muscle fibers. Neuromuscular junctions (NMJs) in TDP-43^{Q331K} mice appeared malformed with an abnormal bleb-like appearance (Figure 2.4F). Quantification of post-synaptic NMJs using a-bungarotoxin staining of the gastrocnemius muscle revealed a significant (30% reduction; p=0.02) in the number of neuromuscular junction endplates in of TDP-43^{Q331K} mice (Figure 2.4G). In contrast, TDP-43$^{Wild\text{-}Type}$, TDP-43$^{Q331K\text{-}Low}$and TDP-43^{M337V} transgenic mice displayed numbers of a-bungarotoxin-positive neuromuscular junction endplates that were not significantly different from non-transgenic animals.

2.3.4. Cytoplasmic mislocalization of TDP-43 is not required for the development of motor neuron dysfunction

A primary pathological feature in ALS patients is the accumulation of cytoplasmic, ubiquitinated and insoluble TDP-43-containing aggregates within the neurons of the nervous system (Neumann et al., 2006). To test whether the development of motor neuron disease was accompanied by a similar alteration in TDP-43 localization, we first performed nuclear and cytoplasmic fractionation of whole spinal cord and brain from 10-12 month old TDP-43 transgenic mice (Figure 2.5A). Immunoblotting for mouse and human TDP-43 in enriched fractions from either cytoplasm (Figure 2.5B, D) or nuclei (Figure 2.5C, E)

derived from cortex or spinal cord revealed that the majority of human TDP-43 remained in the nuclear fraction just as it did in non-transgenic animals (Figure 2.5C, E). Examination of longer exposures revealed a similarly small proportion of both endogenous mouse and human TDP-43 fractionated within the cytosol.

Immunofluorescent staining in lumbar spinal cord sections of TDP-43^{Q331K} mice from two to 10 months of age revealed that the majority of mutant TDP-43 remained nuclear throughout (Figure 2.5F). Additionally, analysis of sequential biochemical extraction using high-salt and urea buffers revealed that the majority of both mouse and human TDP-43 was extracted in the high-salt soluble fraction (Figure 2.12B and C). Analysis for non-transgenic and all transgenic lines of a final extraction of the nuclear pellets with SDS demonstrated that only a small fraction (Figure 2.12D) of human and endogenous mouse TDP-43 was in an initially insoluble form that could be solubilized with SDS.

2.3.5 Widespread splicing changes from altered TDP-43 levels within the CNS

To evaluate if normal patterns of alternative splicing were disrupted upon reduction of mouse TDP-43 and its replacement with wild type or mutant human TDP-43 at or above the level of mouse TDP-43 in normal mice, RNA extracted from cortices of two month old non-transgenic, TDP-43$^{Wild\text{-}Type}$, TDP-43^{Q331K}, and TDP-43$^{Q331K\text{-}low}$ transgenic mice were examined using Affymetrix splicing sensitive microarrays (Figure 2.6A). Analysis of splicing changes in cortices of TDP-43$^{Wild\text{-}Type}$, TDP-43^{Q331K}, and TDP-43$^{Q331K\text{-}Low}$ revealed that 824, 1195, and

208 exons, respectively, were differentially spliced relative to mRNA from non-transgenic mice, using a statistical threshold that captured as many significant changes as possible (absolute separation score of < 0.3) (Du et al., 2010; Sugnet et al., 2006) (Figure 2.6A).

To gain insight into the effects of expressing human TDP-43 proteins on endogenous mouse TDP-43 targets, we focused on the largest represented class of alternative splicing events, namely cassette exons (i.e., exons that can be included or excluded in the final mRNA [white slice of pie charts, Figure 2.6A]). For comparison, we reanalyzed our previous splicing array data (Polymenidou et al., 2011) using a consistent threshold (absolute separation score of < 0.3), identifying 737 cassette exons that were alternatively spliced upon depletion of endogenous mouse TDP-43 in the central nervous system (Figure 2.13). These exons that are normally regulated by TDP-43 levels were then compared with the 314, 533, and 97 cassette exons that were misregulated in human TDP-43$^{\text{Wild-Type}}$, TDP-43$^{\text{Q331K}}$, and TDP-43$^{\text{Q331K-Low}}$ transgenic animals.

To determine if misregulated exons were associated with endogenous TDP-43 binding (as measured by cross-linking and immunoprecipitation followed by deep sequencing (Polymenidou et al., 2011)) we separated the 737 exons into “direct” (175, that contained TDP-43 binding sites within 2 kb of the exon) and “indirect” (562 without TDP-43 binding sites near the exon) targets (Figure 2.6B). Notably, when comparing the percentages of direct and indirect targets that overlapped with TDP-43$^{\text{Q331K}}$-dependent misregulated exons, we observed a statistically significant ($p<0.0005$ by chi-square analysis) 1.8 fold-enrichment of

direct targets (26% (45/175) compared to indirect ones (14% (81/562)). A similar (2.4 fold) enrichment was seen for altered splicing of direct targets in TDP-$43^{Q331K\text{-}Low}$ (6% of direct targets (11/175) compared to 2.6% of indirect targets (15/562)). No significant enrichment was seen in a similar comparison for TDP-$43^{Wild\text{-}Type}$ (9% (16/175) to 7% (39/562)) (Figure 2.6C). Thus, the human mutant transgenes preferentially affect direct, endogenous TDP-43-dependent alternative splicing events.

To test whether the transgene-affected splicing changes for cassette exons reflected a loss or gain of normal TDP-43 function, we compared the directionality of changes of these exons when TDP-43 was depleted relative to the expression of the human protein (Figure 2.6D, i-vi). Of the cassette exon splicing changes observed in the TDP-43 transgenic mice, we found that 53 of 314 in TDP-$43^{Wild\text{-}Type}$ (Figure 2.6D, i-ii), 126 of 533 in TDP-43^{Q331K} (Figure 2.6D, iii-iv), and 26 of 97 TDP-$43^{Q331K\text{-}Low}$ (Figure 2.6D, v-vi) overlapped with cassette exon changes identified following TDP-43 depletion. For directly bound exon targets whose splicing was altered by expression of human TDP-43, the majority of the affected cassette exons overlapping with direct targets were changing in a direction opposite to loss of TDP-43 (TDP-$43^{Wild\text{-}Type}$ [13 of 16], TDP-43^{Q331K} [35 of 45], TDP-$43^{Q331K\text{-}Low}$ [10 of 11]) (in gray, Figure 2.6D, i, iii, and v). Furthermore, at higher TDP-43^{Q331K} levels (and corresponding strong reduction in endogenous mouse TDP-43), splicing of 35 of 45 directly bound cassette exons (Figure 2.6D, iii) changed in a manner consistent with an *elevated* normal function of endogenous mouse TDP-43 (the opposite of TDP-43 depletion).

In other words, cassette exons whose inclusion (or exclusion) was previously shown to be dependent on mouse TDP-43 were more included (or excluded) when human TDP-43^{Q331K} was expressed, consistent with this mutant retaining normal (or enhanced) TDP-43 activity. Nevertheless, in TDP-43^{Q331K} mice, ten direct exon targets were altered in a manner indicative of a *reduction* in endogenous TDP-43 function in regulating the splicing of these TDP-43 target exons (Figure 2.6D, iii), demonstrating that human TDP-43 protein even at high level of expression cannot replace the endogenous mouse TDP-43 for the splicing of these exons.

Exons whose splicing was reported altered by microarray analysis, as well as ones of biological interest but were not represented on the array, were then analyzed by semi-quantitative RT-PCR (Figure 2.6E-F and Table 2.1). To identify and /or validate splicing changes that are specifically affected by ALS-linked mutant of TDP-43, we focused on changes occurred only in both TDP-43^{Q331K} and TDP-43$^{Q331K\text{-}Low}$-transgenic mice, but not in TDP-43$^{Wild\text{-}Type}$ mice (whose accumulated transgene level is similar to that of TDP-43$^{Q331K\text{-}Low}$ transgenic mice). Within these, *Kncip2, Taf1b and Eif4h* changed uniquely in response to the presence of mutant TDP-43 (Figure 2.6E, Table 2.1). Furthermore, consistent with the directionality of splicing changes observed by microarray (Table 2.1), we found that targets that changed uniquely in the presence of the TDP-43^{Q331K} mutant displayed splicing changes consistent both with enhanced normal function (i.e., *Eif4h and Taf1b,* whose exons were more excluded, in contrast to increased inclusion in TDP-43 depletion), as well as loss of normal function

(*Kcnip2;* whose exons were more excluded as in the case of TDP-43 depletion), demonstrating that TDP-43^{Q331K} mutant confers both loss and gain of normal TDP-43 function in splicing regulation.

Additionally, splicing changes in a purely human TDP-43 dose-dependent manner (Figure 2.6F; *Sort1, Ttc3, Kcnd3, Atxn2, and Ahi1*) were also identified, revealing both retention of normal or enhanced function for some RNA substrates and reduced function for others (Figure 2.6F, Table 2.1). Within the exons that overlapped with those that changed upon TDP-43 depletion, we found that these exons primarily displayed a dose-dependent pattern of splicing in the opposite direction to what occurs after TDP-43 depletion (Figure 2.6F, *Sort1* and *Ttc3,* whose exons were more excluded, in contrast to more included in TDP-43 depletion; Table 2.1).

These findings were confirmed globally by a genome-wide analysis of direct TDP-43 targets whose exons were included or excluded upon human TDP-43 expression (Figure 2.6G). On average, ~20% of unaffected exons represented on the array were direct targets (green line in Figure 2.6G). However, when focusing on alternatively changing cassette exons, we found an overall increase in the percentages of direct TDP-43 targets (~43%, TDP-43^{Q331K} and TDP-43$^{Wild-Type}$; up to 53% in TDP-43$^{Q331K-low}$) that were excluded in the presence of the human TDP-43 protein compared with only ~20% of the included exons (Figure 2.6G, ii). Surprisingly, 39% of excluded exons in the TDP-43^{Q331K} animals not previously demonstrated as regulated by endogenous TDP-43 depletion were also direct targets (Figure 2.6G, iii). That is, some exons that were unchanged

following TDP-43 depletion displayed a dose-dependent pattern of splicing in the direction of enhanced exclusion in the presence of the human TDP-43 (Figure 2.6F, Table 2.1, *Atxn2 and Ahi1,* whose exons were more excluded, in contrast to no change upon TDP-43 depletion). This supports a hypothesis that certain exons, although bound by TDP-43, are only misregulated upon elevation of wild-type or mutant TDP-43, but are not altered upon its loss. In other words, elevation or enhancement of TDP-43 activity through dose or mutation produces aberrant splicing events separate from those resulting from loss of TDP-43.

2.3.5 Mutant-specific splicing alterations accompany motor neuron disease development

Having identified that the human transgenes cause both loss and gain of normal function, we focused on alternative splicing changes within the spinal cord, the tissue that harbored the degenerative phenotype. RNA extracted from the spinal cords of 2 month old non-transgenic, TDP-43$^{\text{Wild-Type}}$ and TDP-43$^{\text{Q331K}}$ animals prior to the onset of significant motor dysfunction were analyzed on the same splicing sensitive microarrays (Figure 2.7A). We identified 4462 and 4399 alternative splicing events in the TDP-43$^{\text{Wild-Type}}$ and TDP-43$^{\text{Q331K}}$ spinal cord conditions, respectively, 4 to 5 times greater than the events observed in the cortex (Figure 2.7A). Approximately 38% of changes in TDP-43$^{\text{Wild-Type}}$ cortex (118) and 42% of changes observed in TDP-43$^{\text{Q331K}}$ (226) and were also present in the spinal cord (Figure 2.7B). Notably, with the exception of a cassette exon within the *Kctd9* gene, altered splicing of all 1,060 cassette exons that

overlapped between spinal cord in TDP-43$^{Wild\text{-}Type}$ and TDP-43^{Q331K} mice occurred in the same direction, demonstrating that at least for this subset of RNA targets the mutant remains functionally similar to wild-type TDP-43 (Figure 2.7C).

Use of semi-quantitative RT-PCR validated a set of splicing changes that were consistent with those identified in the cortex (Figure 2.7D and Table 2.2), again demonstrating that TDP-43^{Q331K} mutant confers both loss and gain of normal TDP-43 function. Furthermore, among the 419 splicing events unique in TDP-43^{Q331K} spinal cord were several RNAs whose encoded proteins are involved in neurological function and transmission (Table 2.3), including the synaptic cell-adhesion molecules neurexins 1 and 3 (*Nrxn1* and *Nrxn3*), protein phosphatase 3 (also known as calcineurin (*Ppp3ca*)), and glutamate receptor 2 (*Gria2,* encoding GluR2), which has been proposed to modify motor neuron vulnerability to excitotoxicity (Pizzi et al., 2000; Van Damme et al., 2007; Van Damme et al., 2005). In contrast, the 394 events unique to the TDP-43$^{Wild\text{-}Type}$ spinal cord condition did not include a similar representation from genes involved in neurological function.

2.4 Discussion

Although previous *in vivo* studies using transgenic rodent models (Shan et al., 2010; Tsai et al., 2010; Wegorzewska et al., 2009; Wils et al., 2010; Xu et al., 2010; Zhou et al., 2010) have established that elevated levels of both wild-type and mutant TDP-43, or complete absence of wild-type TDP-43 (Wu et al., 2012), can be inherently toxic to neurons, it had not been determined (1) whether

toxicity from high levels of TDP-43 (mutant or wild type) reflects the toxicity arising in disease pathogenesis in ALS or FLTD, where TDP-43 when expressed at or near normal levels, (2) whether toxicity is mediated through a loss of TDP-43 function or a gain of aberrant toxic property, and (3) whether mutations in TDP-43 affect normal TDP-43 function.

Our generation and analysis of mice expressing wild-type or ALS-linked mutants in TDP-43 at moderate levels (1 -1.5x the normal level of endogenous mouse TDP-43) has revealed that mutant TDP-43 can provoke lower motor neuron disease in a mutant-dependent, age-dependent, dose-dependent manner. Further, toxicity proceeds (1) with loss of endogenous TDP-43 (whose abundance is reduced by TDP-43 autoregulation), (2) without loss of nuclear human TDP-43, and (3) without mutant TDP-43 re-distribution or aggregation within the nucleus or cytoplasm, and (4) without accumulation of a truncated portion of mutant TDP-43. Our findings are supported by evidence from a prior study (Igaz et al., 2011) wherein neurodegeneration correlated not with cytoplasmic accumulation of human TDP-43 but rather with nuclear loss (from autoregulation) of endogenous mouse TDP-43 in the presence of either wild-type human TDP-43 or a TDP-43 variant not found in human disease but containing a mutation in a residue of its nuclear localization sequence.

Through expression of a moderate amount of human wild-type or mutant TDP-43 in the central-nervous system in a pattern that mimics endogenous TDP-43 within neuronal and glial cells, we have demonstrated a mutant TDP-43-dependent contribution to adult-onset motor deficits. Both TDP-43$^{Q331K\text{-}low}$ and

TDP-43^{M337V} mice developed motor deficits by 10 months of age, albeit without further exacerbation of the disease at later ages, whereas mice expressing comparable levels of human wild-type TDP-43 remained phenotypically normal. Furthermore, this motor phenotype was dose-dependent in relation to the amount of human TDP-43, as animals expressing a higher proportion of TDP-43^{Q331K} (and correspondingly lower amount of mouse TDP-43) developed much more severe motor deficits, electrophysiological abnormalities characteristic of lower motor neuron disease, and loss of approximately 35-40% of lower motor neurons and axons. Thus, motor neuron disease can initiate without robust overexpression of human TDP-43. Additionally, analysis of these mice has demonstrated that, despite the development of lower motor neuron disease, these mice lack significant alterations in either the biochemical solubility or nuclear localization of human and mouse TDP-43, contrary to what has been reported in human patients. Together, these data demonstrate that neither insoluble TDP-43 species nor the abnormal accumulation of cytosolic or nuclear TDP-43 is required for the development of lower motor neuron disease.

Rather, systematic genome-wide splicing array and computational analyses have revealed that nearly complete replacement of endogenous TDP-43 with human TDP-43 is accompanied by widespread changes in alternative pre-mRNA splicing, with some changes reflecting an “enhancement of normal function” that is exacerbated by increased accumulation of TDP-43. Furthermore, we find that a subset of splicing changes is uniquely dependent on the TDP-43^{Q331K} mutant protein. Within these mutant-dependent changes, we also find

widespread splicing alterations, with many of the changes reflecting an enhancement of normal function (despite the almost complete replacement of endogenous mouse with human TDP-43), while others are characteristic of TDP-43 loss of function. Hence, the TDP-43^{Q331K} mutant confers both gain and loss of function properties, both of which are associated with mutant-dependent motor neuron disease. Additionally, the high overlap in splicing alterations in both TDP-43$^{Wild\text{-}Type}$ and TDP-43^{Q331K} spinal cord further emphasizes that the TDP-43^{Q331K} mutant remains functionally similar to its wild-type counterpart. Nevertheless, the TDP-43^{Q331K} mutation also produces a subset of unique splicing alterations within the spinal cord, specifically in genes involved in neurological function.

The dependency of some splicing events solely on the level of human TDP-43 - wild-type or mutant (i.e., *Sort1*) - highlights a sensitivity in TDP-43-dependent splicing to levels of accumulated TDP-43 protein. Depletion of endogenous mouse TDP-43 has been demonstrated to have widespread effects on both splicing and levels of mRNAs in the central nervous system (Polymenidou et al., 2011). Our work here demonstrates that an increase in accumulated TDP-43 protein affects splicing just as broadly, results consistent with TDP-43's previously observed role in exon repression in the nervous system (Polymenidou et al., 2011). Together, we propose that maintenance of a homeostatic level of TDP-43 protein is critical for its splicing function in the central nervous system, and that disruption of this level produces widespread aberrant alternative splicing events.

Although it has been demonstrated that TDP-43 itself is intrinsically

aggregation prone (Johnson et al., 2009a) and contains prion-like properties within its C-terminus (Cushman et al., 2010; Fuentealba et al., 2010; Wang et al., 2012), we have found that motor neuron disease develops in the TDP-43 mutant expressing mice without detectable TDP-43 aggregation. Further, the TDP-43 C-terminus has been proposed by others to play a role in association with other proteins in splicing of target genes (Ayala et al., 2005; Buratti et al., 2005; D'Ambrogio et al., 2009; Zhang et al., 2012), although the contribution of mutations in the C-terminus to the disruption of TDP-43 splicing function was not well understood. Indeed, a study using a human cell culture model expressing TDP-43^{Q331K} and TDP-43^{M337V} found that mutations in the TDP-43 C-terminus do not alter the composition of complexes of known TDP-43-interacting hnRNPs, nor the splicing of a CFTR-based splicing reporter (D'Ambrogio et al., 2009). In contrast, using a true *in vivo* context in mice that develop progressive motor neuron disease, we have found widespread splicing alterations in the adult mammalian central nervous system in the presence of nuclear, mutant TDP-43. Furthermore, these splicing alterations occur at an early disease-stage (2-3 months of age). Thus, nuclear loss or cytoplasmic TDP-43 accumulation is not a requirement for the initiation of neurodegeneration.

Finally, our systematic splicing analysis enables us to propose a molecular model for human TDP-43 function in which it drives: (1) dosage-enhanced increases in exon exclusion of normal endogenous mouse TDP-43 targets, (2) mutant-enhanced increases in exon exclusion of normal TDP-43 targets, and (3) mutant-specific decreases in exon exclusion, due to a loss of function on normal

TDP-43 targets (Figure 2.7E). Taken together, the unique splicing changes in TDP-43^{Q331K} transgenic mice within genes in spinal cords encoding proteins involved in neuronal functions provide a molecular basis for selective vulnerability of motor neurons to such mutants.

2.5 Materials and Methods

Generation of transgenic mice expressing floxed wild-type and mutant human TDP-43:

cDNAs containing N-terminal myc-tagged full length wild-type or mutant (Q331K or M337V) TDP-43 were amplified by PCR to insert flanking SalI digestion sites.The resulting products were digested by SalI and cloned into the XhoI insertion site of the MoPrP.XhoI vector (ATCC #JHU-2). The resultant MoPrP.XhoI-^{myc}huTDP-43 construct was then digested upstream of the minimal PrP promoter and downstream of the final PrP exon 3 using BamHI and NotI and subcloned into a shuttle vector containing loxP flanking sites. (Figure 2.1A) The final construct was then linearized using XhoI, injected into the pro-nuclei of fertilized C57Bl6/C3H hybrid eggs and implanted into pseudopregnant female mice. After obtaining multiple founder mice, lines displaying comparable levels of mutant or wild-type transgene accumulation were selected and backcrossed to C57Bl6 to establish the lines detailed in this paper. The mice used for analysis were backcrossed to C57Bl6 for a minimum of four generations. Transgenic mice were genotyped using the following primers: 5'-AGA GGT GTC CGG CTG GTA

G-3’ and 5’-CCT GCA CCA TAA GAA CTT CTC C-3’ (expected product size: 228 bp).

RT-qPCR and Immunoblotting:

Total RNA from half of the mouse spinal cord was isolated using Trizol (Invitrogen) extraction and prepared for reverse transcription according to manufacturer’s instructions. Real time quantitative PCR for mouse and human TDP-43 was performed on 40ng of total cDNA using the iQSYBR Green supermix (Bio-Rad) with the iCycler iQ detection system according to manufacturer's instructions. Mus musculus ribosomal protein S9 (Rps9, NM_029767) and actin gamma subunit protein (Actg1, NM_009609) genes were also measured as endogenous references across all experimental conditions. The protein fraction from each Trizol sample was then isolated and equal volumes (12 μl) were loaded on gels containing 12% polyacrylamide for SDS-PAGE. Following transfer to nitrocellulose membranes overnight at constant voltage (30V), the samples were detected using the following antibodies: rabbit anti-mouse and human TDP-43 (ProteinTech 12892, 1:1000) and mouse anti-GAPDH (AbCam clone 6C5, 1:20000) as a loading control.

Immunohistochemistry

Tissue preparation for immunohistochemistry was performed as described previously (Ilieva et al., 2008) Briefly, anesthetized mice were transcardially perfused with 4% paraformaldehyde in phosphate buffer (pH 7.4). Following

postfixation in 4% paraformaldehyde at 4^{o}C, tissues were cryoprotected in 30% sucrose, and embedded in TissueTek O.C.T. (Sakura) for cryosectioning. 30 mm sections were cut on a cryostat for staining of free-floating sections. Sections were washed three times in PBS before being incubated with blocking solution containing PBS with 1.5% BSA and 0.5% Tween-20 for one hour at room temperature. Sections were then incubated with primary antibody in PBS, 0.3% Triton-X100 overnight at room temperature. The following day, the sections were washed three times with PBS, and incubated with secondary antibody in PBS, 0.3% Triton-X100 for one hour at room temperature. After a final wash in PBS, sections were mounted, dried at room-temperature and cover-slipped in ProLong Gold antifade mounting media (Invitrogen). The following primary antibodies and dilutions used were as follows: anti-c-myc (mouse Sigma clone 4A6 or rabbit Sigma #C3956, 1:500), rabbit anti-TDP-43 (ProteinTech 12892, 1:500), mouse anti-CC1/APC (Calbiochem, 1:500), mouse anti-GFAP (Chemicon, 1:1000), mouse anti-NeuN-488 (directly conjugated; Chemicon, 1:1000), goat anti-ChAT (Millipore, 1:300), and rat anti-Ctip2 (Abcam, 1:500). For detection of primary antibodies, donkey anti-rabbit, anti-mouse, or anti-goat Cy3, Cy5 or FITC-conjugated secondary antibodies (Jackson ImmunoResearch) were diluted at 1:500. Confocal images were acquired on a Nikon Eclipse laser scanning confocal microscope using the Nikon EZ-C1 software.

Quantification of motor axons and neurons

Roots from lumbar level 5 of the spinal cord (L5) were dissected from 3-4 mice per genotype at 2 months and 10-12 months of age and incubated in 2%

osmium tetroxide in 0.05 M cacodylate buffer. They were subsequently washed, dehydrated, and embedded in Epon (Electron Microscopy Sciences) as previously described (Ilieva et al., 2008). 0.75 mm cross-sections were cut and stained with toluidine blue for 30 seconds, rinsed, and dried. L5 axons were quantified as previously described (Ilieva et al., 2008) and are reported as mean ± SD. For lower motor neuron quantification, all lumbar choline acetyl-transferase (ChAT)-positive spinal cord motor neurons were counted in the ventral horn of at least 30 sections per animal (minimum of three animals per genotype) at two and twelve months of age. The number of motor neurons was divided by the number of sections to obtain an average number of motor neurons per section. The data are reported as average ± SD. Quantification of Ctip2-positive neurons in cortex layer five from 10-12 month old animals was performed on 6 consecutive sections of frontal cortex (approximately 2.34mm Bregma), in the motor M1 region in an area of 0.08mm^2 and are reported as the average number of motor neurons per mm^2 ± SEM. Matching sections were chosen for each set of mice.

Quantification of neuromuscular junctions and innervation

Quantification of muscle innervation at the neuromuscular junction was performed using immunohistochemistry on gastrocnemius muscle from 10-12 month-old animals. Briefly, floating 40 mm sections of gastrocnemius were incubated in blocking solution (PBS, 0.5% Tween-20, 1.5% BSA) for four hours at room temperature. Sections were then incubated overnight at room temperature with polyclonal rabbit anti-synaptophysin antibody diluted in PBS, 0.3% Triton-X100 at 1:50 (Invitrogen). The following day, the sections were

washed in PBS and incubated first with donkey anti-rabbit Cy3 (Jackson ImmunoResearch) and α-bungarotoxin-Alexa488 (Invitrogen) at 1:500 for one hour at room temperature and then with fluoromyelin™ red (Invitrogen) at 1:300 for 30 min. Following a final wash, the sections were mounted and dried overnight before coverslipping. Analysis was performed on a Nikon Eclipse laser scanning confocal microscope. A total of approximately 1000 neuromuscular junctions were counted from at least 10 sections of gastrocnemius. To obtain the number of neuromuscular junctions per section, the average number of neuromuscular junctions was divided by the number of sections counted, per animal, with 3 to 4 animals per genotype. Individual NMJs were considered as innervated when colocalization between synaptophysin and α-bungarotoxin staining was over 20%. The average number of neuromuscular junctions per section was reported as mean ± SEM. Statistical analysis was performed using one-way ANOVA with Bonferroni's posthoc test.

Animal Behavior and Electrophysiology

These studies were carried out under protocols approved by the Institutional Animal Care and Use Committee of the University of California, San Diego and were in compliance with Association for Assessment of Laboratory Animal Care guidelines for animal use. All studies were performed in such a manner as to minimize group size and animal suffering.

Accelerating Rotarod

Cohorts of sex-matched, age-matched transgenic animals and littermate controls were tested for time to fall on accelerating rotarod (UGO Basile; 2-40RPM) over three trials with a maximum time of 300 seconds per trial at each time point (21 days, 3-4 months, 6-7 months, 10-12 months and 15-18 months). Latency to fall was recorded in seconds once the mice fell from the bar or rotated once around the bar to eliminate variability from passive rotation in accordance to protocols reported elsewhere (Boudreau et al., 2009; Hockly et al., 2003; Mandillo et al., 2008). Following a one-day training session, trials were repeated over a three-day period for each time point. The data shown is the average of all three trials for the three sessions following the training session ± SEM. Statistical analysis was performed using 1-way ANOVA with Bonferroni's posthoc test for statistical measures.

Grip Strength

Cohorts of sex-matched, age-matched transgenic animals and littermate controls were tested for loss of hindlimb grip strength using a grip strength meter (Columbus Instruments) at 10-12 months of age. Mice were held in front of a horizontal bar such that only the hindlimb paws were able to grasp the bar and gently pulled back with steady force until both paws released the bar. Peak tension was recorded for five consecutive trials over three separate weekly sessions. The data shown is the average ± SEM of trials of all sessions. Statistical analysis was performed using one-way ANOVA with Bonferroni's posthoc test for statistical measures.

Analysis of Tremor or Hindlimb Clasping

A blinded observer subjectively scored mice at each of the time points listed (3-4, 6-7 and 10-12 months of age) as being either affected or unaffected by either of the two phenotypes described. Mice were classified as being affected by tremor if they displayed a persistent tremor when held flat in the observer's hand. Mice were scored as displaying hindlimb clasping if they displayed retraction of the hindlimbs after being lifted by the tail for thirty seconds or less. A percentage of affected animals is shown with statistical analysis performed using Fisher's exact test.

Spinal Cord Surface Motor Evoked potentials (SCMEPs) recording

SCMEPs were recorded from the dorsal surface of the lower thoracic (Th12) spinal cord. Under isoflurane anesthesia (2.0-2.5% maintenance; in room air), animals were mounted into a stereotaxic frame and the scalp over motor cortex was cut open to expose the skull. Stimulation was performed using a pair of stimulating electrodes consisting of one silver ball electrode placed into the skull over the motor cortex and one stainless steel needle inserted into the hard palate behind the upper incisors. A dental drill was used to perform a laminectomy of T11 vertebra exposing the T12 spinal segment. Evoked responses were recorded by a pair of flexible silver ball electrodes placed on the dura surface of the exposed T12 spinal segment. A reference silver-chloride disc electrode was placed subcutaneously on the contralateral side of the recording. After electrode placement, animals were injected with ketamine (150 mg/kg/h, i.p.) and isoflurane anesthesia was discontinued. Stimulation pulses were 0.1 ms long with amplitudes 7 mA delivered by a DS3 constant current isolated

stimulator (Digitimer LTD., Welwyn Garden City, UK). Recording electrodes were connected to an active headstage (3110W Headstage, Warner Instruments LLS) and signal amplified using DP-311 differential amplifier (Warner Instruments LLS). Amplified signal was acquired by the PowerLab 8/30 data acquisition system (ADInstruments, Inc.,Colorado Springs, CO) at sampling frequency of 20 kHz, digitized and stored in PC for analysis.

Myogenic Motor Evoked Potentials (MMEPs) recording

Animals were anesthetized with ketamine (150mg/kg, i.p.) and two 30G stainless steel stimulating electrodes were placed subcutaneously overlying the left and right motor cortex. MEPs were elicited by transcranial electrical stimulation with a pulse duration of 1ms at 7 mA using a DS3 constant current isolated stimulator (Digitimer LTD., Welwyn Garden City, UK). Responses were recorded from the gastrocnemius muscle using a 30G platinum transcutaneous needle electrodes (distance between recording electrodes~1 cm; Grass Technologies, An Astro-Med, Inc., West Warwick, Ri). Recording electrodes were connected to an active headstage (3110W Headstage, Warner Instruments LLS) and signal amplified using DP-311 differential amplifier (Warner Instruments LLS). Amplified signal was acquired by the PowerLab 8/30 data acquisition system (ADInstruments, Inc.,Colorado Springs, CO) at sampling frequency of 20 kHz, digitized and stored in PC for analysis.

Resting Electromyographic (EMG) recording

Animals were anesthetized with 2.5% isoflurane and the left hind limb shaved. To record EMG, two 30G platinum transcutaneous needle electrodes

(Grass Technologies, An Astro-Med, Inc., West Warwick, Ri) were placed into the gastrocnemius muscle (distance between recording electrodes~1 cm). Electrodes were connected to a active headstage (3110W Headstage, Warner Instruments LLS), recorded signal amplified using DP-311 differential amplifier (Warner Instruments LLS) and digitalized by the PowerLab 8/30 data acquisition system (ADInstruments, Inc.,Colorado Springs, CO). Recorded signal was sampled at 20 kHz and stored in PC for analysis.

Statistical analysis

The statistical analysis of electrophysiological data were performed by Student's t-test. $P<0.01$ was considered to be statistically significant. The results were expressed as means ± SE.

Nuclear-cytosolic fractionation

Nuclear-cytosolic fractionation of cortex and spinal cords from young and old mice was performed as described elsewhere (Wils et al.), (Ditsworth et al., 2007). Briefly, cortex and spinal cords were dissected, weighed, and fresh tissue was gently lysed in 10x vol/wt hypotonic buffer A (10 mM Hepes-KOH pH 7.4, 10 mM KCl, 1.5 mM MgCl, 0.5 mM EDTA, 0.5 mM EGTA, 1X protease inhibitors (Roche) using a dounce homogenizer. After 20 min on ice, 2.5M sucrose (0.5x vol/wt) was added and samples were centrifuged at 3000rpm for 5 min. The supernatant was collected as the cytosolic fraction, and the nuclear pellet was washed with buffer A. Following centrifugation, the nuclear pellet was resuspended in 5x vol/wt high salt buffer B (10 mM Hepes-KOH pH 7.4, 0.42 M

NaCl, 2.5% v/v glycerol, 1.5 mM MgCl, 0.5 mM EDTA, 0.5 mM EGTA, 1 mM DTT, 1X protease inhibitors), and incubated at 4°C while rotating at 60 rpm for 1hr. Both the nuclear and cytosolic fractions were then centrifuged at high speed (13000rpm) for 10 min at 4°C. Equivalent volumes were prepared for immunoblotting.

Sequential biochemical fractionation

Sequential biochemical fractionation on cortex and spinal cord was performed as described elsewhere (Giasson et al., 2002). Cortex and spinal cords from mice were dissected, weighed, and homogenized in 4ml/g of high salt buffer (HS buffer: 50mM Tris pH7.5, 750mM NaCl, 5mM EDTA, and protease inhibitor cocktail), and then centrifuged at 45,000g for 30 minutes at 4°C. The pellets were re-extracted with HS buffer, followed by two sequential extractions with HS buffer containing 1% Triton X-100 (TX fractions). Pellets were homogenized in 500µl of HS buffer containing 1M sucrose, and upon centrifugation, floating myelin was removed. Pellets were then extracted with 2ml/g of urea buffer (7M urea, 2M thiourea, 4% CHAPS, 30mM Tris pH8.5), followed by 2ml/g of SDS loading buffer. Equivalent volumes of samples were separated on 4-12% Bis-Tris gradient gels for immunoblotting with the indicated antibodies.

Microarray

Microarray data analysis was performed as previously described (Polymenidou et al.). For each microarray condition, the log2 ratio of skipping intensities to inclusion intensities was estimated using least-squares analysis. Significantly changing splicing events between TDP-43^{Q331K}, TDP-43$^{Q331K\text{-}low}$ and TDP-43$^{Wild\text{-}Type}$ control were identified using a q-value < 0.05 and an absolute separation score > 0.3.

RT-PCR Validation

cDNA was generated by reverse transcribing 1 μg of total RNA extracted from the cortex and spinal cord of 2 month old transgenic animals using oligo (dT) primer and Superscript III reverse transcriptase (Invitrogen) according to the manufacturer's instructions. To test candidate splicing targets as identified by microarray, PCR amplification was performed for 28 cycles using cDNA template with primers falling in exons flanking the alternate cassette exons (all primer sequences are listed in Table 2.4). Products were separated on 10% acrylamide-TBE gels and then stained with SYBR Gold (Invitrogen). Gel imaging and quantification of the isoforms was performed using the Biorad Chemidoc software. The intensity ratios between products including the cassette exon and skipping the cassette exon were averaged for a minimum of 3 biological replicates per genotype.

Acknowledgements

The authors thank Timothy Meerloo and Ying Jones (University of California at San Diego, La Jolla, CA) and Janet Folmer (Johns Hopkins University, Baltimore, MD) for their technical assistance in plastic thin sectioning and staining. We also thank Kevin Clutario, Sandra Lee, Anne Vetto, and Han Jin Park for their technical assistance, and all members of the Cleveland lab for their helpful suggestions and discussion regarding the work. Dr. Chris Shaw (King's College, London, U.K.) very kindly provided clones containing wild-type and mutant human TDP-43 cDNA.

This work was supported by grants to D.W.C. from the NIH and Welcome trust. D.W.C. receives salary support from the Ludwig Institute for Cancer Research. E.S.A. was a recipient of the UC San Diego Genetics Training Grant (NIGMS T32 GM008666). S.-C. L. is a recipient of NIH Neuroplasticity of Aging training grant (T32 AG 000216). S.C.H. is funded by the NSF Graduate Research fellowship. This work was also partially supported by grants NS075449 and HG004659 from the NIH to G.W.Y., an Alfred P. Sloan Research Fellow.

Chapter 2, in part, is being prepared for publication. The dissertation author was the primary researcher and author of this paper. Oleksandr Platoshyn, Melissa McAlonis-Downes, and Dr. Martin Marsala (Marsala Lab, La Jolla, CA) performed electrophysiology experiments and analysis of the resulting data. Ling Ouyang (Salk Institute, La Jolla, CA) performed microarray experiments and Stephanie C. Huelga and Dr. Gene Yeo (Yeo Lab, La Jolla, CA) performed analysis of the resulting data. Drs. Clotilde Lagier-Tourenne and Magdalini Polymenidou performed RT-qPCR experiments. Dr. Holly Kordasiewicz provided

assistance with and performed rotarod experiments. Nuclear-cytoplasmic and biochemical fractionations were performed by Dr. Dara Ditsworth. Drs. Sandrine Da Cruz, and Philippe Parone performed histological staining and quantification for neuromuscular junctions and upper motor neurons.

Chapter 3: Future Directions and Concluding Remarks

3.1 Summary

Much progress has been made towards defining the various properties of TDP-43 that may play a role in neurodegeneration. Nevertheless, much remains unresolved on the relative contribution of each of these properties to disease. Work from our group and others has been crucial in defining the multiple components of TDP-43 biology that may represent points of initiation or accelerate progression of disease. These factors may include but are not limited to the essential role of TDP-43 in development and neurological function, TDP-43's broad role in RNA metabolism, and TDP-43's propensity to aggregate. Careful consideration of each of these properties will be critical to unraveling TDP-43-dependent neurodegeneration and in the downstream design of therapeutic interventions.

Through the generation and characterization of mice expressing wild-type or mutant human TDP-43, I have demonstrated a role for both a mutant-dependent enhancement of TDP-43 function in splicing, as well as a loss of function, in the context of the mammalian nervous system. The principal outcomes of this work were the discovery that: 1) without overexpression, mutant TDP-43 produced age-dependent motor deficits and degeneration in a dose-dependent fashion, 2) alterations in splicing events were observable in the CNS at an early stage of disease, indicative of a gain of aberrant property, and 3) robust accumulation of cytoplasmic or aggregated TDP-43 was not required for the development of neurodegeneration. These findings have important

implications in designing therapeutic strategies fortreating ALS that target TDP-43. Additionally, I have generated rodent models recapitulating clinical and pathological features of age-dependent motor neuron disease. Further study of these animals may reveal additional components underlying the selective degeneration of motor neurons in ALS that are not easily observable in more rapidly progressing models, arising from non-physiologically high levels of either mutant or wild-type TDP-43.

One critical feature distinguishing the transgenic mice that I have built and analyzed from endstage human patient samples is the absence of robust cytoplasmic accumulation of either soluble or insoluble TDP-43. Although I have demonstrated that constitutive nuclear expression of mutant TDP-43 is sufficient to trigger age-dependent neurodegeneration, it is unclear whether cytoplasmic accumulation represents a contributing factor to progression of neurodegeneration or a secondary phenomenon accompanying the process of neurodegeneration. Certainly, my evidence has demonstrated that motor neuron death and motor neuron disease occurs without such accumulations, so such aggregates are not essential for toxicity. Most plausibly, the lack of cytoplasmic TDP-43 accumulation in these mice is likely the combined result of multiple factors. There may be a threshold of protein expression required for the initiation of a seeding process for aggregation, such as has been reported for two other neurodegenerative disease-linked proteins, tau (Frost et al., 2009; Guo and Lee, 2011) and alpha-synuclein (Hansen et al., 2011; Luk et al., 2009). Indeed, the described prion-like properties of TDP-43 (Fuentealba et al., 2010; King et al.,

2012) could conceivably be the basis for what has been described as a “spreading” phenomenon that characterizes ALS. Studies with purified TDP-43 and in cell culture have supported this idea (Furukawa et al., 2011; Pesiridis et al., 2009) of TDP-43-based seeding.

Experiments in vivo have been more variable, however. Several previous mouse models have reported the cytoplasmic accumulation of both wild-type and mutant TDP-43 (Shan et al., 2010; Stallings et al., 2010; Swarup et al., 2011a; Wils et al., 2010; Xu et al., 2010). Whether cytoplasmic misaccumulation is a significant contributor to TDP-43 toxicity is unknown. My evidence establishes that cytoplasmic misaccumulation is not necessarily required for the development of neurodegeneration. Added to my findings are three other reports of transgenic rodent models (Igaz et al., 2011; Shan et al., 2010; Zhou et al., 2010), as well as a Drosophila model of TDP-43 proteinopathy (Voigt et al., 2010), in which cytoplasmic aggregates were reported, but nuclear-localized TDP-43 was also reported to produce neurodegeneration as well. Nonetheless, without direct comparison of each of the models with the mice I have generated it will be difficult to determine the relative proportions of mouse and human TDP-43 between each model, and therefore the variability in production of cytoplasmic TDP-43 species.

Secondly, nuclear clearance of TDP-43 is widely reported in patient samples (Neumann et al., 2006) and has been argued to be an early event (Giordana et al., 2010). Auto-regulated TDP-43 synthesis in multiple cellular and rodent models produces downregulation of endogenous TDP-43 in the presence

of human TDP-43 expression (Ayala et al., 2011; Igaz et al., 2011; Polymenidou et al., 2011). This loss of nuclear TDP-43 function in human disease, either due to physical clearance, or the presence of pathogenic mutations in the presence of a remaining wild-type allele, could presumably contribute to the pathogenesis of ALS and FTLD. In my study, I did not observe any clearance of nuclear TDP-43. Moreover, I demonstrated that human TDP-43 downregulates endogenous mouse TDP-43 with an increasing the proportion of human TDP-43 relative to mouse TDP-43, producing a more severe motor phenotype. Since work from our group has proven the importance of TDP-43 in the maintenance of RNA transcript levels and splicing for hundreds of targets involved in neurological function and disease (Polymenidou et al., 2011). Loss of nuclear TDP-43 will affect motor neuron health. Nevertheless, my work has established that disease can be provoked without nuclear loss of TDP-43 function, instead arising through mutant acquisition of one or more aberrant properties. Additional work is now needed to determine which pathways and transcripts are most central to the disease process.

Finally, studies from genetic models expressing mutant SOD1 have highlighted the importance of glial cell contributions to ALS disease onset and progression (Beers et al., 2006; Beers et al., 2008; Boillee et al., 2006b; Clement et al., 2003; Yamanaka et al., 2008b). Recent evidence from a transgenic rodent model expressing mutant human TDP-43 and human ALS patient spinal cord samples has shown elevated levels of both TDP-43 and NFkB p65 mRNA (Swarup et al., 2011b) and co-activation of p65 by TDP-43. Furthermore,

microglia expressing mutant forms of TDP-43 were demonstrated to be more toxic to primary cultured neurons. Beyond this study, however, a role for TDP-43 in non-neuronal cells has yet to be established. Given the significant role of glial cells in the progression of ALS, and the fact that TDP-43 cytoplasmic accumulations have been reported in both neurons and glia (Igaz et al., 2008; Van Deerlin et al., 2008), this will be a critical avenue of future study. In the initial design of these transgenic mice, I selected the prion promoter due to its expression in both neurons and glial cells (Borchelt et al., 1996; Wang et al., 2005), albeit not in microglia. Additionally, the construct included cre-exciseable LoxP sites, with the intention of testing the relative contribution of various cell types in the CNS, as was previously accomplished using LoxSOD1 transgenic mice (Boillee et al., 2006b; Yamanaka et al., 2008b). A similar study led by Dr. Dara Ditsworth in our group, is now underway to determine the contribution of surrounding cell-types to TDP-43-mediated motor neuron degeneration, using a genetic cross between mice expressing motor-neuron restricted cre (vesicular achetylcholine transporter-cre, or VAchT-cre) and loxPrP-TDP-43^{Q331K} mice.

3.2 Future Directions

This doctoral work has defined a set of mutant-dependent splicing alterations in the context of age-dependent motor degeneration. Much work is now required to understand which alterations are most critical to both disease initiation and progression. Additionally, it remains to be established whether splicing alterations that I have identified are recapitulated in human disease.

Indeed, studies of patient samples have shown a number of splicing alterations that occur in SALS patient spinal cords (Rabin et al., 2010). As dysregulation of RNA metabolism becomes more prominent as a possible cause of ALS, discovering which transcripts are disrupted in the disease process will potentially yield avenues for therapeutic intervention. Comparison of transcription and splicing profiles from the CNS of young and aged loxPrP-TDP-43 mice represents one such experiment to address this question.

One feature of the genetic model of motor neuron degeneration that I have generated is a slow disease progression. Indeed, at present, I have not observed animals that reach fatal paralysis with profound motor neuron loss observed in human disease or SOD1 mutant models of ALS. Although I report a reduction of 35% in both axon and motor neuron numbers, since mutant TDP-43 accumulation continues at comparable levels, this suggests that a population of motor neurons remains more resistant to degeneration, despite the persistent expression of nuclear mutant TDP-43. In their study of ALS patient spinal cord expression and splicing profiles, Rabin et al. have reported a number of compartment-dependent splicing changes through the use of laser microdissection of motor neurons followed by high-throughput sequencing and splicing-sensitive microarray analysis. In an extension of the experiment described previously, rather than examining whole brain or spinal cord alterations, what would now be of advantage would be use of a similar approach to define motor-neuron specific splicing alterations. Such a study could define motor neuron-specific splicing alterations in young and aged loxPrP-TDP-43 animals.

Although I did not focus on alterations in mRNA transcript levels, this is a second and perhaps equally important avenue of future study. In addition to splicing alterations, Polymenidou et al. (2011) have shown that 602 mRNAs showed TDP-43-dependent alterations in transcript levels following TDP-43 depletion. As a parallel and extension of this study, a current postdoc in our group, Dr. Shuying Sun, is currently assessing TDP-43 mutant-dependent alterations in translated RNAs. The use of double transgenic mice expressing cell-type specific eGFP-fused ribosomal proteins (Dougherty et al., 2010) and loxPrP-TDP-43$^{Wild\text{-}Type}$ or loxPrP-TDP-43^{Q331K} will aid in delineating mutant TDP-43-dependent transcriptomic and translational changes in a cell-type specific manner.

Finally, efforts to define threshold levels of TDP-43 accumulation for cellular toxicity and the resulting consequences on both cellular protein quality control and TDP-43 autoregulation potentially represent an interesting topic of study. ALS belongs to a family of proteinopathies, and aggregated TDP-43 is a defining feature of the sporadic form of the disease. Although the RNA-binding function of TDP-43 is clearly an essential component of its toxic properties, the cytoplasmic misaccumulation of the protein is a salient feature of patient samples. Efforts to model ALS and other neurodegenerative diseases at the level of cellular and genetic model organisms cannot completely recapitulate what must be a contribution of components of the protein degradation pathway during aging. Moreover, the recent discovery of mutations in ubiquilin 2 linked to juvenile, X-linked FALS (Deng et al., 2011) is the first demonstration that mutations in a

component of the protein degradation machinery can lead to neurodegeneration and more specifically motor neuron disease. Notably, those authors described a co-localization between ubiqulin 2 inclusions and C-terminal fragments of TDP-43. Considering the previously mentioned prion-like properties of the C-terminal glycine-rich region of TDP-43, study of the impact of dysregulation of TDP-43 on the cellular protein quality control machinery certainly represents an important avenue of study. The proposal that multiple insults (reviewed in (Lee et al., 2012; Polymenidou and Cleveland, 2012) may be required for the onset and progression of TDP-43-dependent neurodegeneration could plausibly represent an intersection of both defects in RNA processing and a feed-forward loop of protein misaccumulation.

Finally, disruption of the TDP-43 autoregulatory pathway certainly has consequences not only for the accumulation of TDP-43, but for the nuclear functions of TDP-43 as well. A current postdoctoral fellow in our group, Dr. Shuo-Chien Ling, has begun testing the impact of increasing or decreasing the amount of TDP-43 expressed in the nervous system. He has employed a genetic strategy of either genetically depleting endogenous TDP-43 in the presence of wild-type or mutant TDP-43. Secondly, he has increased the dosage of wild-type or mutant TDP-43 through a genetic cross between loxPrP-TDP-43 mice and mice expressing both endogenous TDP-43 as well as a monogenic BAC transgene expressing the full-length human TDP-43 gene. Through these two strategies, Dr. Ling has devised an *in vivo* milieu to modulate and test the effects of different dosages of either wild-type or mutant TDP-43.

3.3 Concluding Remarks

In closing, my thesis work has defined a set of mutant-dependent alterations in TDP-43 function in the context of the mammalian nervous system. I have also proposed that the cytoplasmic accumulation of TDP-43 is not a required component of neurodegeneration. Finally, I have generated novel genetic models of human motor neuron disease that recapitulate certain pathological and clinical aspects of disease. Together, these contributions may help guide a dissection of the disease process in ALS. As the role of defects in RNA splicing and metabolism become more clearly linked to ALS, future studies using these genetic models may have important implications on the development of therapeutic strategies and targets in ALS and other TDP-43-linked neurodegenerative diseases.

Figures and Tables

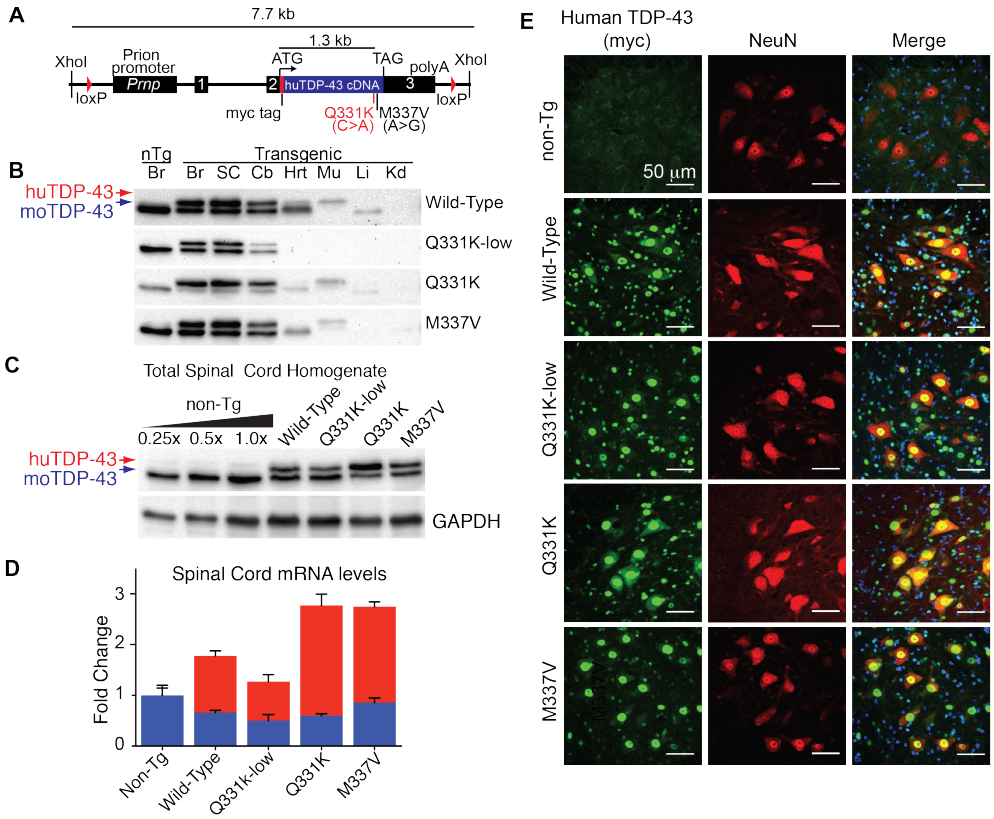

Figure 2.1: Generation and establishment of multiple lines of transgenic mice expressing wild-type, Q331K or M337V-mutant human TDP-43.

(A) Schematic of the PrP-TDP-43 transgene. A cDNA containing myc-tagged human TDP-43 transgene with either wild-type or either of two ALS-linked point mutations (Q331K or M337V) was cloned into the prion protein promoter construct (mPrP.XhoI) and flanked with loxP sites to allow excision in the presence of cre-recombinase.

(B) Immunoblotting using an antibody that recognizes both mouse and human TDP-43 in whole organ lysates from transgenic animals demonstrates that the Prnp promoter drives CNS-specific expression of TDP-43 and closely mimics the pattern of endogenous TDP-43. Br = Brain, Cb = Cerebellum, SC=Spinal Cord, Hrt = Heart, Mu = Skeletal Muscle, Liv = Liver, Kid = Kidney. Equal protein amounts were loaded per lane.

(C) Immunoblotting for using an antibody that recognizes both mouse and human TDP-43 in whole spinal cord lysates from transgenic mice shows accumulated human TDP-43 protein and a corresponding downregulation of endogenous mouse TDP-43 in all lines analyzed

(D) Accumulated mRNA expression levels of the human transgene in the spinal cords from PrP-TDP-43 transgenic mice recapitulates the downregulation of the endogenous mouse TDP-43 transcript as observed by immunoblotting in **(C)**.

(E) The human transgene accumulates in the nuclei of neurons as well as glial cells in a pattern that mimics endogenous TDP-43. Representative single-plane confocal images of the ventral horn of lumbar-level spinal cord from 2-month old animals. Immunofluorescent staining for the human transgene was performed using a rabbit polyclonal antibody raised against c-myc (Sigma C3956), co-stained with the neuronal marker, NeuN (Sigma). Scale bar = 50 μm

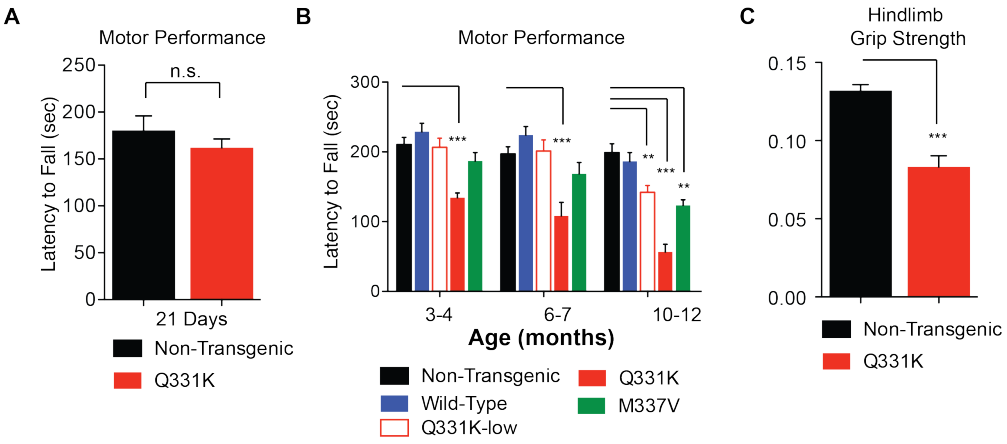

Figure 2.2: TDP-43^{Q331K} and TDP-43^{M337V} mice develop age-dependent, progressive motor deficits.

(A-B) Motor deficits as measured by rotarod are exacerbated in a dose dependent manner in TDP-43^{Q331K} mice. N≥11 for each genotype and each time point. Data shown is the average ± SEM. Statistical analysis was performed using 1-way ANOVA for each time point with Bonferroni's posthoc test for statistical measures (** $p<0.01$ and *** $p<0.001$).

(C) 10-12 month old TDP-43^{Q331K} high-expressing animals developed hindlimb weakness as measured by a hindlimb grip strength assay ($p=0.0002$ by 1-way ANOVA with Bonferroni's posthoc test). Data shown is the average ± SEM. N=12 per genotype.

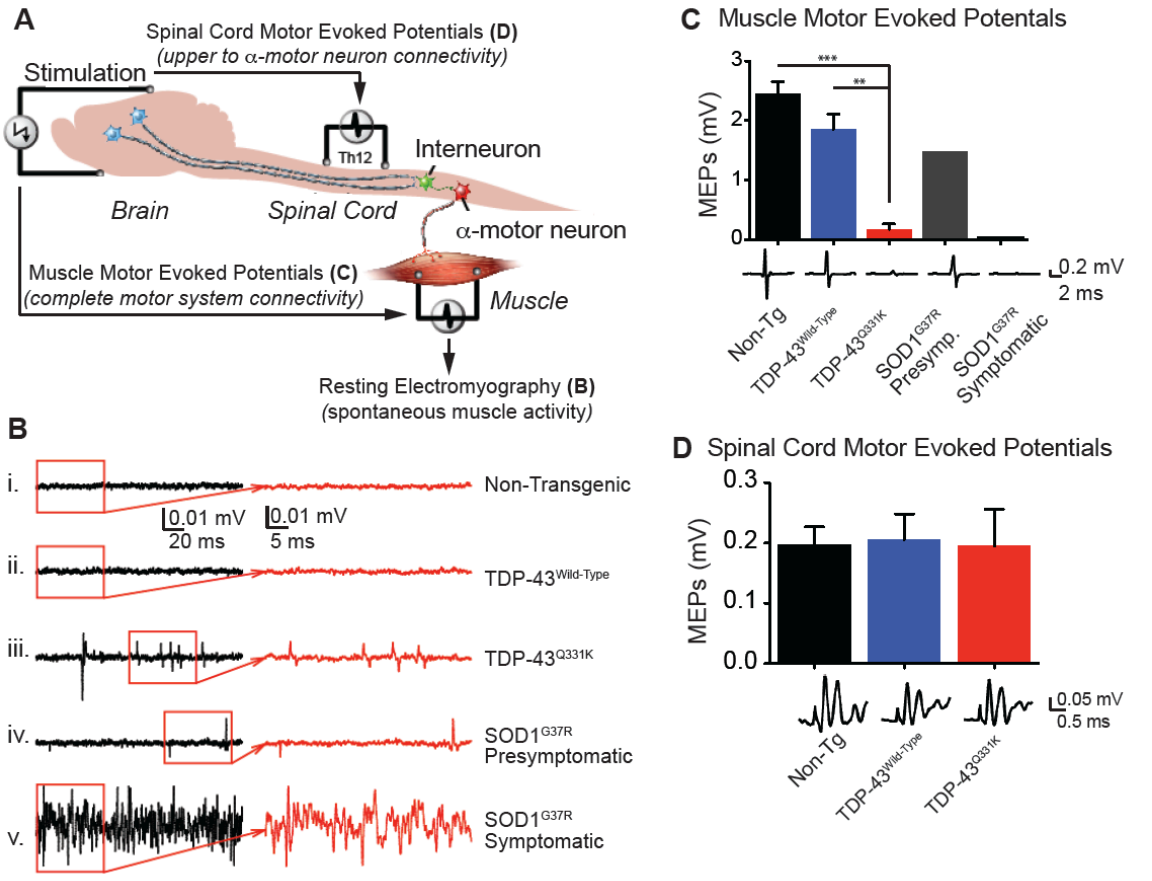

Figure 2.3: Analysis of electrophysiology in TDP-43 transgenic animals confirms deficits in lower motor neuron function in aged mutant-expressing TDP-43 transgenic mice.

(A) To identify the conductivity of descending motor axons and their functional connectivity with lumbar α-motoneurons, motor evoked potentials were elicited by electrical stimulation of motor cortex and extra-pyramidal system and responses recorded from the exposed T12 spinal segments (spinal cord surface MEPs) or from the gastrocnemius muscle (myogenic motor evoked potentials-MMEPs). The presence of muscle fibrillations was identified by EMG recording in the gastrocnemius muscle in isoflurane anesthetized animals in the absence of any stimulus (resting EMG).

(B) Resting electromyography recording from the gastrocnemius muscle showed no detectable muscle activity over the background "noise" in non-transgenic and wild type animals (i and ii). In contrast, a consistent presence of muscle fibrillations was recorded in Q331K and in presymptomatic SOD1^{G37R} mice (iii and iv). In symptomatic SOD1^{G37R} mice a high frequency muscle fibrillation was recorded (v).

(C) Myogenic motor evoked potentials (MMEPs) recordings from the gastrocnemius muscle showed a significant decrease in recorded amplitudes in TDP-43^{Q331K} mice; the magnitude of MMEP amplitude decrease was similar as recorded in symptomatic SOD1^{G37R} mice.

(D) Spinal cord surface MEP recordings showed no significant difference in recorded amplitudes between non-transgenic, TDP-43$^{Wild-Type}$ and TDP-43^{Q331K} mice.

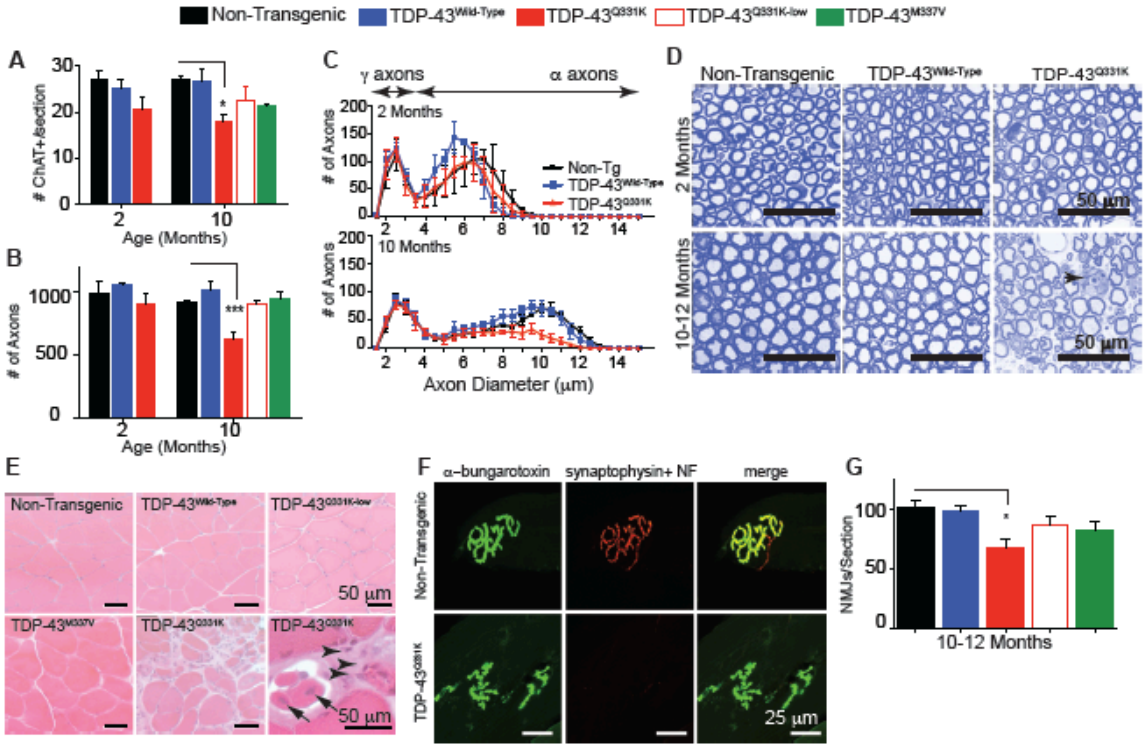

Figure 2.4: TDP-43^{Q331K} transgenic mice develop age-dependent lower motor neuron degeneration.

(A) Quantification of ChAT-positive motor neurons in lumbar spinal cords from TDP-43 transgenice mice showed a reduction of ~35% (17.9 ± 3.0 vs 27.3 ± 1.0 motor neurons in non-transgenic animals) in the number of a-motor neurons in TDP-43^{Q331K} transgenic animals (n=3 per genotype per time point). Statistical analysis was performed using one-way ANOVA with Bonferroni's posthoc test (*p=0.0448). Data shown is the average ± SD.

(B) Quantification of motor axons in (**D**) revealed a significant age-dependent reduction of large caliber motor axons in TDP-43^{Q331K} transgenic at 10-12 months of age (N≥3 per genotype per time point). The statistical analyses shown were performed using one-way ANOVA with Bonferroni's posthoc test (***p <0.001). Data shown is the average ± SD.

(C) The diameter distributions of L5 motor axons determined from images in **(D)** shows a specific loss of large-caliber motor axons in 10-12 month old TDP-43^{Q331K} transgenic animals, corresponding to the loss of a-motor neurons.

(D) Representative images of lumbar level 5 (L5) motor axon roots from TDP-43$^{Wild-Type}$ or TDP-43^{Q331K} transgenic animals stained with Toluidine blue. Note the appearance of degenerating axons in TDP-43^{Q331K} transgenic mice (arrowhead), but not in TDP-43$^{Wild-Type}$. Scale bar = 50 μm

(E) Hematoxylin and eosin staining of gastrocnemius muscle in TDP-43^{Q331K} transgenic animals shows regions of atrophied fibers of varying sizes (arrowheads) and regenerating fibers characterized by centralized nuclei (arrows). Scale bar = 50 μm.

(F) Representative neuromuscular junctions (NMJs) from non-transgenic and TDP-43^{Q331K}-expressing animals. Scale bar = 25 μm.

(G) 10-12 month old TDP-43 transgenic animals showed a 30% reduction in the number of neuromuscular junctions per section. Data shown is the average number of neuromuscular junctions per section ± SEM (*p=0.0235, by one-way ANOVA with Bonferroni's posthoc test).

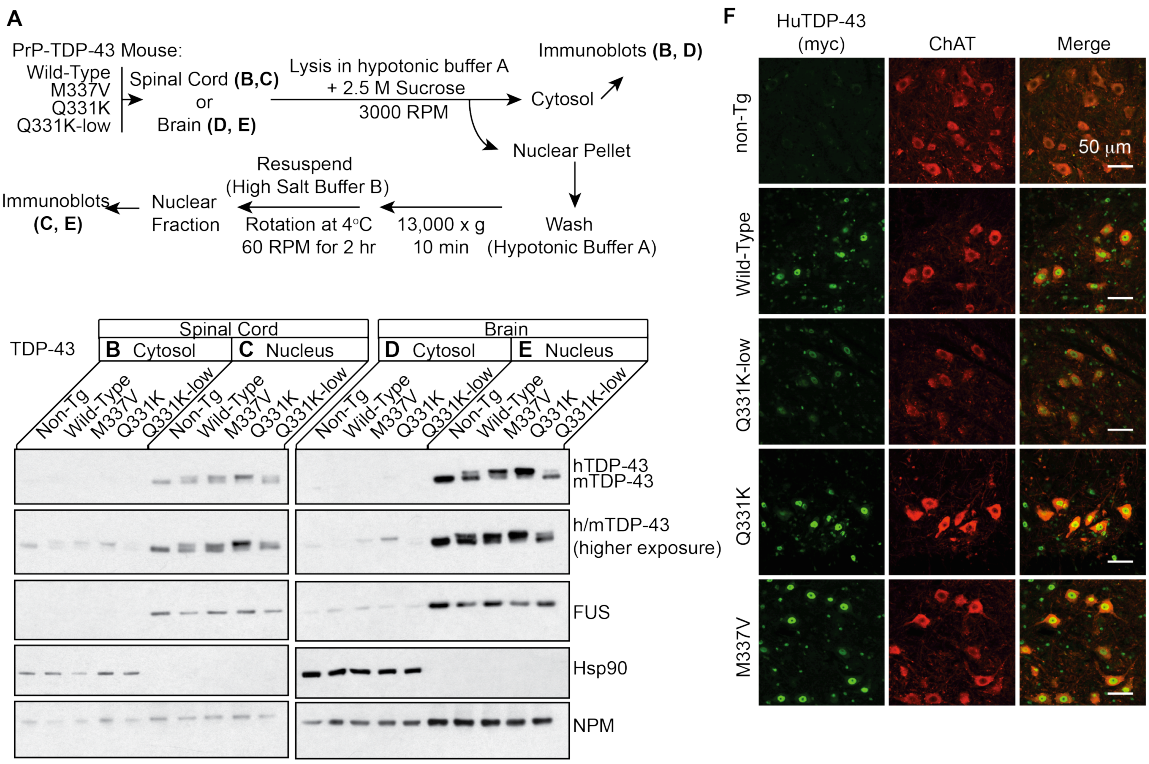

Figure 2.5: Neither wild-type nor mutant TDP-43 show aberrant cytosolic localization in the brain and spinal cords of TDP-43 transgenic mice.

(A) Schematic outlining fractionation of mouse brain or spinal cord into nuclear and cytosolic fractions. TDP43$^{Wild\text{-}Type}$, TDP43^{Q331K}, TDP-43$^{Q331K\text{-}low}$ or TDP-43^{M337V} mice were used.

(B-E) Immunoblots of enriched cytosolic or nuclear extracts of spinal cord **(B, C)** or brain **(D, E)** in 10-12 month old wild-type and mutant TDP-43 transgenic animals showing the presence of endogenous and human TDP-43 in both fractions. Note the enrichment of Hsp90 in the cytosolic extract and (FUS) in the nuclear extract, indicating the efficiency of separation

(F) Immunofluorescent co-labeling of the human transgene and ChAT showed that the human transgene remained predominantly localized to the nuclease of surviving ammunofluorescenin aged TDP-43 transgenic animals. Scale bar = 50 μm

Figure 2.6: Targets directly bound by the TDP-43^{Q331K} transgene show splicing alterations primarily consistent with enhanced normal function, but also some loss of function.

(A) Experimental strategy to identify differentially regulated splicing events in TDP-43^{Q331K} transgenic animals. RNA extracted from the cortices of 2-month old non-transgenic, TDP-43$^{Wild-Type}$, TDP-43^{Q331K}, or TDP-43$^{Q331K-Low}$ transgenic mice was subjected to Affymetrix splicing sensitive microarray analysis. After comparison to non-transgenic splicing arrays, pie charts display the total alternative splicing events significantly altered in the transgenic mice. Pie chart colors represent the types of events represented on the array and are displayed schematically to the right.

(B) TDP-43 regulated cassette exons identified from TDP-43 depletion experiments in mouse (Polymenidou et al., 2011). Cassette exons are divided into direct targets, bound by TDP-43 within 2 kilobases, and indirect targets, not bound by TDP-43.

(C) Bar plot displaying the fraction of overlap of TDP-43-regulated exons, direct (dark green) and indirect (light green), with exons that changed upon expression of TDP-43$^{Wild-Type}$, TDP-43^{Q331K} and TDP-43$^{Q331K-low}$. The TDP-43^{Q331K} and TDP-43$^{Q331K-low}$ overlapping exons show a significant enrichment (by chi-square analysis: $p<0.0005$) in the fraction that are direct TDP-43 regulated exons compared to the fraction that are indirect TDP-43 regulated exons. No enrichment was found in TDP-43$^{Wild-Type}$.

(D) The overlap of significantly changed cassette exons observed in the cortices from TDP-43 transgenic mice with TDP-43 regulated cassette exons. Direct and indirect exons that are also regulated in TDP-43 transgenic mice are represented as exons that are changed in the opposite direction of TDP-43 depletion (colored gray) and as exons that are changed in the same direction of TDP-43 depletion (included or excluded in both, colored white).

(E-F) RT-PCR validation for a subset of cortex alternate cassette exons identified by splicing sensitive microarrays. **(E)** includes targets that changed uniquely in the presence of the TDP-43^{Q331K} mutant (both TDP-43^{Q331K} and TDP-43$^{Q331K-low}$ conditions, "Mutant-Dependent"). **(F)** shows targets that changed primarily in a dose-dependent manner (in TDP-43$^{Wild-Type}$, TDP-43^{Q331K} and TDP-43$^{Q331K-low}$ conditions). The bar plots show the ratio of inclusion to exclusion calculated from the mean intensities of a minimum of three biological replicates ± S.D. of RT-PCR products as analyzed on 10% acrylamide-TBE resolving gels (representative gel images shown, with duplicate biological replicates). Splicing alterations significantly different from the non-transgenic condition were determined with Student's T-test, *$p<0.05$, **$p<0.01$ and ***$p<0.001$. "in/ex" = ratio of inclusion to exclusion.

(**G**) Bar graph depicting the percentages of differentially included or excluded exons upon transgene expression. The green dashed line represents the fraction of unchanged exons in any cortex experiment (TDP-43$^{Wild-Type}$, TDP-43^{Q331K}, TDP-43$^{Q331K-low}$) that have binding.

(i) "All Changing Exons" includes all exons that were either included or excluded. 25% of the cassette exons that were included and excluded were direct targets.

(ii) "Overlapping Exons with TDP-43 KD" depicts only exons that changed following TDP-43 depletion (i.e. regulated by endogenous TDP-43). A significant increase was found in the percentage of direct targets (~43% for TDP-43^{Q331K} and TDP-43$^{Wild-Type}$, and 53% for TDP-43$^{Q331K-low}$) for cassette exons that are excluded upon transgene expression, with only a modest ~20% of included exons that are direct targets.

(iii) "Non-overlapping exons with TDP-43 KD" includes only exons not previously shown to be regulated by endogenous TDP-43 depletion, in which 39% of excluded exons in the TDP-43^{Q331K} animals were direct targets.

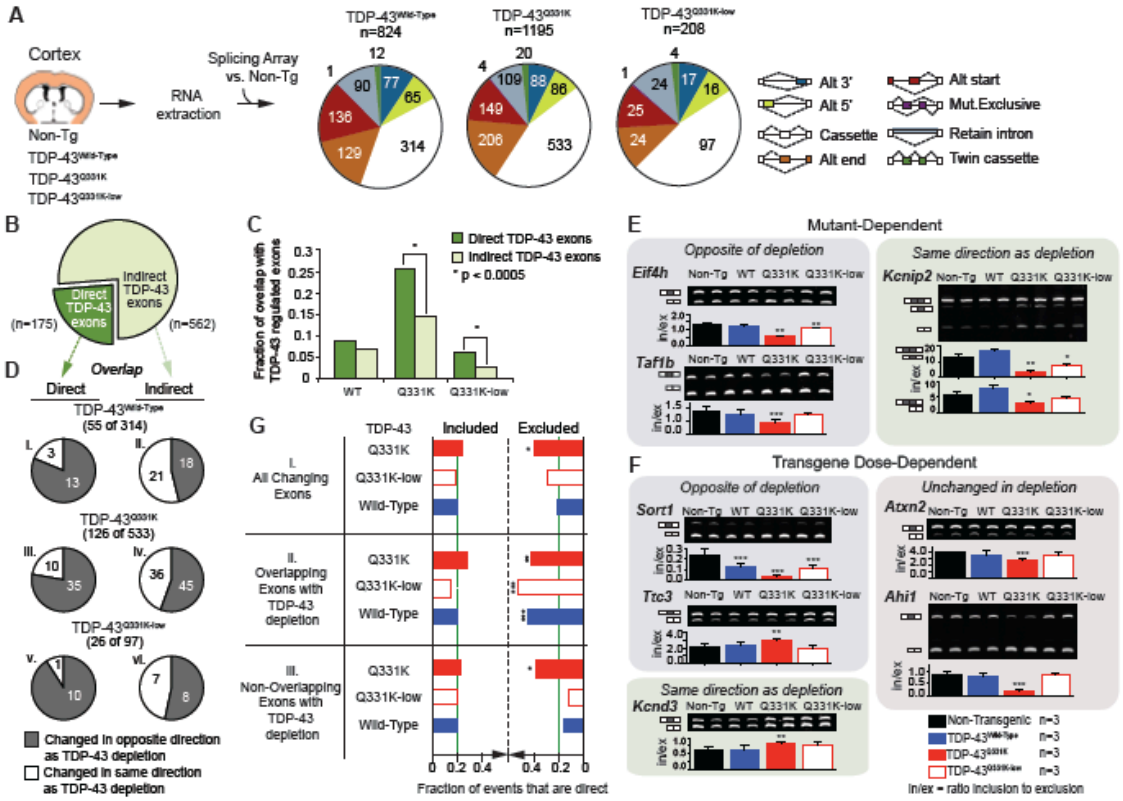
A
Cortex
Non-Tg
TDP-43Wild-Type
TDP-43Q331K
TDP-43Q331K-low
RNA extraction
Splicing Array vs. Non-Tg
TDP-43Wild-Type n=824
TDP-43Q331K n=1195
TDP-43Q331K-low n=208
Alt 3'
Alt 5'
Cassette
Alt end
Alt start
Mut.Exclusive
Retain intron
Twin cassette
B
Direct TDP-43 exons
Indirect TDP-43 exons
(n=175)
(n=562)
C
Direct TDP-43 exons
Indirect TDP-43 exons
* p < 0.0005
Fraction of overlap with TDP-43 regulated exons
WT
Q331K
Q331K-low
D
Overlap
Direct
Indirect
TDP-43Wild-Type (55 of 314)
TDP-43Q331K (126 of 533)
TDP-43Q331K-low (26 of 97)
Changed in opposite direction as TDP-43 depletion
Changed in same direction as TDP-43 depletion
E
Mutant-Dependent
Opposite of depletion
Eif4h
Taf1b
Same direction as depletion
Kcnip2
Non-Tg WT Q331K Q331K-low
in/ex
F
Transgene Dose-Dependent
Opposite of depletion
Sort1
Ttc3
Same direction as depletion
Kcnd3
Unchanged in depletion
Atxn2
Ahi1
Non-Transgenic n=3
TDP-43Wild-Type n=3
TDP-43Q331K n=3
TDP-43Q331K-low n=3
in/ex = ratio inclusion to exclusion
G
TDP-43
Included
Excluded
I. All Changing Exons
II. Overlapping Exons with TDP-43 depletion
III. Non-Overlapping Exons with TDP-43 depletion
Q331K
Q331K-low
Wild-Type
Fraction of events that are direct

Figure 2.7: TDP-43^{Q331K} mice show unique splicing alterations in the spinal cord including changes in genes involved in neurological function and transmission.

(A) Experimental strategy to identify differentially regulated splicing events in TDP-43^{Q331K} transgenic animals. RNA extracted from the spinal cords of 2-month old non-transgenic, TDP-43$^{Wild\text{-}Type}$, or TDP-43^{Q331K} transgenic mice was subjected to Affymetrix splicing sensitive microarray analysis. After comparison to non-transgenic splicing arrays, pie charts display the total alternative splicing events significantly altered in the spinal cords of transgenic mice. Pie chart colors represent the types of events represented on the array and are displayed schematically to the right.

(B) Diagram showing the overlap between events changing in cortex and spinal cord for the TDP-43$^{Wild\text{-}Type}$ and TDP-43^{Q331K} conditions. Overall, 38% (118 of 196) of changes found in TDP-43$^{Wild\text{-}Type}$ cortex were present in TDP-43$^{Wild\text{-}Type}$ spinal cord, and 42% (226 of 307) of changes found in TDP-43^{Q331K} cortex were present in TDP-43^{Q331K} spinal cord.

(C) Overlap of spinal cord TDP-43$^{Wild\text{-}Type}$ and TDP-43^{Q331K} alternative cassette exons shows a set of 1060 common splicing events, 1059 of which change in the same direction. Additionally, 394 events unique to the TDP-43$^{Wild\text{-}Type}$ condition and 419 events unique to the TDP-43^{Q331K} condition were identified.

(D) RT-PCR validation for a subset of spinal cord alternate cassette exons identified using splicing sensitive microarrays that also overlap with changes observed in cortex. Bar plots show the mean intensities of a minimum of three biological replicates ± S.D of RT-PCR products as analyzed on 10% acrylamide-TBE resolving gels (representative gel images shown, with duplicate biological replicates). Splicing alterations significantly different from the non-transgenic condition were determined with Student's T-test, *$p<0.05$, **$p<0.01$ and ***$p<0.001$.

(E) Modes of TDP-43 Action in Exon Splicing. TDP-43 normally acts to repress exon inclusion, causing exon exclusion. Increased levels of wild-type or mutant TDP-43 protein produce increased exon exclusion, which may be mimicked in some cases through a mutant-specific enhancement of normal TDP-43 function. Depletion of TDP-43, either through loss of nuclear TDP-43, or targeted depletion using anti-sense oligonucleotides as in (Polymenidou et al., 2011), produces a decrease in exon exclusion. This decrease in exon exclusion may also be mimicked through mutant-specific loss of normal TDP-43 function.

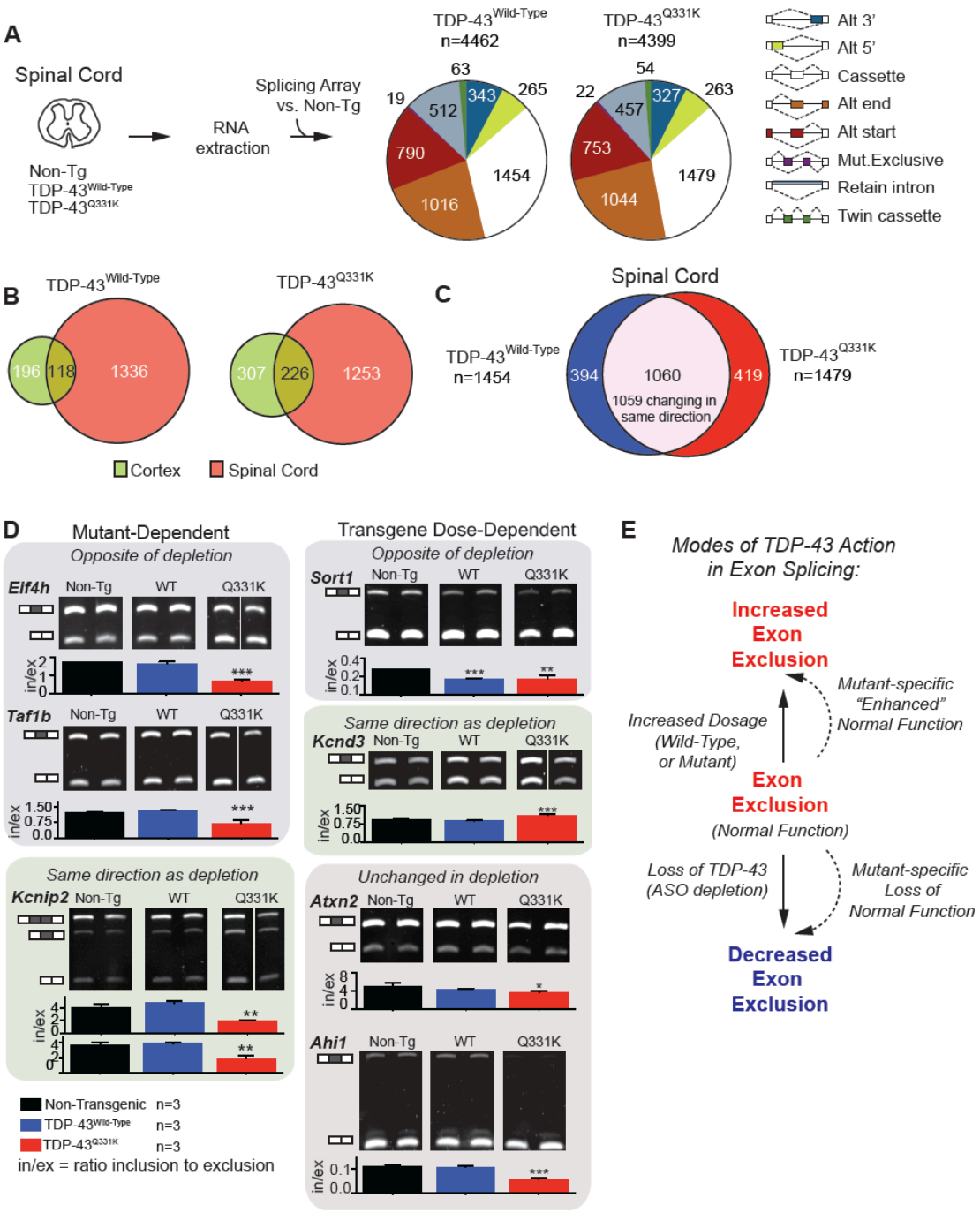
A
Spinal Cord
Non-Tg
TDP-43Wild-Type
TDP-43Q331K
RNA extraction
Splicing Array vs. Non-Tg
TDP-43Wild-Type n=4462
63
19
512
343
265
790
1454
1016
TDP-43Q331K n=4399
54
22
457
327
263
753
1479
1044
Alt 3'
Alt 5'
Cassette
Alt end
Alt start
Mut.Exclusive
Retain intron
Twin cassette
B
TDP-43Wild-Type
TDP-43Q331K
196
118
1336
307
226
1253
Cortex
Spinal Cord
C
Spinal Cord
TDP-43Wild-Type n=1454
394
1060
1059 changing in same direction
419
TDP-43Q331K n=1479
D
Mutant-Dependent
Opposite of depletion
Eif4h
Non-Tg
WT
Q331K
in/ex
***
Taf1b
Non-Tg
WT
Q331K
in/ex
***
Same direction as depletion
Kcnip2
Non-Tg
WT
Q331K
in/ex
**
**
Non-Transgenic n=3
TDP-43Wild-Type n=3
TDP-43Q331K n=3
in/ex = ratio inclusion to exclusion
Transgene Dose-Dependent
Opposite of depletion
Sort1
Non-Tg
WT
Q331K
in/ex
***
**
Same direction as depletion
Kcnd3
Non-Tg
WT
Q331K
in/ex
***
Unchanged in depletion
Atxn2
Non-Tg
WT
Q331K
in/ex
*
Ahi1
Non-Tg
WT
Q331K
in/ex
***
E
Modes of TDP-43 Action in Exon Splicing:
Increased Exon Exclusion
Mutant-specific "Enhanced" Normal Function
Increased Dosage (Wild-Type, or Mutant)
Exon Exclusion
(Normal Function)
Loss of TDP-43 (ASO depletion)
Mutant-specific Loss of Normal Function
Decreased Exon Exclusion

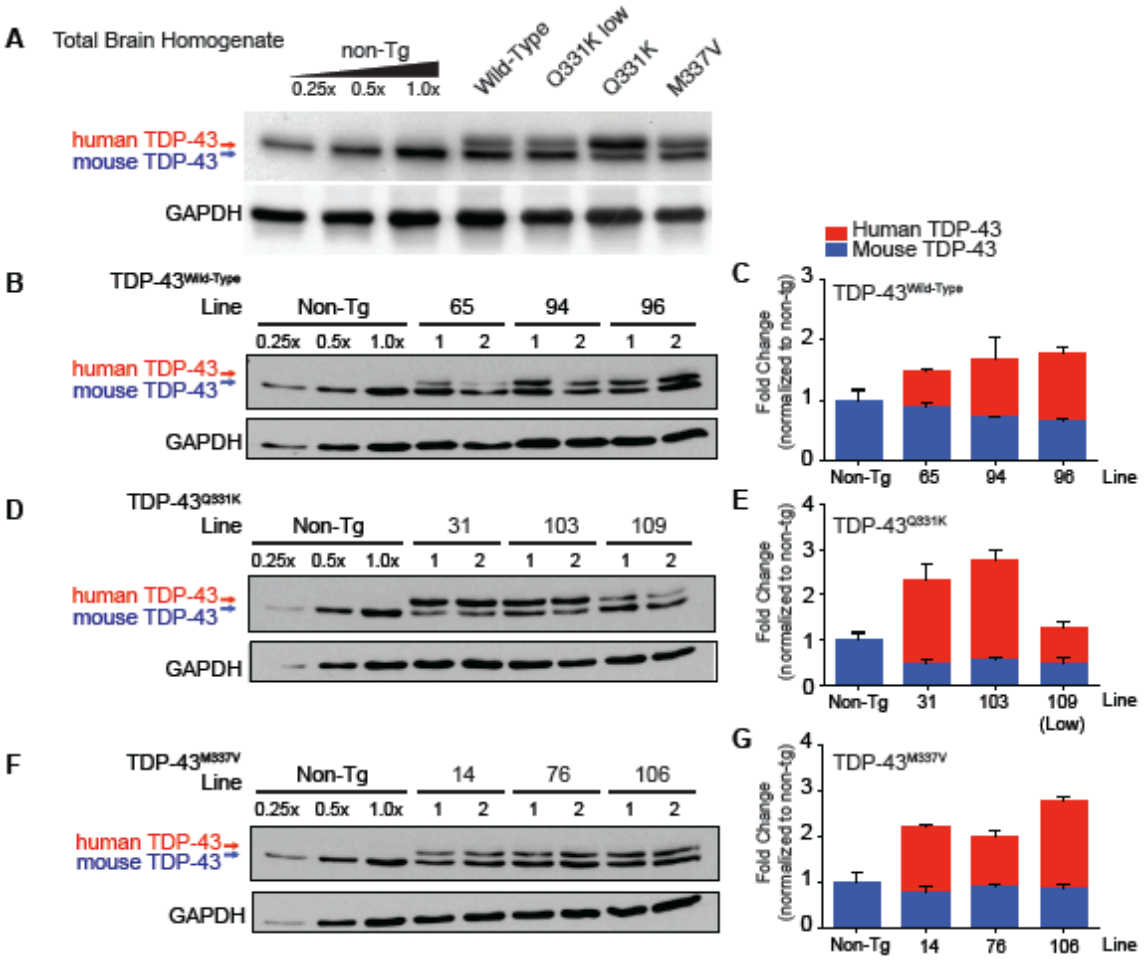

Figure 2.8: Accumulated protein and mRNA expression levels of the human transgene in brains and spinal cords from TDP-43 transgenic mice

(A) Accumulated protein from whole brain lysate from TDP-43 transgenic mice.

(B-C) Accumulated protein and mRNA expression levels of the human transgene in the spinal cords from the founder lines of TDP-43$^{Wild\text{-}Type}$-expressing transgenic mice. Based on protein and RNA expression levels, TDP-43$^{Wild\text{-}Type}$ Line 96 was selected to be characterized, and is referred to as "TDP-43$^{Wild\text{-}Type}$" in the text.

(D-E) Accumulated protein and mRNA expression levels of the human transgene in the spinal cords from the founder lines of TDP-43^{Q331K}-expressing transgenic mice. TDP-43^{Q331K} Line 103 and TDP-43^{Q331K} Line 109 were selected to be characterized, and are referred to as "TDP-43^{Q331K}" and "TDP-43$^{Q331K\text{-}low}$", respectively.

(F-G) Accumulated protein and mRNA expression levels of the human transgene in the spinal cords from the founder lines of TDP-43^{M337V}-expressing transgenic mice. TDP-43^{M337V} Line 106 was selected to be characterized, and is referred to as TDP-43^{M337V}.

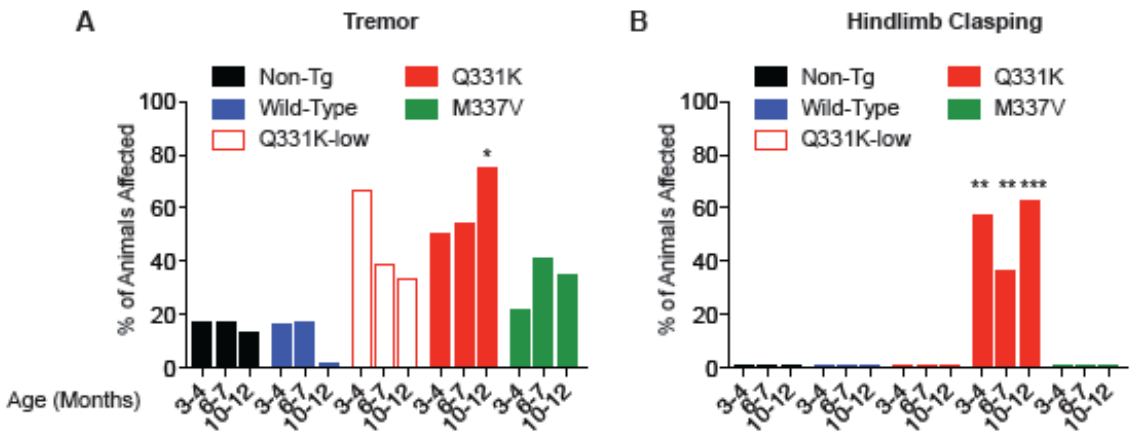

Figure 2.9: Development of tremor and clasping phenotype in TDP-43^{Q331K} transgenic mice.

(A) A tremor phenotype observed in TDP-43^{Q331K} mice as early as 3-4 months of age and progressively increased as the animals aged. N≥8 per genotype per time point.

(B) Hindlimb clasping was observed in TDP-43^{Q331K} mice but in no other genotypes. N≥8 per genotype per time point. For both **(A)** and **(B)**, a percentage of affected animals is shown with statistical analysis performed using Fisher's exact test (**p<0.01 and ***p<0.001).

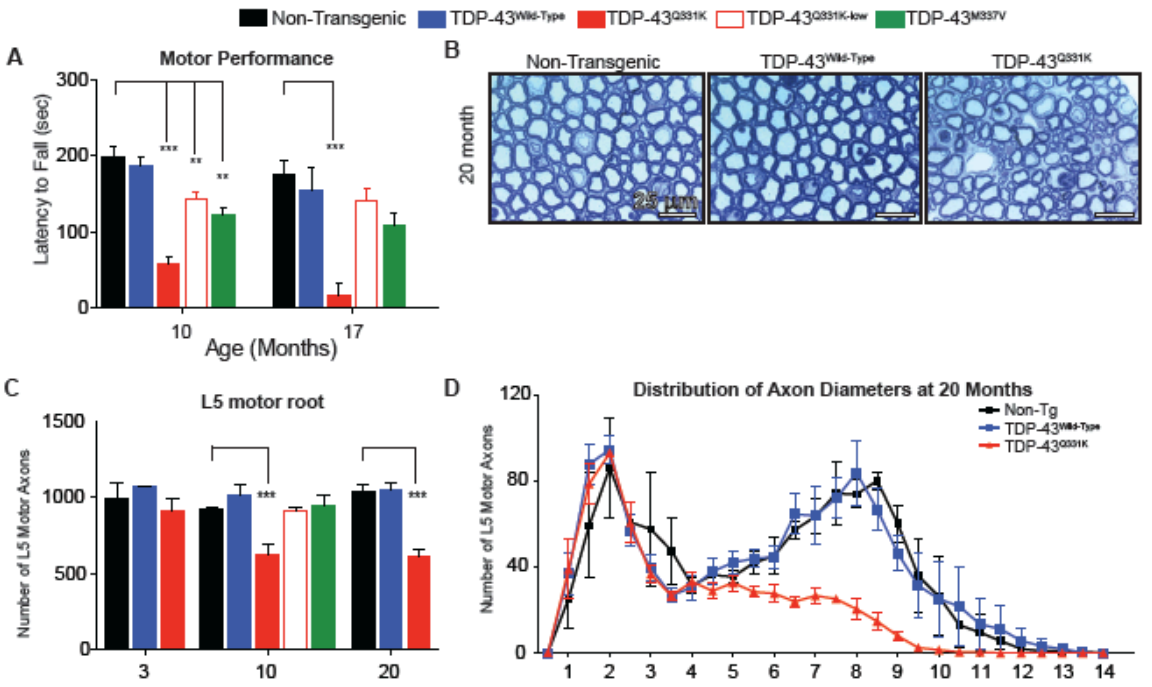

Figure 2.10: Late-stage plateau in adult-onset motor deficits in TDP-43^{Q331K}, TDP-43$^{Q331K\text{-}low}$, and TDP-43^{M337V} mice.

(A) Animals were tested on rotarod at 17 months of age. TDP-43^{Q331K}, TDP-43$^{Q331K\text{-}low}$ and TDP-43^{M337V} mice showed no further progression of motor deficits demonstrated at 10 months of age. The motor performance of 17 month old animals has been plotted alongside data from 10 month old animals as shown in Figure 2.2B in order to better visualize the data. Data shown is the average ± SEM. Statistical analyses were performed using one-way ANOVA with Bonferroni's posthoc test (**p< 0.01 and ***p <0.001). Non-Transgenic: n=6 males, TDP-43$^{Wild\text{-}Type}$: n=6 males, TDP-43^{Q331K}: n=3 males, TDP-43$^{Q331K\text{-}low}$: n=8 males, TDP-43^{M337V}: n=7 males.

(B) Representative images of L5 Motor Axon cross-sections in 20 month-old non-transgenic and TDP-43 transgenic mice. Scale bar = 25 μm.

(C) Quantification of images in **(B)** showed no further loss of L5 motor axons. Data shown is the average ± SD. Statistical analyses were performed using one-way ANOVA with Bonferroni's posthoc test (***p <0.001). The quantification of L5 motor axons from 20 month old animals has been plotted alongside data from 10 month old animals as shown in Figure 2.4B in order to better visualize the data.

(D) Motor axon distribution calculated from images in **(B)**. TDP-43 transgenic animals show loss of primarily large caliber axons corresponding to a-motor neurons.

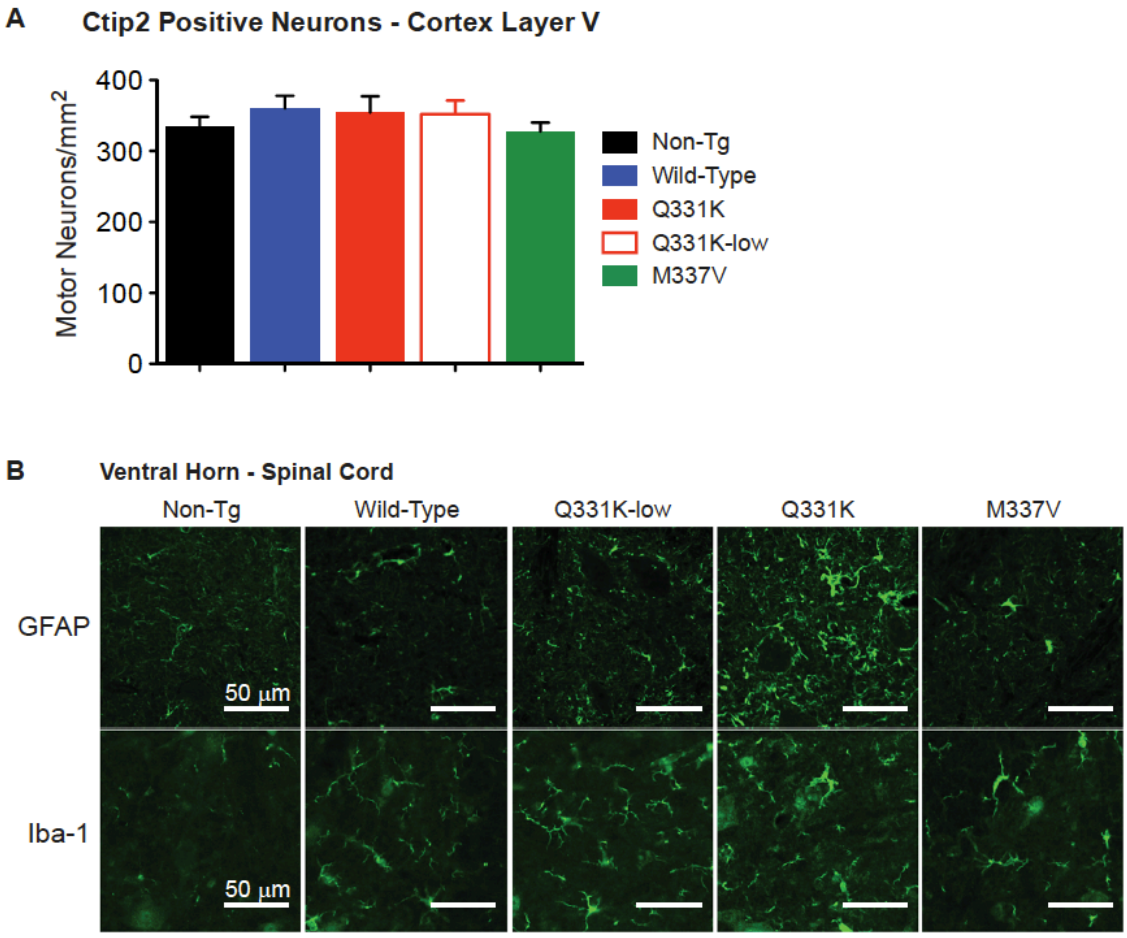

Figure 2.11: TDP-43-mutant expressing animals show no loss of upper motor neurons in aged mutant TDP-43 expressing animals, but display reactive astrocytes and microgliosis in the ventral horn of the spinal cord.
(A) Quantification of Ctip2-positive upper motor neurons in cortex layer V showed no loss in TDP-$43^{Wild\text{-}Type}$ or mutant (TDP-43^{Q331K} and TDP-43^{M337V}) transgenic animals. Data shown is the average number of Ctip2-positive upper motor neurons per section from 3-4 animals per genotype, ± SEM. Statistical analysis was performed using one-way ANOVA with Bonferroni's posthoc test.
(B) Aged TDP-43 transgenic animals showed enhanced GFAP and Iba-1 immuoreactivity in the spinal cord, indicating reactive astrocytosis and infiltration of microglia, respectively, absent in non-transgenic controls. Scale bar = 50 μm.

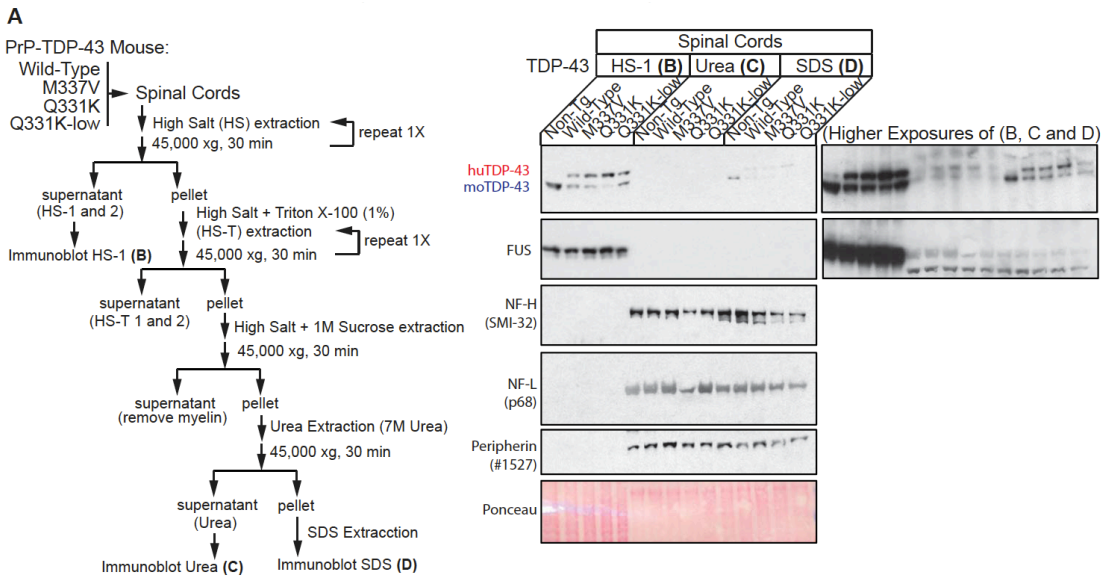

Figure 2.12: Low levels of the wild-type (mouse and human) and mutant TDP-43 are recovered in the insoluble (urea and SDS) fractions after sequential biochemical fractionation of spinal cords from 10-12 month old transgenic animals.

(A) Experimental scheme for the sequential biochemical extraction of spinal cords from non-transgenic and TDP-43 transgenic animals.

(B) Immunoblotting using a polyclonal antibody equally recognizing both mouse and human demonstrated that the majority of both endogenous and human TDP-43 is recovered in the high-salt fraction.

(C-D) Immunoblotting using a polyclonal antibody recognizing both mouse and human of **(C)** urea and **(D)** SDS-extracted pellets from spinal cords of 10-12 month old animals showed that a small fraction of both endogenous and human (wild-type and mutant) was recovered from the **(C)** urea and **(D)** SDS-insoluble fractions from 10-12 month old animals. Note that neurofilament and peripherin fractionate to the insoluble fractions, as expected.

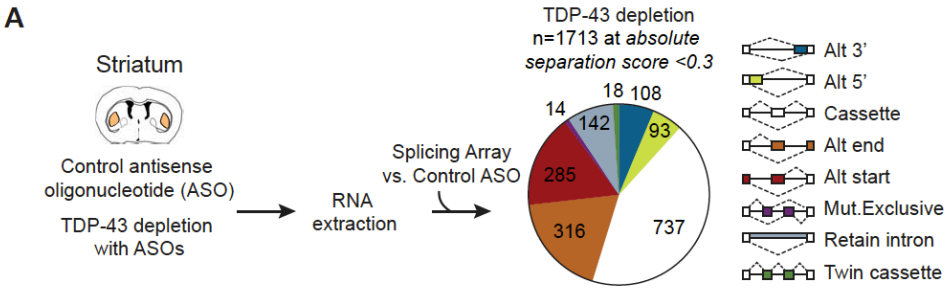

Figure 2.13: Experimental strategy for the re-analysis of alternative splicing events following TDP-43 depletion.

Experimental strategy to identify differentially regulated splicing events following depletion of mouse TDP-43 using anti-sense oligonucleotides targeted against mouse TDP-43, as described in a previous study from our group (Polymenidou et al., 2011). RNA extracted from the striatum of mice treated with TDP-43 or Control ASOs was subjected to Affymetrix splicing sensitive microarray analysis. After comparison to control ASO splicing arrays, pie charts display the total alternative splicing events significantly altered in TDP-43 depleted mice, utilizing a commonly used statistical threshold of absolute separation score of <0.3. Pie chart colors represent the types of events represented on the array and are displayed schematically below.

Table 1.1: Mutations in Genes linked to Autosomal Dominant, Adult-Onset ALS

Locus	Gene	Protein	Mutations	Proportion of Inherited ALS	Date Discovered	Reference
21q22.1	*SOD1*	Cu/Zn superoxide dismutase	> 150*	20%	1993	Rosen et al., 1993
9p13.2-21.3	*C9ORF72*	C9Orf72	Variable length hexanucleotide repeat expansions, >~23 repeats	20%	2011	Renton et al., 2011; DeJesus-Hernandez et al., 2011
1q36	*TARDBP*	TDP-43	>40*	5%	2008	Kabashi et al., 2008; Sreedharan et al., 2008; Gitcho et al., 2008
16p11.2	*FUS*	FUS/TLS	>40*	4%	2009	Vance et al., 2009; Kwiatkowski et al., 2009
9p13.3	*VCP*	Valosin-containing protein	5	1-2%	2010	Johnson et al., 2010
10p15-14	*OTPN*	Optineurin	1	1-2%	2010	Maruyama et al., 2010
6q21	*FIG4*	PI(3,5)P(2) 5-phosphatase	5*	1%	2009	Chow et al., 2009
12q24	*DAO*	D-amino acid oxidase	1	1%	2010	Mitchell et al., 2010
14q11	*ANG*	angiogenin	>10	<1%	2006	Greenway et al., 2006
*Including sporadic ALS cases						
Adapted from Da Cruz and Cleveland, 2011						

Table 2.1: Summary of Exon Changes in Cortices from TDP-43 Transgenic Mice from RT-PCR Confirmation Gels and Microarrays

Cortex							
	RT-PCR Confirmation Gels				Microarray Separation Score (compared to non-transgenic; absolute threshold <0.3)		
Target	**Wild-Type**	**Q331K**	**Q331K-low**	**TDP-43 Depletion (Polymenidou et al. 2011)**	**Wild-Type**	**Q331K**	**Q331K-low**
Mutant Dependent							
Eif4h	NS	More Excluded *	More Excluded *	More Included	0	-1.521	-0.367
Taf1b	NS	More Excluded *	More Excluded	More Included	0	-2.02	-0.564
Kcnip2	Not Significant (NS)	More Excluded *	More Excluded *	More excluded	ND	ND	ND
Dose Dependent							
Sort1	More Excluded*	More Excluded *	More Excluded *	More Included	-0.946	-0.401	-0.802
Ttc3	More excluded	More excluded	More excluded	More Included	-0.604	-2.518	-0.802
Kcnd3	NS	More included*	NS	More included	0	0.357	0
Atxn2	NS	More Excluded	NS	not changed	0	-0.75	0
Ahi1	NS	More Excluded	NS	not changed	0	-1.982	0

- = statistically significant by Student's T-test with $p<0.05$, compared to non-tg

ND: not determined

same direction as knowdown, suggestive of loss-of-function

opposite direction as knockdown, suggestive of enhancement-of-function

changed by transgene but unchanged in knockdown, , suggestive of enhancement-of-function

Table 2.2: Summary of Exon Changes in Spinal Cord from TDP-43 Transgenic Mice from RT-PCR Confirmation Gels and Microarrays

Spinal Cord					
	RT-PCR Confirmation Gels			Microarray Separation Score (compared to non-transgenic; absolute threshold <0.3)	
Target	**Wild-Type**	**Q331K**	**TDP-43 Depletion** (Polymenidou et al. 2011)	**Wild-Type**	**Q331K**
Mutant-specific					
Eif4h	NS	More Excluded*	More included	0	-1.259
Taf1b	NS	More Excluded*	more included	0	-1.341
Kcnip2	NS	More Excluded*	More excluded	ND	ND
Transgene dose-dependent					
Sort1	More Excluded*	More Excluded*	More included	-0.752	-0.882
Kcnd3	NS	More included*	More included	0	0.34
Atxn2	NS	More Excluded	not changed	0	-0.478
Ahi1	NS	More Excluded*	not changed	0	-0.836

- = statistically significant by Student's T-test with $p<0.05$, compared to non-tg

ND= not determined

opposite direction as knockdown, suggestive of enhancement-of-function

same direction as knowdown, suggestive of loss-of-function

changed by transgene but unchanged in knockdown, , suggestive of enhancement-of-function

Table 2.3: Genes in containing splicing changes in TDP-43^{Q331K} spinal cord involved in neurological processing and transmission

Gene Symbol	Gene Name	Microarray Separation Score (compared to non-transgenic; absolute threshold <0.3)
APBA2	amyloid beta A4 precursor protein-binding family	-0.526
CHRM1	muscarinic acetylcholine receptor M1	0.36
COCH	cochlin precursor	0.384
GAL3ST1	galactosylceramide sulfotransferase	0.381
GRIA2	glutamate receptor 2 isoform 3 precursor	-0.306
GTF3C2	general transcription factor 3C polypeptide 2	0.326
NR2F6	nuclear receptor subfamily 2 group F member 6	-0.303
NRXN1	neurixin-1-alpha	0.37
NRXN3	neurexin-3-alpha	-0.775
OLFR1033	olfactory receptor 1033	-0.408
OPA1	dynamin-like 120 kDa protein, mitochondrial	-0.313
PDE6D	retinal rod rhodopsin-sensitive cGMP	0.576
PICK1	PRKCA-binding protein	0.33
PPP3CA	calcineurin or serine/threonine-protein phosphatase 2B	-0.553
RIMS1	regulating synaptic membrane exocytosis protein	-0.574
SCRIB	protein scribble homolog	-0.584
STX3	syntaxin-3	0.316
UNC13B	protein unc-13 homolog B	0.332

Table 2.4: RT-PCR forward and reverse primer sequences (5' to 3') used for validation of TDP-43-dependent-events.

Gene	Forward Primer 5' to 3'	Reverse Primer 5' to 3'
mKcnip2	CGGCTCCTATGACCAGCTTA	GGAGTTGTTCCAGACCCTCA
mEif4h	ACTTCGTGTGGACATTGCAG	CCCCCTACCCCCTAAGAAGT
mKcnd3	GGCAAGACCACCTCACTCAT	AGTGGCTGGACAGAGAAGGA
mSort1	CAGGAGACAAATGCCAAGGT	TGGCCAGGATAATAGGGACA
mTaf1b	CCCCAACACCAAGATCAACT	AGGCCTGTTTGCTCTTCTGA
mAhi1	CCCCTCCTTTAACTCCCAAG	AGGGGTCTGCCCTTACTGAG
mTtc3	TGCTGAGGGAGGTCTCAGTT	GGAGAGTGGCTTACTGCACC
mAtxn2	CACATGCTCAGCCTGGTTTA	GGATGGGGAGTATGTGGATG

Table A.1: Antibody Dilutions Used for Immunofluorescent Staining in Arnold et al., 2012

Antibody	Species	Dilution	Source
Choline acetyl-transferase (ChAT)	Goat	1:300	Chemicon
Ctip2	Rat	1:500	Abcam
Glial fibrillary acidic protein (GFAP)	Mouse (Clone 6C5)	1:500	Chemicon
Glial fibrillary acidic protein (GFAP)	Rabbit	1:500	Dako
Iba-1	Rabbit	1:500	Wako
Myc	Mouse (Clone 4A6)	1:500	Chemicon
Myc	Rabbit	1:500	Sigma
NeuN-488	Mouse	1:1000	Chemicon
Mouse/Human TDP-43 (10782)	Rabbit	1:500	ProteinTech
Mouse/Human TDP-43 (12892)	Rabbit	1:500	ProteinTech

Appendix: Protocols

A.1: Protocol for the Genotyping of PrP-TDP-43 Transgenic Mice

A.1.1 PCR Set-Up

Template DNA should be extracted according to the chosen method (high-salt extraction was preferred for rapidity and the purity of DNA) with a minimum starting amount of 50 nanograms per reaction. A range between 100 nanograms to 150 nanograms is preferable.

Reaction Mix for 1x:

10x PCR Buffer (Invitrogen)	2.5 μl
10 mM dNTPs	0.75 μl
F Primer 1 (10 μM)	0.75 μl
F Primer 2 (10 μM)	0.75 μl
R Primer 1 (10 μM)	0.75 μl
R Primer 2 (10 μM)	0.75 μl
50 mM MgCl2	0.75 μl
Taq (Invitrogen)	0.25 μl
ddH2O	16.75 μl
DNA Template	1.0 μl
TOTAL	25 μl

Cycling Conditions

Temperature	**Time**	
94°C	5 min	
94°C	30 sec	X 35
58°C	1 min	Cycles
72°C	1 min	
72°C	7 min	
4°C	HOLD	

Primer Set 1

RT-hT-2F	agaggtgtccggctggtag
RT-hT-3R	cctgcaccataagaacttctcc
Expected size:	228 bp

Primer Set 2

mTDP-43-3uTR 1F	TTTTCATACACGGCGGTACA
mTDP-43-3uTR 1R	GCCGCTCATGCTGTATATGA
Expected size:	371 bp

A.2: Protocol for the Semi-quantitative RT-PCR Validation of Splicing Sensitive Microarrays

A.4.1 Preparation of cDNA

1 μg of Trizol-extracted RNA was prepared for reverse transcription according to the manufacturer's specifications (Superscript III Reverse Transcriptase, Invitrogen # 18080-044).

A.4.2 RT-PCR Primers

See Table 2.4. Primers were designed using Primer3 Software (http://frodo.wi.mit.edu/) for regions flanking the splice junction sites included on the splicing-sensitive array.

A.4.3 PCR Protocol

Reaction Mix for 1x:	
10x PCR Buffer (Invitrogen)	5 μl
10 mM dNTPs	1 μl
F Primer 1 (10 μM)	1 μl
F Primer 2 (10 μM)	1 μl
50 mM MgCl2	1.5 μl
Taq (Invitrogen)	0.4 μl
DEPC H2O	39.1 μl
cDNA Template	1.0 μl
TOTAL	49 μl

Cycling Conditions

Temperature	**Time**	
94°C	5 min	
94°C	30 sec	X 35
58°C	1 min	Cycles
72°C	1 min	
72°C	7 min	
4°C	HOLD	

A.4.4 Quantification of Bands

Prepare 10% acrylamide/TBE DNA gels as follows:

10% acrylamide DNA gels	
30% Acrylamide	5 ml
10X TBE	2 ml
Water	13 ml
10% APS	100 μl
TEMED	20 μl
TOTAL	20.12 ml

Following electrophoresis (120V for approximately 30-40 minutes), stain gels in SYBR Gold (Invitrogen, Catalog #S-11494) at 1:1000 (20 μl per 200 ml is sufficient for multiple gels

References

Abhyankar, M.M., Urekar, C., and Reddi, P.P. (2007). A novel CpG-free vertebrate insulator silences the testis-specific SP-10 gene in somatic tissues: role for TDP-43 in insulator function. J Biol Chem *282*, 36143-36154.

Acharya, K.K., Govind, C.K., Shore, A.N., Stoler, M.H., and Reddi, P.P. (2006). cis-requirement for the maintenance of round spermatid-specific transcription. Dev Biol *295*, 781-790.

Alberti, S., Halfmann, R., King, O., Kapila, A., and Lindquist, S. (2009). A systematic survey identifies prions and illuminates sequence features of prionogenic proteins. Cell *137*, 146-158.

Arai, T., Hasegawa, M., Akiyama, H., Ikeda, K., Nonaka, T., Mori, H., Mann, D., Tsuchiya, K., Yoshida, M., Hashizume, Y.*, et al.* (2006). TDP-43 is a component of ubiquitin-positive tau-negative inclusions in frontotemporal lobar degeneration and amyotrophic lateral sclerosis. Biochem Biophys Res Commun *351*, 602-611.

Arai, T., Hasegawa, M., Nonoka, T., Kametani, F., Yamashita, M., Hosokawa, M., Niizato, K., Tsuchiya, K., Kobayashi, Z., Ikeda, K.*, et al.* (2010). Phosphorylated and cleaved TDP-43 in ALS, FTLD and other neurodegenerative disorders and in cellular models of TDP-43 proteinopathy. Neuropathology.

Ash, P.E., Zhang, Y.J., Roberts, C.M., Saldi, T., Hutter, H., Buratti, E., Petrucelli, L., and Link, C.D. (2010). Neurotoxic effects of TDP-43 overexpression in C. elegans. Hum Mol Genet *19*, 3206-3218.

Ayala, Y.M., De Conti, L., Avendano-Vazquez, S.E., Dhir, A., Romano, M., D'Ambrogio, A., Tollervey, J., Ule, J., Baralle, M., Buratti, E.*, et al.* (2011). TDP-43 regulates its mRNA levels through a negative feedback loop. EMBO J *30*, 277-288.

Ayala, Y.M., Pantano, S., D'Ambrogio, A., Buratti, E., Brindisi, A., Marchetti, C., Romano, M., and Baralle, F.E. (2005). Human, Drosophila, and C.elegans TDP43: nucleic acid binding properties and splicing regulatory function. J Mol Biol *348*, 575-588.

Beers, D.R., Henkel, J.S., Xiao, Q., Zhao, W., Wang, J., Yen, A.A., Siklos, L., McKercher, S.R., and Appel, S.H. (2006). Wild-type microglia extend survival in PU.1 knockout mice with familial amyotrophic lateral sclerosis. Proc Natl Acad Sci U S A *103*, 16021-16026.

Beers, D.R., Henkel, J.S., Zhao, W., Wang, J., and Appel, S.H. (2008). CD4+ T cells support glial neuroprotection, slow disease progression, and modify glial morphology in an animal model of inherited ALS. Proc Natl Acad Sci U S A *105*, 15558-15563.

Belzil, V.V., Daoud, H., Dion, P.A., and Rouleau, G.A. (2011). No effect on SOD1 splicing by TARDP or FUS mutations. Arch Neurol *68*, 395-396.

Bensimon, G., Lacomblez, L., and Meininger, V. (1994). A controlled trial of riluzole in amyotrophic lateral sclerosis. ALS/Riluzole Study Group. N Engl J Med *330*, 585-591.

Boillee, S., Vande Velde, C., and Cleveland, D.W. (2006a). ALS: a disease of motor neurons and their nonneuronal neighbors. Neuron *52*, 39-59.

Boillee, S., Yamanaka, K., Lobsiger, C.S., Copeland, N.G., Jenkins, N.A., Kassiotis, G., Kollias, G., and Cleveland, D.W. (2006b). Onset and progression in inherited ALS determined by motor neurons and microglia. Science *312*, 1389-1392.

Borchelt, D.R., Davis, J., Fischer, M., Lee, M.K., Slunt, H.H., Ratovitsky, T., Regard, J., Copeland, N.G., Jenkins, N.A., Sisodia, S.S.*, et al.* (1996). A vector for expressing foreign genes in the brains and hearts of transgenic mice. Genet Anal *13*, 159-163.

Boudreau, R.L., McBride, J.L., Martins, I., Shen, S., Xing, Y., Carter, B.J., and Davidson, B.L. (2009). Nonallele-specific silencing of mutant and wild-type huntingtin demonstrates therapeutic efficacy in Huntington's disease mice. Mol Ther *17*, 1053-1063.

Bruijn, L.I., Becher, M.W., Lee, M.K., Anderson, K.L., Jenkins, N.A., Copeland, N.G., Sisodia, S.S., Rothstein, J.D., Borchelt, D.R., Price, D.L.*, et al.* (1997). ALS-linked SOD1 mutant G85R mediates damage to astrocytes and promotes

rapidly progressive disease with SOD1-containing inclusions. Neuron *18*, 327-338.

Buratti, E., and Baralle, F.E. (2001). Characterization and functional implications of the RNA binding properties of nuclear factor TDP-43, a novel splicing regulator of CFTR exon 9. J Biol Chem *276*, 36337-36343.

Buratti, E., and Baralle, F.E. (2008). Multiple roles of TDP-43 in gene expression, splicing regulation, and human disease. Front Biosci *13*, 867-878.

Buratti, E., Brindisi, A., Giombi, M., Tisminetzky, S., Ayala, Y.M., and Baralle, F.E. (2005). TDP-43 binds heterogeneous nuclear ribonucleoprotein A/B through its C-terminal tail: an important region for the inhibition of cystic fibrosis transmembrane conductance regulator exon 9 splicing. J Biol Chem *280*, 37572-37584.

Buratti, E., Brindisi, A., Pagani, F., and Baralle, F.E. (2004). Nuclear factor TDP-43 binds to the polymorphic TG repeats in CFTR intron 8 and causes skipping of exon 9: a functional link with disease penetrance. Am J Hum Genet *74*, 1322-1325.

Buratti, E., Dork, T., Zuccato, E., Pagani, F., Romano, M., and Baralle, F.E. (2001). Nuclear factor TDP-43 and SR proteins promote in vitro and in vivo CFTR exon 9 skipping. Embo J *20*, 1774-1784.

Cannon, A., Yang, B., Knight, J., Farnham, I.M., Zhang, Y., Wuertzer, C.A., D'Alton, S., Lin, W.L., Castanedes-Casey, M., Rousseau, L.*, et al.* (2012). Neuronal sensitivity to TDP-43 overexpression is dependent on timing of induction. Acta Neuropathol.

Charcot, J.M., and Joffroy, A. (1869). Deux cas d'atrophie musculaire progressive avec lesion de la substance grise et des faisceaux antero-lateraux de la moelle epiniere. Arch Physiol Neurol Path, Arch. Physiol. Neurol. Path.

Chiang, P.M., Ling, J., Jeong, Y.H., Price, D.L., Aja, S.M., and Wong, P.C. (2010). Deletion of TDP-43 down-regulates Tbc1d1, a gene linked to obesity, and alters body fat metabolism. Proc Natl Acad Sci U S A.

Clement, A.M., Nguyen, M.D., Roberts, E.A., Garcia, M.L., Boillee, S., Rule, M., McMahon, A.P., Doucette, W., Siwek, D., Ferrante, R.J.*, et al.* (2003). Wild-type nonneuronal cells extend survival of SOD1 mutant motor neurons in ALS mice. Science *302*, 113-117.

Couthouis, J., Hart, M.P., Shorter, J., DeJesus-Hernandez, M., Erion, R., Oristano, R., Liu, A.X., Ramos, D., Jethava, N., Hosangadi, D.*, et al.* (2011). A yeast functional screen predicts new candidate ALS disease genes. Proc Natl Acad Sci U S A *108*, 20881-20890.

Cushman, M., Johnson, B.S., King, O.D., Gitler, A.D., and Shorter, J. (2010). Prion-like disorders: blurring the divide between transmissibility and infectivity. J Cell Sci *123*, 1191-1201.

D'Ambrogio, A., Buratti, E., Stuani, C., Guarnaccia, C., Romano, M., Ayala, Y.M., and Baralle, F.E. (2009). Functional mapping of the interaction between TDP-43 and hnRNP A2 in vivo. Nucleic Acids Res *37*, 4116-4126.

Da Cruz, S., and Cleveland, D.W. (2011). Understanding the role of TDP-43 and FUS/TLS in ALS and beyond. Curr Opin Neurobiol *21*, 904-919.

Daoud, H., Valdmanis, P.N., Kabashi, E., Dion, P., Dupre, N., Camu, W., Meininger, V., and Rouleau, G.A. (2008). Contribution of TARDBP mutations to sporadic amyotrophic lateral sclerosis. J Med Genet.

DeJesus-Hernandez, M., Mackenzie, I.R., Boeve, B.F., Boxer, A.L., Baker, M., Rutherford, N.J., Nicholson, A.M., Finch, N.A., Flynn, H., Adamson, J.*, et al.* (2011). Expanded GGGGCC hexanucleotide repeat in noncoding region of C9ORF72 causes chromosome 9p-linked FTD and ALS. Neuron *72*, 245-256.

Deng, H.X., Chen, W., Hong, S.T., Boycott, K.M., Gorrie, G.H., Siddique, N., Yang, Y., Fecto, F., Shi, Y., Zhai, H.*, et al.* (2011). Mutations in UBQLN2 cause dominant X-linked juvenile and adult-onset ALS and ALS/dementia. Nature *477*, 211-215.

Deng, H.X., Hentati, A., Tainer, J.A., Iqbal, Z., Cayabyab, A., Hung, W.Y., Getzoff, E.D., Hu, P., Herzfeldt, B., Roos, R.P.*, et al.* (1993). Amyotrophic lateral sclerosis and structural defects in Cu,Zn superoxide dismutase. Science *261*, 1047-1051.

Ditsworth, D., Zong, W.X., and Thompson, C.B. (2007). Activation of poly(ADP)-ribose polymerase (PARP-1) induces release of the pro-inflammatory mediator HMGB1 from the nucleus. J Biol Chem *282*, 17845-17854.

Dougherty, J.D., Schmidt, E.F., Nakajima, M., and Heintz, N. (2010). Analytical approaches to RNA profiling data for the identification of genes enriched in specific cells. Nucleic Acids Res *38*, 4218-4230.

Du, H., Cline, M.S., Osborne, R.J., Tuttle, D.L., Clark, T.A., Donohue, J.P., Hall, M.P., Shiue, L., Swanson, M.S., Thornton, C.A.*, et al.* (2010). Aberrant alternative splicing and extracellular matrix gene expression in mouse models of myotonic dystrophy. Nat Struct Mol Biol *17*, 187-193.

Elden, A.C., Kim, H.J., Hart, M.P., Chen-Plotkin, A.S., Johnson, B.S., Fang, X., Armakola, M., Geser, F., Greene, R., Lu, M.M.*, et al.* (2010). Ataxin-2 intermediate-length polyglutamine expansions are associated with increased risk for ALS. Nature *466*, 1069-1075.

Feiguin, F., Godena, V.K., Romano, G., D'Ambrogio, A., Klima, R., and Baralle, F.E. (2009). Depletion of TDP-43 affects Drosophila motoneurons terminal synapsis and locomotive behavior. FEBS Lett *583*, 1586-1592.

Fiesel, F.C., Voigt, A., Weber, S.S., Van den Haute, C., Waldenmaier, A., Gorner, K., Walter, M., Anderson, M.L., Kern, J.V., Rasse, T.M.*, et al.* (2010). Knockdown of transactive response DNA-binding protein (TDP-43) downregulates histone deacetylase 6. EMBO J *29*, 209-221.

Frost, B., Ollesch, J., Wille, H., and Diamond, M.I. (2009). Conformational diversity of wild-type Tau fibrils specified by templated conformation change. J Biol Chem *284*, 3546-3551.

Fuentealba, R.A., Udan, M., Bell, S., Wegorzewska, I., Shao, J., Diamond, M.I., Weihl, C.C., and Baloh, R.H. (2010). Interaction with polyglutamine aggregates reveals a Q/N-rich domain in TDP-43. J Biol Chem *285*, 26304-26314.

Furukawa, Y., Kaneko, K., Watanabe, S., Yamanaka, K., and Nukina, N. (2011). A seeding reaction recapitulates intracellular formation of Sarkosyl-insoluble transactivation response element (TAR) DNA-binding protein-43 inclusions. J Biol Chem *286*, 18664-18672.

Giasson, B.I., Duda, J.E., Quinn, S.M., Zhang, B., Trojanowski, J.Q., and Lee, V.M. (2002). Neuronal alpha-synucleinopathy with severe movement disorder in mice expressing A53T human alpha-synuclein. Neuron *34*, 521-533.

Giordana, M.T., Piccinini, M., Grifoni, S., De Marco, G., Vercellino, M., Magistrello, M., Pellerino, A., Buccinna, B., Lupino, E., and Rinaudo, M.T. (2010). TDP-43 redistribution is an early event in sporadic amyotrophic lateral sclerosis. Brain Pathol *20*, 351-360.

Gitcho, M.A., Baloh, R.H., Chakraverty, S., Mayo, K., Norton, J.B., Levitch, D., Hatanpaa, K.J., White, C.L., 3rd, Bigio, E.H., Caselli, R.*, et al.* (2008). TDP-43 A315T mutation in familial motor neuron disease. Ann Neurol *63*, 535-538.

Guo, J.L., and Lee, V.M. (2011). Seeding of normal Tau by pathological Tau conformers drives pathogenesis of Alzheimer-like tangles. J Biol Chem *286*, 15317-15331.

Gurney, M.E., Pu, H., Chiu, A.Y., Dal Canto, M.C., Polchow, C.Y., Alexander, D.D., Caliendo, J., Hentati, A., Kwon, Y.W., Deng, H.X.*, et al.* (1994). Motor neuron degeneration in mice that express a human Cu,Zn superoxide dismutase mutation. Science *264*, 1772-1775.

Hansen, C., Angot, E., Bergstrom, A.L., Steiner, J.A., Pieri, L., Paul, G., Outeiro, T.F., Melki, R., Kallunki, P., Fog, K.*, et al.* (2011). alpha-Synuclein propagates from mouse brain to grafted dopaminergic neurons and seeds aggregation in cultured human cells. J Clin Invest *121*, 715-725.

Hanson, K.A., Kim, S.H., Wassarman, D.A., and Tibbetts, R.S. (2010). Ubiquilin modifies TDP-43 toxicity in a Drosophila model of amyotrophic lateral sclerosis (ALS). J Biol Chem *285*, 11068-11072.

Ho, Y.S., Gargano, M., Cao, J., Bronson, R.T., Heimler, I., and Hutz, R.J. (1998). Reduced fertility in female mice lacking copper-zinc superoxide dismutase. J Biol Chem *273*, 7765-7769.

Hockly, E., Woodman, B., Mahal, A., Lewis, C.M., and Bates, G. (2003). Standardization and statistical approaches to therapeutic trials in the R6/2 mouse. Brain Res Bull *61*, 469-479.

Hodges, J.R., Davies, R.R., Xuereb, J.H., Casey, B., Broe, M., Bak, T.H., Kril, J.J., and Halliday, G.M. (2004). Clinicopathological correlates in frontotemporal dementia. Ann Neurol *56*, 399-406.

Huang, C., Tong, J., Bi, F., Zhou, H., and Xia, X.G. (2012). Mutant TDP-43 in motor neurons promotes the onset and progression of ALS in rats. J Clin Invest *122*, 107-118.

Igaz, L.M., Kwong, L.K., Chen-Plotkin, A., Winton, M.J., Unger, T.L., Xu, Y., Neumann, M., Trojanowski, J.Q., and Lee, V.M. (2009). Expression Of TDP-43 C-terminal fragments in vitro recapitulates pathological features of TDP-43 proteinopathies. J Biol Chem.

Igaz, L.M., Kwong, L.K., Lee, E.B., Chen-Plotkin, A., Swanson, E., Unger, T., Malunda, J., Xu, Y., Winton, M.J., Trojanowski, J.Q.*, et al.* (2011). Dysregulation of the ALS-associated gene TDP-43 leads to neuronal death and degeneration in mice. J Clin Invest *121*, 726-738.

Igaz, L.M., Kwong, L.K., Xu, Y., Truax, A.C., Uryu, K., Neumann, M., Clark, C.M., Elman, L.B., Miller, B.L., Grossman, M.*, et al.* (2008). Enrichment of C-terminal fragments in TAR DNA-binding protein-43 cytoplasmic inclusions in brain but not in spinal cord of frontotemporal lobar degeneration and amyotrophic lateral sclerosis. Am J Pathol *173*, 182-194.

Ilieva, H., Polymenidou, M., and Cleveland, D.W. (2009). Non-cell autonomous toxicity in neurodegenerative disorders: ALS and beyond. J Cell Biol *187*, 761-772.

Ilieva, H.S., Yamanaka, K., Malkmus, S., Kakinohana, O., Yaksh, T., Marsala, M., and Cleveland, D.W. (2008). Mutant dynein (Loa) triggers proprioceptive axon loss that extends survival only in the SOD1 ALS model with highest motor neuron death. Proc Natl Acad Sci U S A *105*, 12599-12604.

Johnson, B.S., McCaffery, J.M., Lindquist, S., and Gitler, A.D. (2008). A yeast TDP-43 proteinopathy model: Exploring the molecular determinants of TDP-43 aggregation and cellular toxicity. Proc Natl Acad Sci U S A *105*, 6439-6444.

Johnson, B.S., Snead, D., Lee, J.J., McCaffery, J.M., Shorter, J., and Gitler, A.D. (2009a). TDP-43 is intrinsically aggregation-prone and ALS-linked mutations accelerate aggregation and increase toxicity. J Biol Chem.

Johnson, B.S., Snead, D., Lee, J.J., McCaffery, J.M., Shorter, J., and Gitler, A.D. (2009b). TDP-43 is intrinsically aggregation-prone, and amyotrophic lateral sclerosis-linked mutations accelerate aggregation and increase toxicity. J Biol Chem *284*, 20329-20339.

Kabashi, E., Lin, L., Tradewell, M.L., Dion, P.A., Bercier, V., Bourgouin, P., Rochefort, D., Bel Hadj, S., Durham, H.D., Vande Velde, C.*, et al.* (2009). Gain and loss of function of ALS-related mutations of TARDBP (TDP-43) cause motor deficits in vivo. Hum Mol Genet *19*, 671-683.

Kabashi, E., Valdmanis, P.N., Dion, P., Spiegelman, D., McConkey, B.J., Vande Velde, C., Bouchard, J.P., Lacomblez, L., Pochigaeva, K., Salachas, F.*, et al.* (2008). TARDBP mutations in individuals with sporadic and familial amyotrophic lateral sclerosis. Nat Genet *40*, 572-574.

Kawase, M., Murakami, K., Fujimura, M., Morita-Fujimura, Y., Gasche, Y., Kondo, T., Scott, R.W., and Chan, P.H. (1999). Exacerbation of delayed cell injury after transient global ischemia in mutant mice with CuZn superoxide dismutase deficiency. Stroke *30*, 1962-1968.

Kim, S.H., Shi, Y., Hanson, K.A., Williams, L.M., Sakasai, R., Bowler, M.J., and Tibbetts, R.S. (2008). Potentiation of ALS-associated TDP-43 aggregation by the proteasome-targeting factor, Ubiquilin 1. J Biol Chem.

King, O.D., Gitler, A.D., and Shorter, J. (2012). The tip of the iceberg: RNA-binding proteins with prion-like domains in neurodegenerative disease. Brain Res.

Kondo, T., Reaume, A.G., Huang, T.T., Carlson, E., Murakami, K., Chen, S.F., Hoffman, E.K., Scott, R.W., Epstein, C.J., and Chan, P.H. (1997). Reduction of CuZn-superoxide dismutase activity exacerbates neuronal cell injury and edema formation after transient focal cerebral ischemia. J Neurosci *17*, 4180-4189.

Kraemer, B.C., Schuck, T., Wheeler, J.M., Robinson, L.C., Trojanowski, J.Q., Lee, V.M., and Schellenberg, G.D. (2010). Loss of murine TDP-43 disrupts motor

function and plays an essential role in embryogenesis. Acta Neuropathol *119*, 409-419.

Kuo, P.H., Doudeva, L.G., Wang, Y.T., Shen, C.K., and Yuan, H.S. (2009). Structural insights into TDP-43 in nucleic-acid binding and domain interactions. Nucleic Acids Res *37*, 1799-1808.

Kwiatkowski, T.J., Jr., Bosco, D.A., Leclerc, A.L., Tamrazian, E., Vanderburg, C.R., Russ, C., Davis, A., Gilchrist, J., Kasarskis, E.J., Munsat, T.*, et al.* (2009). Mutations in the FUS/TLS gene on chromosome 16 cause familial amyotrophic lateral sclerosis. Science *323*, 1205-1208.

Lagier-Tourenne, C., Polymenidou, M., and Cleveland, D.W. (2010). TDP-43 and FUS/TLS: emerging roles in RNA processing and neurodegeneration. Hum Mol Genet *19*, R46-64.

Laird, A.S., Van Hoecke, A., De Muynck, L., Timmers, M., Van den Bosch, L., Van Damme, P., and Robberecht, W. (2010). Progranulin is neurotrophic in vivo and protects against a mutant TDP-43 induced axonopathy. PLoS ONE *5*, e13368.

Lee, E.B., Lee, V.M., and Trojanowski, J.Q. (2012). Gains or losses: molecular mechanisms of TDP43-mediated neurodegeneration. Nat Rev Neurosci *13*, 38-50.

Li, Y., Ray, P., Rao, E.J., Shi, C., Guo, W., Chen, X., Woodruff, E.A., 3rd, Fushimi, K., and Wu, J.Y. (2010). A Drosophila model for TDP-43 proteinopathy. Proc Natl Acad Sci U S A.

Liachko, N.F., Guthrie, C.R., and Kraemer, B.C. (2010). Phosphorylation promotes neurotoxicity in a Caenorhabditis elegans model of TDP-43 proteinopathy. J Neurosci *30*, 16208-16219.

Ling, S.C., Albuquerque, C.P., Han, J.S., Lagier-Tourenne, C., Tokunaga, S., Zhou, H., and Cleveland, D.W. (2010). ALS-associated mutations in TDP-43 increase its stability and promote TDP-43 complexes with FUS/TLS. Proc Natl Acad Sci U S A *107*, 13318-13323.

Lino, M.M., Schneider, C., and Caroni, P. (2002). Accumulation of SOD1 mutants in postnatal motoneurons does not cause motoneuron pathology or motoneuron disease. J Neurosci *22*, 4825-4832.

Liscic, R.M., Grinberg, L.T., Zidar, J., Gitcho, M.A., and Cairns, N.J. (2008). ALS and FTLD: two faces of TDP-43 proteinopathy. Eur J Neurol *15*, 772-780.

Lomen-Hoerth, C., Anderson, T., and Miller, B. (2002). The overlap of amyotrophic lateral sclerosis and frontotemporal dementia. Neurology *59*, 1077-1079.

Lu, Y., Ferris, J., and Gao, F.B. (2009). Frontotemporal dementia and amyotrophic lateral sclerosis-associated disease protein TDP-43 promotes dendritic branching. Mol Brain *2*, 30.

Luk, K.C., Song, C., O'Brien, P., Stieber, A., Branch, J.R., Brunden, K.R., Trojanowski, J.Q., and Lee, V.M. (2009). Exogenous alpha-synuclein fibrils seed the formation of Lewy body-like intracellular inclusions in cultured cells. Proc Natl Acad Sci U S A *106*, 20051-20056.

Mandillo, S., Tucci, V., Holter, S.M., Meziane, H., Banchaabouchi, M.A., Kallnik, M., Lad, H.V., Nolan, P.M., Ouagazzal, A.M., Coghill, E.L.*, et al.* (2008). Reliability, robustness, and reproducibility in mouse behavioral phenotyping: a cross-laboratory study. Physiol Genomics *34*, 243-255.

Miguel, L., Frebourg, T., Campion, D., and Lecourtois, M. (2011). Both cytoplasmic and nuclear accumulations of the protein are neurotoxic in Drosophila models of TDP-43 proteinopathies. Neurobiol Dis *41*, 398-406.

Neumann, M., Kwong, L.K., Lee, E.B., Kremmer, E., Flatley, A., Xu, Y., Forman, M.S., Troost, D., Kretzschmar, H.A., Trojanowski, J.Q.*, et al.* (2009). Phosphorylation of S409/410 of TDP-43 is a consistent feature in all sporadic and familial forms of TDP-43 proteinopathies. Acta Neuropathol *117*, 137-149.

Neumann, M., Sampathu, D.M., Kwong, L.K., Truax, A.C., Micsenyi, M.C., Chou, T.T., Bruce, J., Schuck, T., Grossman, M., Clark, C.M.*, et al.* (2006). Ubiquitinated TDP-43 in frontotemporal lobar degeneration and amyotrophic lateral sclerosis. Science *314*, 130-133.

Ou, S.H., Wu, F., Harrich, D., Garcia-Martinez, L.F., and Gaynor, R.B. (1995). Cloning and characterization of a novel cellular protein, TDP-43, that binds to human immunodeficiency virus type 1 TAR DNA sequence motifs. J Virol *69*, 3584-3596.

Pesiridis, G.S., Lee, V.M., and Trojanowski, J.Q. (2009). Mutations in TDP-43 link glycine-rich domain functions to amyotrophic lateral sclerosis. Hum Mol Genet *18*, R156-162.

Pizzi, M., Benarese, M., Boroni, F., Goffi, F., Valerio, A., and Spano, P.F. (2000). Neuroprotection by metabotropic glutamate receptor agonists on kainate-induced degeneration of motor neurons in spinal cord slices from adult rat. Neuropharmacology *39*, 903-910.

Polymenidou, M., and Cleveland, D.W. (2012). Prion-like spread of protein aggregates in neurodegeneration. J Exp Med *209*, 889-893.

Polymenidou, M., Lagier-Tourenne, C., Hutt, K.R., Huelga, S.C., Moran, J., Liang, T.Y., Ling, S.C., Sun, E., Wancewicz, E., Mazur, C.*, et al.* (2011). Long pre-mRNA depletion and RNA missplicing contribute to neuronal vulnerability from loss of TDP-43. Nat Neurosci *14*, 459-468.

Pramatarova, A., Laganiere, J., Roussel, J., Brisebois, K., and Rouleau, G.A. (2001). Neuron-specific expression of mutant superoxide dismutase 1 in transgenic mice does not lead to motor impairment. J Neurosci *21*, 3369-3374.

Rabin, S.J., Kim, J.M., Baughn, M., Libby, R.T., Kim, Y.J., Fan, Y., La Spada, A., Stone, B., and Ravits, J. (2010). Sporadic ALS has compartment-specific aberrant exon splicing and altered cell-matrix adhesion biology. Hum Mol Genet *19*, 313-328.

Reaume, A.G., Elliott, J.L., Hoffman, E.K., Kowall, N.W., Ferrante, R.J., Siwek, D.F., Wilcox, H.M., Flood, D.G., Beal, M.F., Brown, R.H., Jr.*, et al.* (1996). Motor neurons in Cu/Zn superoxide dismutase-deficient mice develop normally but exhibit enhanced cell death after axonal injury. Nat Genet *13*, 43-47.

Renton, A.E., Majounie, E., Waite, A., Simon-Sanchez, J., Rollinson, S., Gibbs, J.R., Schymick, J.C., Laaksovirta, H., van Swieten, J.C., Myllykangas, L.*, et al.*

(2011). A hexanucleotide repeat expansion in C9ORF72 is the cause of chromosome 9p21-linked ALS-FTD. Neuron *72*, 257-268.

Ripps, M.E., Huntley, G.W., Hof, P.R., Morrison, J.H., and Gordon, J.W. (1995). Transgenic mice expressing an altered murine superoxide dismutase gene provide an animal model of amyotrophic lateral sclerosis. Proc Natl Acad Sci U S A *92*, 689-693.

Ritson, G.P., Custer, S.K., Freibaum, B.D., Guinto, J.B., Geffel, D., Moore, J., Tang, W., Winton, M.J., Neumann, M., Trojanowski, J.Q.*, et al.* (2010). TDP-43 mediates degeneration in a novel Drosophila model of disease caused by mutations in VCP/p97. J Neurosci *30*, 7729-7739.

Rosen, D.R., Siddique, T., Patterson, D., Figlewicz, D.A., Sapp, P., Hentati, A., Donaldson, D., Goto, J., O'Regan, J.P., Deng, H.X.*, et al.* (1993). Mutations in Cu/Zn superoxide dismutase gene are associated with familial amyotrophic lateral sclerosis. Nature *362*, 59-62.

Sephton, C.F., Cenik, C., Kucukural, A., Dammer, E.B., Cenik, B., Han, Y., Dewey, C.M., Roth, F.P., Herz, J., Peng, J.*, et al.* (2011). Identification of neuronal RNA targets of TDP-43-containing ribonucleoprotein complexes. J Biol Chem *286*, 1204-1215.

Sephton, C.F., Good, S.K., Atkin, S., Dewey, C.M., Mayer, P., Herz, J., and Yu, G. (2009). TDP-43 is a developmentally-regulated protein essential for early embryonic development. J Biol Chem.

Shan, X., Chiang, P.M., Price, D.L., and Wong, P.C. (2010). Altered distributions of Gemini of coiled bodies and mitochondria in motor neurons of TDP-43 transgenic mice. Proc Natl Acad Sci U S A.

Sreedharan, J., Blair, I.P., Tripathi, V.B., Hu, X., Vance, C., Rogelj, B., Ackerley, S., Durnall, J.C., Williams, K.L., Buratti, E.*, et al.* (2008). TDP-43 mutations in familial and sporadic amyotrophic lateral sclerosis. Science *319*, 1668-1672.

Stallings, N.R., Puttaparthi, K., Luther, C.M., Burns, D.K., and Elliott, J.L. (2010). Progressive motor weakness in transgenic mice expressing human TDP-43. Neurobiol Dis *40*, 404-414.

Strong, M.J., Volkening, K., Hammond, R., Yang, W., Strong, W., Leystra-Lantz, C., and Shoesmith, C. (2007). TDP43 is a human low molecular weight neurofilament (hNFL) mRNA-binding protein. Mol Cell Neurosci *35*, 320-327.

Sugnet, C.W., Srinivasan, K., Clark, T.A., O'Brien, G., Cline, M.S., Wang, H., Williams, A., Kulp, D., Blume, J.E., Haussler, D.*, et al.* (2006). Unusual intron conservation near tissue-regulated exons found by splicing microarrays. PLoS Comput Biol *2*, e4.

Swarup, V., Phaneuf, D., Bareil, C., Robertson, J., Rouleau, G.A., Kriz, J., and Julien, J.P. (2011a). Pathological hallmarks of amyotrophic lateral sclerosis/frontotemporal lobar degeneration in transgenic mice produced with TDP-43 genomic fragments. Brain *134*, 2610-2626.

Swarup, V., Phaneuf, D., Dupre, N., Petri, S., Strong, M., Kriz, J., and Julien, J.P. (2011b). Deregulation of TDP-43 in amyotrophic lateral sclerosis triggers nuclear factor kappaB-mediated pathogenic pathways. J Exp Med *208*, 2429-2447.

Tollervey, J.R., Curk, T., Rogelj, B., Briese, M., Cereda, M., Kayikci, M., Konig, J., Hortobagyi, T., Nishimura, A.L., Zupunski, V.*, et al.* (2011). Characterizing the RNA targets and position-dependent splicing regulation by TDP-43. Nat Neurosci *14*, 452-458.

Tsai, K.J., Yang, C.H., Fang, Y.H., Cho, K.H., Chien, W.L., Wang, W.T., Wu, T.W., Lin, C.P., Fu, W.M., and Shen, C.K. (2010). Elevated expression of TDP-43 in the forebrain of mice is sufficient to cause neurological and pathological phenotypes mimicking FTLD-U. J Exp Med.

Turner, B.J., and Talbot, K. (2008). Transgenics, toxicity and therapeutics in rodent models of mutant SOD1-mediated familial ALS. Prog Neurobiol *85*, 94-134.

Van Damme, P., Bogaert, E., Dewil, M., Hersmus, N., Kiraly, D., Scheveneels, W., Bockx, I., Braeken, D., Verpoorten, N., Verhoeven, K.*, et al.* (2007). Astrocytes regulate GluR2 expression in motor neurons and their vulnerability to excitotoxicity. Proc Natl Acad Sci U S A *104*, 14825-14830.

Van Damme, P., Braeken, D., Callewaert, G., Robberecht, W., and Van Den Bosch, L. (2005). GluR2 deficiency accelerates motor neuron degeneration in a

mouse model of amyotrophic lateral sclerosis. J Neuropathol Exp Neurol *64*, 605-612.

Van Deerlin, V.M., Leverenz, J.B., Bekris, L.M., Bird, T.D., Yuan, W., Elman, L.B., Clay, D., Wood, E.M., Chen-Plotkin, A.S., Martinez-Lage, M.*, et al.* (2008). TARDBP mutations in amyotrophic lateral sclerosis with TDP-43 neuropathology: a genetic and histopathological analysis. Lancet Neurol *7*, 409-416.

Vance, C., Rogelj, B., Hortobagyi, T., De Vos, K.J., Nishimura, A.L., Sreedharan, J., Hu, X., Smith, B., Ruddy, D., Wright, P.*, et al.* (2009). Mutations in FUS, an RNA processing protein, cause familial amyotrophic lateral sclerosis type 6. Science *323*, 1208-1211.

Voigt, A., Herholz, D., Fiesel, F.C., Kaur, K., Muller, D., Karsten, P., Weber, S.S., Kahle, P.J., Marquardt, T., and Schulz, J.B. (2010). TDP-43-mediated neuron loss in vivo requires RNA-binding activity. PLoS ONE *5*, e12247.

Wang, H.Y., Wang, I.F., Bose, J., and Shen, C.K. (2004). Structural diversity and functional implications of the eukaryotic TDP gene family. Genomics *83*, 130-139.

Wang, I.F., Chang, H.Y., Hou, S.C., Liou, G.G., Way, T.D., and James Shen, C.K. (2012). The self-interaction of native TDP-43 C terminus inhibits its degradation and contributes to early proteinopathies. Nat Commun *3*, 766.

Wang, J., Xu, G., Slunt, H.H., Gonzales, V., Coonfield, M., Fromholt, D., Copeland, N.G., Jenkins, N.A., and Borchelt, D.R. (2005). Coincident thresholds of mutant protein for paralytic disease and protein aggregation caused by restrictively expressed superoxide dismutase cDNA. Neurobiol Dis *20*, 943-952.

Wegorzewska, I., Bell, S., Cairns, N.J., Miller, T.M., and Baloh, R.H. (2009). TDP-43 mutant transgenic mice develop features of ALS and frontotemporal lobar degeneration. Proc Natl Acad Sci U S A *106*, 18809-18814.

Wils, H., Kleinberger, G., Janssens, J., Pereson, S., Joris, G., Cuijt, I., Smits, V., Groote, C.C., Van Broeckhoven, C., and Kumar-Singh, S. (2010). TDP-43 transgenic mice develop spastic paralysis and neuronal inclusions characteristic of ALS and frontotemporal lobar degeneration. Proc Natl Acad Sci U S A.

Winton, M.J., Igaz, L.M., Wong, M.M., Kwong, L.K., Trojanowski, J.Q., and Lee, V.M. (2008). Disturbance of nuclear and cytoplasmic TAR DNA-binding protein (TDP-43) induces disease-like redistribution, sequestration, and aggregate formation. J Biol Chem *283*, 13302-13309.

Wu, L.S., Cheng, W.C., Hou, S.C., Yan, Y.T., Jiang, S.T., and Shen, C.K. (2010). TDP-43, a neuro-pathosignature factor, is essential for early mouse embryogenesis. Genesis *48*, 56-62.

Wu, L.S., Cheng, W.C., and Shen, C.K. (2012). Targeted Depletion of TDP-43 Expression in the Spinal Cord Motor Neurons Leads to the Development of Amyotrophic Lateral Sclerosis-like Phenotypes in Mice. J Biol Chem *287*, 27335-27344.

Xiao, S., Sanelli, T., Dib, S., Sheps, D., Findlater, J., Bilbao, J., Keith, J., Zinman, L., Rogaeva, E., and Robertson, J. (2011). RNA targets of TDP-43 identified by UV-CLIP are deregulated in ALS. Mol Cell Neurosci *47*, 167-180.

Xu, Y.F., Gendron, T.F., Zhang, Y.J., Lin, W.L., D'Alton, S., Sheng, H., Casey, M.C., Tong, J., Knight, J., Yu, X.*, et al.* (2010). Wild-type human TDP-43 expression causes TDP-43 phosphorylation, mitochondrial aggregation, motor deficits, and early mortality in transgenic mice. J Neurosci *30*, 10851-10859.

Xu, Y.F., Zhang, Y.J., Lin, W.L., Cao, X., Stetler, C., Dickson, D.W., Lewis, J., and Petrucelli, L. (2011). Expression of mutant TDP-43 induces neuronal dysfunction in transgenic mice. Mol Neurodegener *6*, 73.

Yamanaka, K., Boillee, S., Roberts, E.A., Garcia, M.L., McAlonis-Downes, M., Mikse, O.R., Cleveland, D.W., and Goldstein, L.S. (2008a). Mutant SOD1 in cell types other than motor neurons and oligodendrocytes accelerates onset of disease in ALS mice. Proc Natl Acad Sci U S A *105*, 7594-7599.

Yamanaka, K., Chun, S.J., Boillee, S., Fujimori-Tonou, N., Yamashita, H., Gutmann, D.H., Takahashi, R., Misawa, H., and Cleveland, D.W. (2008b). Astrocytes as determinants of disease progression in inherited amyotrophic lateral sclerosis. Nat Neurosci *11*, 251-253.

Yazawa, I., Giasson, B.I., Sasaki, R., Zhang, B., Joyce, S., Uryu, K., Trojanowski, J.Q., and Lee, V.M. (2005). Mouse model of multiple system atrophy alpha-

synuclein expression in oligodendrocytes causes glial and neuronal degeneration. Neuron *45*, 847-859.

Zhang, T., Hwang, H.Y., Hao, H., Talbot, C., Jr., and Wang, J. (2012). Caenorhabditis elegans RNA-processing Protein TDP-1 Regulates Protein Homeostasis and Life Span. J Biol Chem *287*, 8371-8382.

Zhang, Y.J., Xu, Y.F., Cook, C., Gendron, T.F., Roettges, P., Link, C.D., Lin, W.L., Tong, J., Castanedes-Casey, M., Ash, P.*, et al.* (2009). Aberrant cleavage of TDP-43 enhances aggregation and cellular toxicity. Proc Natl Acad Sci U S A *106*, 7607-7612.

Zhang, Y.J., Xu, Y.F., Dickey, C.A., Buratti, E., Baralle, F., Bailey, R., Pickering-Brown, S., Dickson, D., and Petrucelli, L. (2007). Progranulin mediates caspase-dependent cleavage of TAR DNA binding protein-43. J Neurosci *27*, 10530-10534.

Zhou, H., Huang, C., Chen, H., Wang, D., Landel, C.P., Xia, P.Y., Bowser, R., Liu, Y.J., and Xia, X.G. (2010). Transgenic rat model of neurodegeneration caused by mutation in the TDP gene. PLoS Genet *6*, e1000887.